ROLE OF INTERSUBUNIT INTERFACES IN HIV-1 CAPSID ASSEMBLY AND STABILITY

By

Ernest L. Yufenyuy

Dissertation

Submitted to the Faculty of the

Graduate School of Vanderbilt University

in partial fulfillment of the requirements

for the degree of

DOCTOR OF PHILOSOPHY

in

Microbiology and Immunology

May, 2013

Nashville, Tennessee

Approved:

Dr. Earl Ruley

Dr. Chris Aiken

Dr. Ellen Fanning

Dr. Benjamin Spiller

Dr. Mark Denison

ACKNOWLEDGEMENTS

I look at the past four years with great admiration and appreciation for the sacrifices that so many have made to help me along this journey. It was during the 1996 Democratic National Convention that Hillary Clinton, the wife of former President Clinton and the United States Secretary of State under the Obama administration, made popular the African proverb that "it takes a village to raise a child." This could not be more true for training a PhD student. It takes the enormous work and dedication from one's advisor and committee, along with the support from one's friends, family, and department staff. These are the hidden forces behind my successful completion of this program. So with a joyful heart I would like to thank my advisor, Dr. Christopher Aiken, for all he has done and been, for all he has provided towards my success. The platform he provided for my training was encouraging, demanding, and challenging, and now I can confidently say it was rewarding. I have learned so much from him, both formally and informally. I have learned to think critically, analytically, to question myself, and to appreciate the wonder of science, which I will carry with me into the next phase of my life. For all these and much more, I say thank you.

I want to thank my thesis committee, headed by Dr. Earl Ruley as Chair, Dr. Mark Denison, Dr. Ben Spiller, and Dr. Ellen Fanning for their commitment to this adventure of raising science children. Your ability to look at things from different angles provided me with multiple views on a scientific question that kept me constantly thinking, and it only made me a better science student. I would like to extend my appreciation to Dr. Ruley for keeping his door open whenever I needed him. I owe all of

you by deepest gratitude.

I would like to thank members of the Aiken Laboratory, both past and present, whom I was fortunate to meet. I appreciate all your help in orienting me in the lab. My stay in the Aiken lab has been graced by the diversity of cultures and personalities which you brought forth. Anybody that has been to this lab will immediately concur that the wealth of diversity makes science and research more fun. I have learned so much about other cultures just by being around the lab for the past four years. I know I will be remembered as the loud one, but I must confess it was all for the purpose of keeping things upbeat. I have also been fortunate to work with a group of talented scientists and collaborators from Pittsburgh under the auspices of Dr. Peijun Zhang. Thank you for the great work that we did together.

My friends have been a wonderful support in my life and I cannot thank them enough. Sometimes life rears its ugliness with challenges that are real and which come at times that we least expect, or from sources that are least imaginable. But the presence of friends and family will always soften these moments and place us once again on the train of hope. My friends have been awesome and my special thanks go to all of them, for they have been a part of my life in a way I will never forget.

I have been blessed with a big family, my wife, wonderful brothers and sisters, nieces and nephews, my sister in-law, my endearing mother, and a very wise father (of late). I largely attribute my success in life to all your support, love, and encouragement. My special thanks go to my father whose wisdom and principles have always guided me wherever I go. I especially thank my brother Ellison Yufenyuy and Mr. Patrick Doyle for all their support. Special thanks also go to my wife Mamboh Yufenyuy, whose love and

encouragement have gone a long way to lift me up. Thanks, Ma!

A wise woman once said that when our thoughts wander they draw us naturally to those people who have affected our lives in a special way. I am greatly indebted to all these groups of people for their support. Because of all that you did, I can continue to resound this motto: “And the net was not torn!”

LIST OF TABLES

TABLE OF CONTENTS

LIST OF FIGURES

LIST OF ABBREVIATIONS

AIDS	Acquired immune deficiency syndrome
BBS	BES-buffered saline
BBS	Bovine serum albumin
CA	Capsid protein, p24
CANC	CA-SP-NC
CA5	CA-SP1
CCR5	CC chemokine receptor 5
CD4+	Protein marker on surface of HIV-1 target cells
CDC	Centers for Disease Control
CLP	Capsid-like particle
CryoEM	Cryo-electron microscopy
CsA	Cyclosporin A
CTD	Carboxy-terminal domain
CypA	Cyclophilin A
CXCR4	CX chemokine receptor 4
DMEM	Dulbecco's modified Eagle's medium
DMSO	Dimethyl sulfoxide
dNTP	Deoxynucleotide
DNA	Deoxyribonucleic acid
DTT	Dithiothreitol
EFV	Efavirenz

ELISA	Enzyme-linked immunosorbent assay
EM	Electron microscopy
Env	Envelope glycoproteins
Gag	Group specific antigen
GFP	Green fluorescent protein
gp120	Envelope glycoprotein gp120; SU
HIV	Human immunodeficiency virus
HIV-1	Human immunodeficiency virus type 1
IN	Integrase
kb	Kilobases
LTR	Long terminal repeat
MA	Matrix protein, p17
MLV	Murine leukemia virus
NaCl	Sodium chloride
NC	Nucleocapsid protein, p7
Nef	Negative factor
nm	nanometer
NTD	Amino-terminal domain
OMK	Owl monkey kidney cells
PBS	Phosphate-buffered saline
PCR	Polymerase chain reaction
PIC	Pre-integration complex
Pol	Polymerase gene

PPT	Polypurine tract
PR	Viral protease
Ref1	Restriction factor 1
REV	Regulator of virion protein expression
RNA	Ribonucleic acid
RNP	Ribonucleoprotein complex
RSV	Rous sarcoma virus
RT	Reverse transcriptase
RTC	Reverse transcription complex
qPCR	Quantitative PCR
SDS	Sodium dodecyl sulfate
SU	Viral surface envelope protein
Tat	HIV transactivator of transcription
TEM	Transmission electron microscopy
TRIM	Tripartite motif
TRIMCypA	Tripartite motif fused with cyclophilin A
Vif	Viral infectivity factor
VLP	Virus-like particle
VSV	Vesicular stomatitis virus
VSV-G	VSV glycoprotein

CHAPTER I

BACKGROUND AND RESEARCH OBJECTIVES

HIV/AIDS

The etiologic agent of acquired immune deficiency syndrome (AIDS) is the small but highly pathogenic human immunodeficiency virus (HIV-1). HIV-1 infections are worldwide, causing an epidemic with a prevalence of over 34 million infections, 23 million of which are in sub-Saharan Africa. AIDS was responsible for over 1.8 million deaths in 2010 (UNAIDS), of which sub-Saharan Africa accounted for over three-quarters of the deaths. Although deaths related to HIV/AIDS have declined over the years, the incidence rate of HIV-1 is still high at over 2.7 million new infections in 2010; 14.4% of which were children below the age of 15. The hardest-hit regions of HIV/AIDS are less developed countries, resulting in severe economic and social problems. The compounding effects are numerous; escalating cycles of poverty because of low availability of an age-working group, increase in orphaned population, breakdown in social systems.

At present, there is no cure for HIV infection and there is no vaccine on the market. Highly active anti-retroviral therapy (HAART) has proven to control the disease by targeting multiple steps in the viral lifecycle, but would not completely eradicate the virus but reduce viral loads. However, toxicity, cost (given that most people infected are from poor backgrounds) and drug resistance remain some of the major concerns involved with current therapies. Therefore, an understanding of the steps in the viral life cycle

could help in designing novel drug targets for antiviral therapy. One of these steps in the viral life cycle is the process of uncoating, broadly defined as the disassembly of the viral capsid. This process is still poorly understood. My research project, as presented in this dissertation, was to identify viral determinants of HIV-1 capsid stability as related to uncoating. Additionally, the process of maturation from an immature virus to a mature viral particle is important. Understanding HIV-1 stability and the process of maturation of the capsid is important in order to exploit these processes as pharmacologic targets for antiviral therapies.

Progression of AIDS

Infection with HIV-1 can be transmitted by sexual contact and by sharing of contaminated needles in drug injections. In some cases, transmissions from mother to child occur during childbirth or during breast-feeding. The virus crosses the mucosal surfaces and makes contacts with $CD4^+$ T cells, which are the primary target cells of the virus. Once infected with the virus, disease progression can vary from individual to individual. Individuals can be classified as slow progressors, where AIDS develops slowly in a span of 3-10 years; fast progressors, where AIDS develops within 2 to 3 years; and long term non-progressors or elite controllers, who are people with undetectable viral loads for more than 10 years. However, stages in disease progression are similar in all individuals and can be divided into acute infection, clinical latency, and severe clinical immunodeficiency, also called AIDS (UNAIDS, 2007). During the acute phase, viral load in peripheral blood is high with symptoms occurring within few weeks of infection. Most common symptoms encountered in more than 70% of the cases include flu-like symptoms. The virus spreads

throughout the body, seeding in spleen, lymph nodes, thymus. Viral replication during the acute phase results in a dramatic decline in $CD4^+$ T cells. Increase in viral replication prompts innate immune response to react along with cellular and humoral immune responses. Counterattack by the innate immune system results in a reduction in the levels of viral replication, causing T cells to rebound in the clinical latency phase. In the clinical latency phase, the individual remains asymptomatic and viral load and $CD4^+$ T cells are in equilibrium with viral replication. This can last from weeks to about 20 years. Eventually, viral replication will slowly increase, leading to a reduction in immune cells and eventually causing a collapse of the immune system. Without antiretroviral treatment, the patient becomes exposed to opportunistic infections such as pneumonia, brain infections, and histoplasmosis. This is the final phase of severe clinical immunodeficiency phase or AIDS.

Structure of the virion

The HIV-1 virion, of the lentivirus subfamily of retroviruses, measures about 120 nm in diameter and roughly spherical. On the outer surface of the virion is a host-cell derived lipid envelope that surrounds a conical capsid. The viral genome is contained within the capsid and is made up of two identical single strands of RNA. Viral RNA is associated with the nucleocapsid protein. With a genome of 9.2 Kb, each single-stranded RNA molecule has nine open reading frames (ORF), of which three include the genes that code for the Gag, Env and Pol polyproteins that are cleaved by a protease during the process of maturation. Gag is a polyprotein that is cleaved into MA, CA, NC, p6 and two spacer proteins SP1 and SP2. The Pol polyprotein is cleaved into proteins that mediate viral enzymatic reactions including protease (PR, for viral processing), reverse transcriptase

(RT, for reverse transcription) and integrase (IN, for integration into host genome). The Env polyprotein is cleaved into gp120 and gp41, which constitute the surface glycoprotein and trans membrane proteins, respectively. Both membrane proteins mediate attachment and fusion of the virus to the target cells. HIV-1 also encodes four accessory proteins (Vif, Nef, Vpr, Vpu) and two regulatory proteins (Tat and Rev) that are both important for viral pathogenesis and replication. In immature particles, the Gag polyprotein remains attached to the inner viral, membrane through its N-terminal myristic acid group. This radial arrangement of Gag makes the core of an immature virus to be spherical (Figure 1-3 and Figure 1-4).

HIV-1 life cycle: an overview

The life cycle of HIV-1 can be divided into two distinct phases; an early phase of cell fusion, uncoating, reverse transcription, nuclear entry and integration; and a late phase that constitutes events after integration such as nuclear export, translation, assembly, budding and maturation (Figure 1-1). The early phase events begin when the virus, via gp120, binds a $CD4^+$ cell either as T lymphocytes or macrophages. In addition to CD4, one of two co-receptors, CCR5 and CXCR4, is also involved in binding (Freed, 2001). Binding to coreceptor results in a conformational change that exposes the gp41 fusion peptide to the target the cell membrane. This brings the virus membrane and the cell membrane in close proximity initiating fusion between the two membranes (Gallo et al., 2001). Fusion results in the release of viral capsid into the cytoplasm of the cell where two key events of the early phase take place: uncoating (broadly defined as the disassembly of the capsid, releasing the reverse transcription complex into the cytoplasm) (Aiken, 2006), and reverse

transcription. The sequence of events involving uncoating and reverse transcription are not well understood, and it is unclear whether uncoating takes place before reverse transcription or vice versa, or whether both events take place at the same time. However, it is understood that these processes are critical for viral infection. The core contains the ribonucleoprotein particle (RNP) and, the viral enzymes integrase and reverse transcriptase.

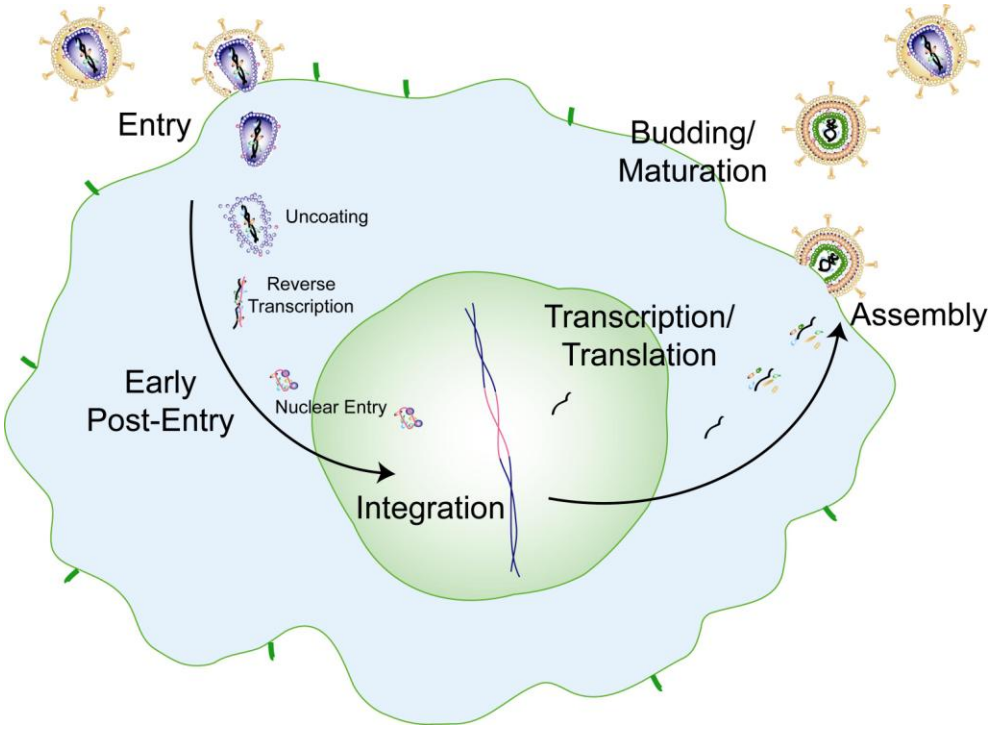

Figure 1-1. A schematic of the HIV-1 life cycle. An overview of the viral life cycle is described on page 4. Briefly the virus enters the cell and viral DNA is formed. The formed viral DNA undergoes integration, which leads to transcription and translation of viral proteins, assembly, budding and maturation. (This drawing was provided by David Dismuke).

Reverse transcription is catalyzed by reverse transcriptase and occurs in the cytoplasm in a step-wise process. The final product of reverse transcription is a double-stranded linear DNA, which constitutes part of the PIC called the provirus (Miller et al., 1997). Efficient reverse transcription appears to be associated with capsid stability: unstable CA mutants fail to undergo reverse transcription (Forshey et al., 2002; Jiang et al., 2011a; Leschonsky et al., 2007; Yang and Aiken, 2007; Yang et al., 2012). This suggests that uncoating is a balanced process that requires a capsid of optimal stability that will disassemble at a proper rate in target cells. CA mutants with reduced capsid stability often exhibit impaired infectivity, a phenotype that is well correlated with impairments in reverse transcription. Imaging studies of HIV-1 CA mutants in target cells further provided evidence for a role of reverse transcription in facilitating uncoating, suggesting that deviations in capsid stability might affect reverse transcription (Hulme et al., 2011). The role of reverse transcription in the process of uncoating is not well understood (Dismuke and Aiken, 2006; Forshey and Aiken, 2003; Yang and Aiken, 2007).

The PIC once formed is transported into the nucleus by the help of several host factors (e.g. TNPO3) working in close collaboration with viral proteins. The proviral DNA is then integrated into the host genome with the aid of the viral enzyme, integrase. Host factors then bind to the 5' LTR of the inserted viral genome in the host cell to promote transcription of the viral proteins, Tat, Rev and Nef. More Tat leads to potent up-regulation of transcription of the viral genome (Wei et al., 1998). The synthesized viral transcripts are exported from the nucleus to undergo translation in the cytoplasm. This process is regulated by Rev, where increased levels of the Rev leads to transport or exit of unspliced

viral transcripts from the nucleus. These will later produce the structural components of the capsid, including Gag (p55), and Gag-Pol.

Viral maturation

The Gag polyprotein assembles by radially arranging its myristoylated amino terminus MA domain on the inner leaflet of the viral membrane. The carboxyl terminus projects toward the center of the viral particle (Fuller et al., 1997; Wilk et al., 2001). This assembly leads to the formation of an immature, non-infectious spherical viral particle. In order to become infectious, the immature virus must undergo maturation, which is characterized by ordered cleavage of sites within Gag molecule as the virus buds from the cell (Figure 1-3). This process is mediated by the viral protease and results in dramatic morphological changes that lead to the formation of a conical, centralized viral core. Gag cleavage generates structural proteins (MA, CA, NC) and the spacer proteins (SP1 and SP2). Initially, cleavage occurs between the SP1 and NC. Subsequent cleavage between MA and CA-SP1 results in the refolding of a 13 N-terminal amino acid stretch to form a β-hairpin. Recent studies have suggested that cleavage between CA/SP1 destabilizes the immature lattice by destroying a helix formed by CA-SP1 (Datta et al., 2011). The β-hairpin is stabilized by a salt bridge formed between Pro1 and Asp 51 (Pornillos et al., 2009; Tang et al., 2002). It is thought that the final cleavage event, which occurs between CA and SP1, disrupts an α-helix that spans CA-SP1 resulting in rearrangement of the C-terminal domain of CA to form the various capsid interfaces and the full condensation of the capsid shell around the viral genome coated by NC (Wiegers et al., 1998) (Figure 1-3).

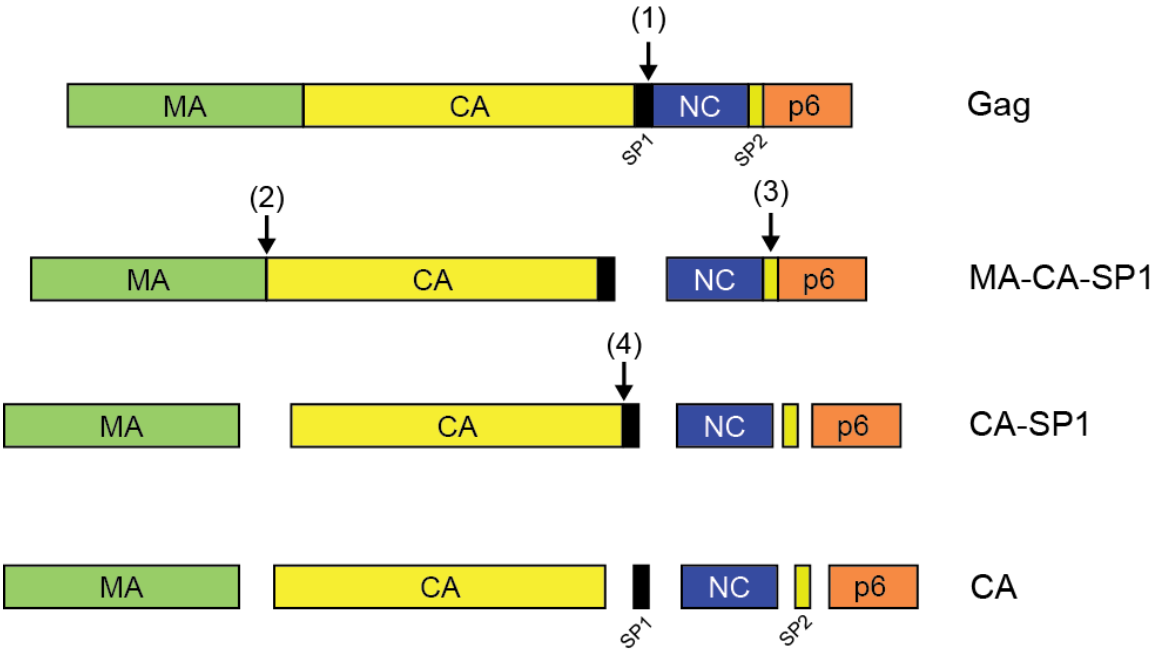

Figure 1-2: Diagram of HIV-1 $Pr55^{gag}$ and the sequential cleavage of Gag polyprotein. Shown are structures of full-length Gag and the sequence of cleavage with cleavage intermediates shown.

However, the precise mechanism that governs the maturation process from the spherical immature core to a conical mature viral core in HIV-1 has not been described. More specifically, it is not known whether the intermolecular capsid interfaces that are present in mature HIV-1 capsid are similar to those present in immature HIV-1 particles, or are only formed during maturation. Part of my research, as described in Chapter IV of this dissertation, was focused on understanding when and how these capsid interfaces are formed.

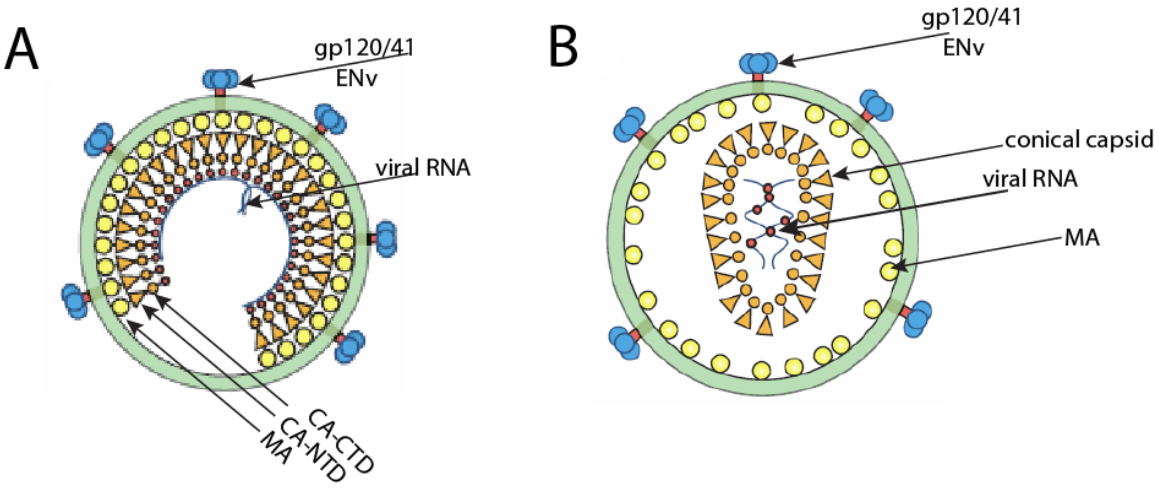

Figure 1-3: Diagram of the immature (A), and mature (B) HIV-1 virion. (A) Gag molecules align through attachment of the MA domain to the inner leaflet of the membrane to form a spherical inner core that is not completely closed. (B) MA remains attached to the membrane while CA condenses and form a conical shell around NC-coated genomic RNA. This picture is modified and adapted from J. Mol. Biol. (2011) 410, 534–552.

Uncoating and HIV-1 Capsid

The process of uncoating is thought to occur in the cytoplasm following viral entry into the cell (Figure 1-4). Compared with other steps in the viral life cycle, uncoating is one of the least well understood. Our laboratory and others have worked developed biochemical assays to study the process of uncoating in vitro (Aiken, 2009; Forshey and Aiken, 2003; Forshey et al., 2002; Kotov et al., 1999; Shah and Aiken, 2011b). The capsid of HIV-1 has been extensively studied via mutations to the CA protein that comprises the capsid. In this light, the effects of mutagenesis on the CA have been studied for capsid structure, capsid stability and viral infectivity.

Recent studies from our laboratory and others have focused on the structure and stability of the capsid, and its impact on viral infectivity (Forshey et al., 2002; Jiang et al., 2011b; von Schwedler et al., 1998; Yang and Aiken, 2007). Members of our lab have purified HIV-1 cores from wild type and mutant particles by treatments with detergent followed by sucrose density gradient ultracentrifugation. For the wild type, the percentage of CA associated with cores was found to be fairly constant, averaging 17% ±2 standard deviation. This is referred to as the core-associated CA. The CA associated with cores can dissociate spontaneously at a particular rate for wild type and under various conditions of temperature, pH, salt concentrations. For CA mutants, deviations in the percentage of CA associated with cores from wild type and deviations from wild type kinetics of disassembly reflect changes in the stability of the capsid. These measurements have allowed the classification of mutants as having unstable, and hyperstable capsids.

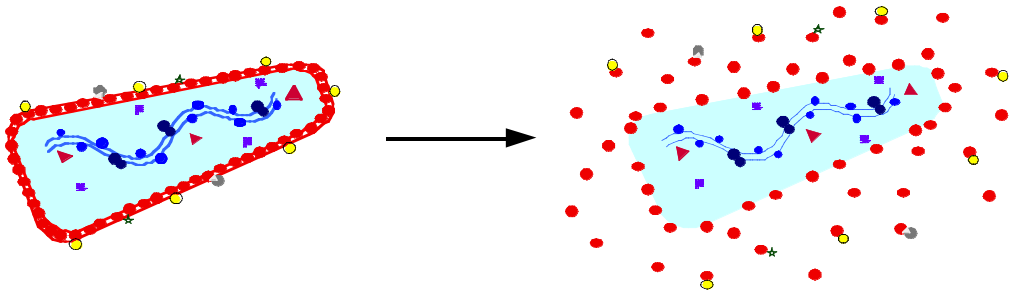

Figure 1-4: A schematic of HIV-1 uncoating. The capsid shell disassembles and releases the core contents, specifically the viral ribonucleoprotein complex (RNP) into the cytoplasm (Aiken, 2006).

Mutagenesis studies have indicated that subunit interactions in the capsid lattice confer specific intrinsic stability to the HIV-1 capsid. Mutations at the NTD-NTD and CTD-CTD intersubunit interfaces affect capsid stability (Byeon et al., 2009; Forshey and Aiken, 2003; Forshey et al., 2002; Wacharapornin et al., 2007; Yang and Aiken, 2007). CA mutants with reduced capsid stability often exhibit impaired infectivity, suggesting that the intact capsid performs a critical function following penetration into the target cell. Imaging studies of HIV-1 CA mutants in target cells further provided evidence for a role of reverse transcription in facilitating uncoating, suggesting that deviations in capsid stability might affect reverse transcription (Hulme et al., 2011). The process of uncoating is not well understood (Dismuke and Aiken, 2006; Forshey and Aiken, 2003; Yang and Aiken, 2007).

A viral DNA "flap" has been implicated in the process of uncoating: research has shown that mutations preventing the formation of the viral DNA flap prevent nuclear entry of the viral cores and lead to the accumulation of cores at the nuclear membrane (Arhel et al., 2007). The authors argued that uncoating occurs after reverse transcription and before nuclear entry. Recent studies have shown that the process of uncoating might occur at the same time as reverse transcription: that is reverse transcription and uncoating might be coupled (Hulme et al., 2011). In this study it was shown that inhibition of reverse transcription had a negative effect on the rate of uncoating.

Several host factors have also been implicated in HIV-1 uncoating. Cyclophilin A (CypA), a cellular peptidylprolyl isomerase, binds to the HIV-1 at the NTD (Gamble et al., 1996; Luban et al., 1993). The binding of CypA to CA is important and disruption of this binding by mutations on the CA binding loop (G89A, P90A) or addition of cyclosporine, inhibits HIV-1 infection (Franke et al., 1994; Towers et al., 2003). The role of CypA in HIV-

1 replication is still not fully understood, but it was suggested by studies from our laboratory and others that CypA plays a role in capsid stability and uncoating (Li et al., 2009; Luban, 1996; Shah et al., 2013). Another host factor, TRIM5α, is a restriction factor that is linked to capsid stability and uncoating. TRIM5α binds to the capsid of HIV-1 and inhibit infectivity apparently by accelerating uncoating (Stremlau et al., 2004; Stremlau et al., 2006). TRIMCyp was also identified to bind to the capsid and inhibit infection of HIV-1 via a similar mechanism to TRIM5α (Sayah et al., 2004). What is important about these two restriction factors is that their mechanisms of action are similar, promoting rapid uncoating and impairments in reverse transcription reminiscent of capsid mutants with unstable cores (Hatziioannou et al., 2004; Nisole et al., 2004; Owens et al., 2004; Owens et al., 2003). Our lab has also observed that TNPO3 stimulated the uncoating of HIV-1 cores in vitro. Hence, TNPO3 and CypA may coordinately control the process of uncoating.

Small molecule compounds have been found to inhibit viral replication by interacting with the viral capsid and altering capsid structure and stability (Blair et al., 2010; Kelly et al., 2007; Kortagere et al., 2012; Lemke et al., 2012; Phillips et al., 2008; Tang et al., 2003; Ternois et al., 2005). One of these molecules, PF-3450074 (PF74), binds the NTD in the region of the NTD-CTD interface and destabilizes the capsid, while amino acid substitutions at the interface can lead to resistance by blocking the binding of the drug (Blair et al., 2010; Shi et al., 2011). Overall, the emerging picture is that the capsid is a critical component of HIV-1 viral replication whose structure, assembly and disassembly need to be better understood and exploited to develop novel and effective antiviral therapies that target the capsid.

HIV-1 CA and CA-CA interactions

The CA protein of HIV-1 is a product of Gag polyprotein cleavage. CA is highly helical and contains 231 amino acids, has two globular domains; an N-terminal domain (NTD) and a C-terminal domain (CTD) (Figure 1-5). These two domains fold independently and are joined by a flexible helical linker (Berthet-Colominas et al., 1999; Gamble et al., 1997). The NTD, residues 1-151, is composed of seven α-helices and two β-hairpins (Berthet-Colominas et al., 1999; Momany et al., 1996), while the CTD constitutes residues 152-231 and consist of 4 alpha helices and a 3-10 helix. Two endogenous cysteines form an intramolecular disulfide bond between residues C198 and C218 (Mateu, 2002; Pornillos et al., 2009).

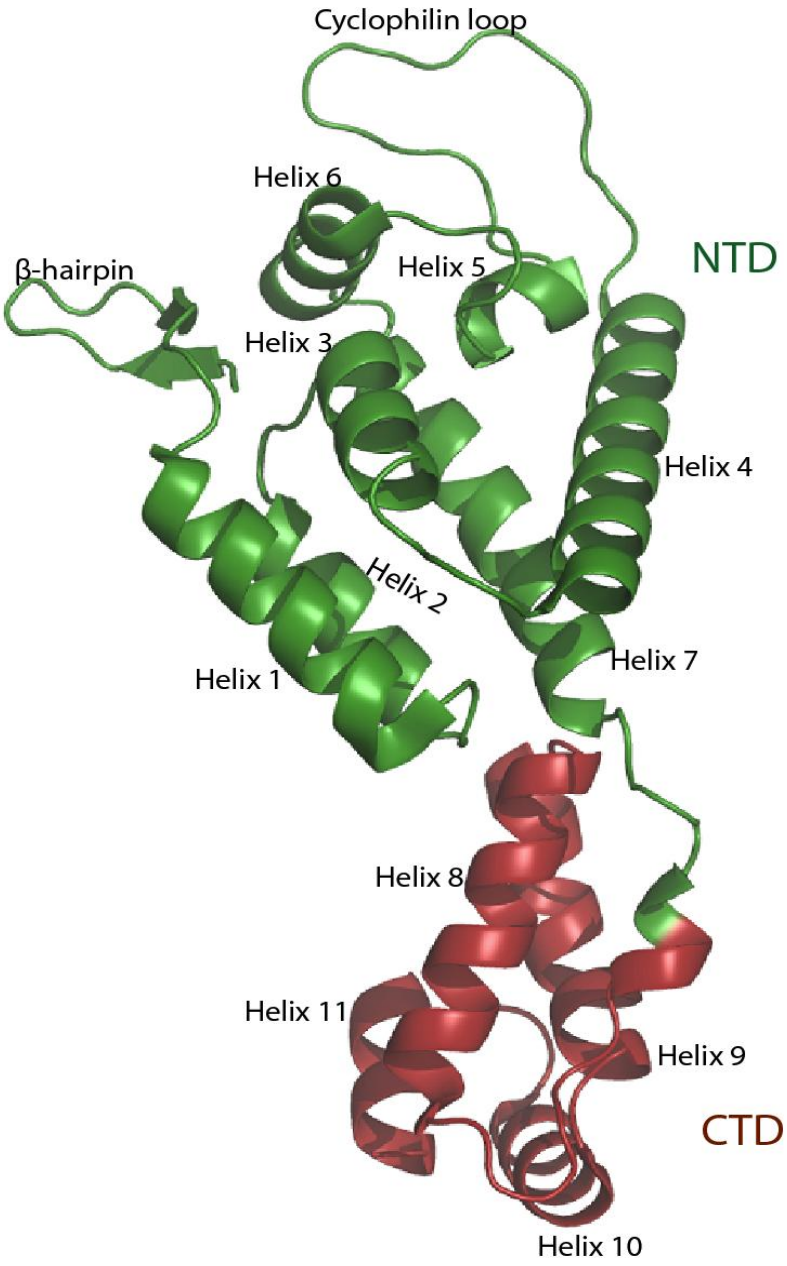

Figure 1-5: Ribbon diagram of the mature HIV-1 CA protein. The NTD (helix 1-7) is shown in green while the CTD (helix 8-11) is shown in red. This structure is based on data from the X-ray crystal structure of the hexamer (PBD 3H4E), Pornillos et al., 2009.

Transmission electron microscopy and cryoEM of HIV-1 particles produced from transfected cells have shown that the capsid of mature HIV-1 is conical and surrounds the viral core (Briggs et al., 2003; Ganser et al., 1999; Li et al., 2000). The capsid lattice is made up of about 250 hexamers (1500 molecules of CA protein) (Briggs et al., 2004; Ganser et al., 1999). A molecular model by direct imaging analysis suggested that the mature HIV-1 capsid forms a fullerene cone, composed of array of hexamers. The cone is closed at the ends by the insertion pentamers (Briggs et al., 2003; Ganser et al., 1999; Li et al., 2000). Although these studies established the general architecture of capsid, the resolution was not sufficient to define intermolecular contacts within the capsid. Recent studies using X-ray crystallography provided a model for capsid assembly with a more detailed structure of the HIV-1 fullerene core (Ganser-Pornillos et al., 2007; Pornillos et al., 2009). This demonstrates that the mature HIV-1 capsid lattice is stabilized by four major intermolecular interfaces:

1. NTD-NTD interface: This interface is essential for the formation of the CA hexamer and hence is termed the "hexamerization" interface (Byeon et al., 2009; Ganser-Pornillos et al., 2007; Li et al., 2000; Pornillos et al., 2009). The CA hexamer is held together by an 18-helix bundle that involves interactions between helices 1, 2, and 3 of one CA subunit with the corresponding bundle of the adjacent CA subunit (Pornillos et al., 2009). This model is supported by hydrogen-deuterium exchange experiments (Lanman et al., 2003), crosslinking with disulfide mutants (Pornillos et al., 2009), and mutational studies, which have shown severe impairments in infectivity for mutations located at this interface (Dismuke and Aiken, 2006; Forshey et al., 2002).

2. CTD-CTD dimerization interface: The CTD-CTD dimer interface is formed between hexamers of the mature HIV-1 capsid when helix 9 dimerizes with a neighboring helix 9 (Byeon et al., 2009; Gamble et al., 1997; Ganser-Pornillos et al., 2007; Worthylake et al., 1999). Analysis of mutations at the interface have shown impaired capsid assembly *in vitro* and *in vivo* (Ganser-Pornillos et al., 2007; von Schwedler et al., 2003). Similar experiments using amide hydrogen-deuterium exchange showed slower and decreased exchange at this interface in assembled HIV-1 particles, indicating that amino acids in this region were involved in some form of interaction (Lanman et al., 2003). Knowledge from this interface has led to efforts to design antiviral drugs that mimic helix 9 and inhibit assembly at this interface (Neira, 2009).

3. CTD-CTD threefold axis: Although not evident by the X-ray crystal structure, cryoEM modeling predicts the presence of a CTD-CTD interface located at a three-fold axis of symmetry (Byeon et al., 2009). The presence of this interface has been confirmed by crosslinking. Mutational analysis revealed that this interface was critically important for viral infectivity and uncoating, as K203A and Q219A formed unstable capsids; while E213A and E213Q both stabilized the capsid. However, the low resolution cryoEM structure could not reveal secondary structural elements of the trimer interface. My studies in Chapter III of this dissertation, will address the structure of the high resolution three-fold cryoEM structure.

4. NTD-CTD interface: This is an X-ray crystallographically defined CA interface formed by the insertion of NTD helices 4 and 7 into a groove formed by CTD helices 8 and 11. The NTD-CTD interactions were initially suggested by in vitro kinetic assembly studies of full-

length CA protein and truncated N-terminus and C-terminus proteins (Lanman et al., 2002). This initial suggestion was further enhanced by observations that hydrogen-deuterium (H/D) exchange on in vitro assembled CA occurred slowly at the NTD and at the CTD regions suggesting that these regions are protected. Chemical crosslinking and high-resolution mass spectrometry in the same study showed that Lys 70 on one subunit is in proximity to Lys 182 on a different CA subunit (Lanman et al., 2003). This interface was later visualized in atomic resolution in the crystal structure of a CA hexamer (Pornillos et al., 2009). Structural and genetic studies of other retroviruses, specifically RSV and SIV (both showing second-site suppressors), also indicate the presence of an interdomain interaction in the capsid involving the NTD of one subunit and the CTD of an adjacent subunit (Bowzard et al., 2001; Cardone et al., 2009; Inagaki et al., 2010), The interface is formed by helices 4 and 7 on the NTD of one subunit and helices 8 and 11 on the CTD of the adjacent subunit (Ganser-Pornillos et al., 2007; Pornillos et al., 2009). This is consistent with the overall structural conservation exhibited by retroviral CA proteins (Ako-Adjei et al., 2005; Berthet-Colominas et al., 1999; Khorasanizadeh et al., 1999; Kingston et al., 2000; Momany et al., 1996). Although the NTD-CTD interface is present in assemblies of recombinant CA, the presence of the interface within the native viral capsid has not been established. However, using H/D exchange experiments, the NTD of CA in virus-like particles was protected but the CTD was not shown (Lanman et al., 2004). It is not known whether the NTD-CTD interface is present in mature HIV-1 virions and how it might contribute to mature HIV-1 capsid structure and stability. Furthermore, it was not known if some of the aforementioned intersubunit interfaces are present in immature virions and how the mechanism that governs intersubunit formation and structural changes from the immature virion to the mature virion are achieved.

My studies described in Chapters II, III and IV of this dissertation were performed to answer these questions.

Research Objectives

HIV-1 particles undergo disassembly following entry into the target cell. For the disassembly process to successfully result in infection, the capsid must be of correct structure and proper stability. The determinants of capsid stability are still not well understood. Optimal stability to the HIV-1 might be conferred to the capsid intrinsically; via the coordinated interaction of capsid interfaces as these interfaces might provide the structural integrity and functionality of the capsid. Mutations at the NTD-NTD and CTD-CTD intersubunit interfaces alter capsid stability (Byeon et al., 2009; Forshey and Aiken, 2003; Forshey et al., 2002; Wacharapornin et al., 2007; Yang and Aiken, 2007). Although the NTD-CTD interface is present in assemblies of recombinant CA, the presence of the interface and its function within the native viral capsid had not been established. The main objectives of my dissertation were (1) to determine if the NTD-CTD interface is present in the mature HIV-1 capsid; (2) determine the functional role, if any, of the NTD-CTD interface on capsid structure and stability; (3) validate a high-resolution structural model of the CTD-CTD trimer interface; and (4) determine the effects of particle maturation on the formation of capsid interfaces.

To accomplish the first goal, I rationally targeted the NTD-CTD interface by using Pymol, a molecular graphics program to determine if residues on one NTD of HIV-1 CA were in close proximity to residues on an adjacent CTD of another subunit in the X-ray crystal structure of the CA hexamer. I then engineered cysteines on those residues

that lie within close proximity (~5 Å (Cβ-Cβ)) between amino acid residues from the NTD to the CTD. In Chapter II of this dissertation, I show evidence for engineered disulfide crosslinking that an NTD-CTD interface exists in HIV-1 virions. Mutant HIV-1 particles with substitutions of Cys for M68 and E212 of CA spontaneously formed disulfide-linked oligomers including dimers, trimers, tetramers, pentamers, and hexamers, supporting the existence of the interface in mature HIV-1 particles. To investigate the role of the NTD-CTD intersubunit interface in capsid structure and stability, I used the X-ray crystal structure of the HIV-1 CA hexamer as a guide to create and characterize a panel of HIV-1 mutants encoding substitutions in the NTD-CTD interface. Assays of capsid function in vitro and ex-vivo revealed that the mutations perturbed HIV-1 capsid structure, stability, and infectivity. In Chapter III, in collaboration with Dr. Peijun Zhang from the University of Pittsburgh, I validated a newly-generated cryoEM structural model of the HIV-1 trimer interface showing a disulfide crosslink in A204C. The cryoEM showed A204 to belong to the hydrophobic core of the trimer interface. A thorough mutational analysis revealed its importance in capsid stability. In Chapter IV, I used engineered disulfide crosslinking as a probe to study the presence of different capsid interfaces during HIV-1 particle maturation. Using probes for the different capsid interfaces in mature particles my analyses of immature particles containing these cysteine mutations support a maturation model involving reorganization of capsid interfaces, rather than complete disassembly and reassembly. Collectively, my research has provided evidence that an NTD-CTD interface exists in mature HIV-1 virions and that this interface and the CTD-CTD trimer interface are critical for capsid structure and stability. In collaboration with Dr. Peijun Zhang's group,

I also showed how the HIV-1 capsid assembles and the role of the trimer interface in assembly. This study provided a detailed understanding of how assembly occurs and how maturation results in the formation of capsid interfaces. My research has, therefore, uncovered genetic and structural details of capsid assembly and stability that can provide a basis for therapeutic targeting.

CHAPTER II

THE NTD-CTD INTERSUBUNIT INTERFACE IS CRITICAL FOR CAPSID ASSEMBLY AND STABILITY

Introduction

The mature HIV-1 capsid is a cone-shaped structure formed from assembly of approximately 1500 subunits of the viral CA protein into a lattice of hexamers with pentamers closing the ends (Ganser et al., 1999; Ganser-Pornillos et al., 2008). The capsid lattice is stabilized by intersubunit interactions within the hexamers and between hexamers. The amino-terminal and carboxyl-terminal domains (designated NTD and CTD, respectively) of CA are predominantly alpha-helical and fold independently (Gamble et al., 1997; Gitti et al., 1996). Recent structural studies have provided a detailed model of the capsid and have defined protein interfaces in the NTD and CTD through which the subunits interact (Byeon et al., 2009; Ganser-Pornillos et al., 2007; Pornillos et al., 2009; Pornillos et al., 2011). These interfaces include a six-fold intra-hexameric NTD-NTD interface (Ganser-Pornillos et al., 2007; Pornillos et al., 2009); a dimeric inter-hexamer interface formed between CTDs (Byeon et al., 2009; Gamble et al., 1997; Ganser-Pornillos et al., 2007; Worthylake et al., 1999); and a CTD-CTD trimeric interface that connects the hexamers (Byeon et al., 2009). The structures have also revealed the presence of an NTD-CTD intersubunit interface between adjacent CA subunits within the hexamers (Pornillos et al., 2009).

The viral capsid plays a critical role in early events in the HIV-1 life cycle. Following fusion of the HIV-1 particle with a susceptible host cell, the capsid undergoes

disassembly from the ribonucleoprotein complex in a process termed uncoating. Uncoating is a poorly understood stage in the HIV-1 life cycle. Mutagenesis studies have indicated that subunit interactions in the capsid lattice confer specific intrinsic stability to the HIV-1 capsid. Mutations at the NTD-NTD and CTD-CTD intersubunit interfaces affect capsid stability (Byeon et al., 2009; Forshey et al., 2002; Wacharapornin et al., 2007; Yang and Aiken, 2007). CA mutants with reduced capsid stability often exhibit impaired infectivity, suggesting that the intact capsid performs a critical function following penetration into the target cell. Imaging studies of HIV-1 CA mutants in target cells further provided evidence for a role of reverse transcription in facilitating uncoating, suggesting that deviations in capsid stability might affect reverse transcription (Hulme et al., 2011). Furthermore, capsid-targeting cellular restriction factors that block infection at an early phase of replication appear to act by inducing premature uncoating in target cells (Sayah et al., 2004; Stremlau et al., 2004; Stremlau et al., 2006). Mutagenesis studies have also shown that CA surfaces are important for both particle assembly and capsid formation; CA mutants that exhibit abnormal core morphology are poorly infectious (Dorfman et al., 1994; Jiang et al., 2011a; Noviello et al., 2011; von Schwedler et al., 1998; von Schwedler et al., 2003). Thus, the emerging view is that the capsid is a critical component of the virion whose structure, assembly, and disassembly require a better understanding for antiviral targeting.

The NTD-CTD interactions were initially suggested by in vitro kinetic assembly studies of full-length CA protein and truncated N-terminus and C-terminus proteins (Lanman et al., 2002). This initial suggestion was further enhanced by observations that hydrogen-deuterium (H/D) exchange on in vitro assembled CA occurred slowly at the

NTD and at the CTD regions suggesting that these regions are protected. Chemical crosslinking and high-resolution mass spectrometry in the same study showed that Lys 70 on one subunit is in proximity to Lys 182 on a different CA subunit (Lanman et al., 2003). This interface was later visualized in atomic resolution in the crystal structure of a CA hexamer (Pornillos et al., 2009). Structural and genetic studies of other retroviruses, specifically RSV and SIV (both showing second-site suppressors), also indicate the presence of an interdomain interaction in the capsid involving the NTD of one subunit and the CTD of an adjacent subunit (Bowzard et al., 2001; Cardone et al., 2009; Inagaki et al., 2010), The interface is formed by helices 4 and 7 on the NTD of one subunit and helices 8 and 11 on the CTD of the adjacent subunit (Ganser-Pornillos et al., 2007; Pornillos et al., 2009). This is consistent with the overall structural conservation exhibited by retroviral CA proteins (Ako-Adjei et al., 2005; Berthet-Colominas et al., 1999; Khorasanizadeh et al., 1999; Kingston et al., 2000; Momany et al., 1996). Although the NTD-CTD interface is present in assemblies of recombinant CA, the presence of the interface within the native viral capsid has not been established. However, using H/D exchange experiments, the NTD of CA in virus-like particles was protected but the CTD was not shown (Lanman et al., 2004).

To investigate the role of the NTD-CTD intersubunit interface in capsid assembly and stability, I used the crystal structure of the HIV-1 CA hexamer as a guide to design a panel of HIV-1 mutants encoding substitutions in the NTD-CTD interface. I confirmed via engineered disulfide crosslinking that the NTD-CTD interface exists in HIV-1 particles. Analysis of a panel of single amino acid substitution mutants for capsid

functions in vitro and ex vivo revealed that the interface is critical for HIV-1 capsid structure and stability, and for viral infectivity.

Results

Engineered cysteine substitutions at the NTD-CTD interface result in spontaneous disulfide crosslinking of CA in virion

The X-ray structure of the HIV-1 CA hexamer capsid revealed the presence of an intermolecular interface between the NTD of one CA subunit and the CTD of the adjacent subunit (Pornillos et al., 2009). To test whether the NTD-CTD interface is formed within the viral capsid lattice, I made full-length HIV-1 molecular clones encoding double Cys substitutions across the interface. Using the structural display program Pymol, I quantified distances between interface residues in the X-ray structure of the HIV-1 CA hexamer (PDB code 3H4E, Figure 2-1). Distances within ~5 Å (Cβ-Cβ) were targeted. I reasoned that if the interface is present within the viral mature capsid, adjacent subunits with mutant cysteine residues should form spontaneous disulfide crosslinks. In a previous study, our lab had successfully employed this approach to provide evidence for the existence of a CTD-CTD trimeric interface in mature HIV-1 particles (Byeon et al., 2009). I targeted a total of 5 pairs spanning the interface (Figure 2-1). The mutant viruses were produced by transfection of 293T cells with the mutant plasmids, pelleted, and analyzed for CA-CA crosslinking by non-reducing SDS-PAGE and immunoblotting. When tested on TZM-bl cells, the double Cys mutants were not infectious (data not shown). The A64C/L211C and M68C/L211C mutants did not exhibit crosslinked CA bands higher than dimers (Figure 2-2A), but the M144C/M215C mutant

exhibited dimer and trimer CA species, may be as a result of geometric constraints. Q63C/Y169A and M68C/E212C particles exhibited ladders of oligomers corresponding to dimers, trimers, tetramers, pentamers, and hexamers (Figure 2-2A). Of the mutants, M68C/E212C exhibited the greatest extent of crosslinking. Upon treatment with reducing agent, all higher CA bands of the double mutants were converted into the monomeric form (Figure 2-2B), demonstrating that the oligomeric species were stabilized by disulfide bond formation. When M68C/E212C virions were analyzed by transmission electron microscopy (TEM), the particles exhibited a variety of shapes and sizes, suggesting that these residues may be involved in the initial assembly of the immature particle. The capsids varied in size and shape, but still exhibited spherical and conical structures (data not shown).

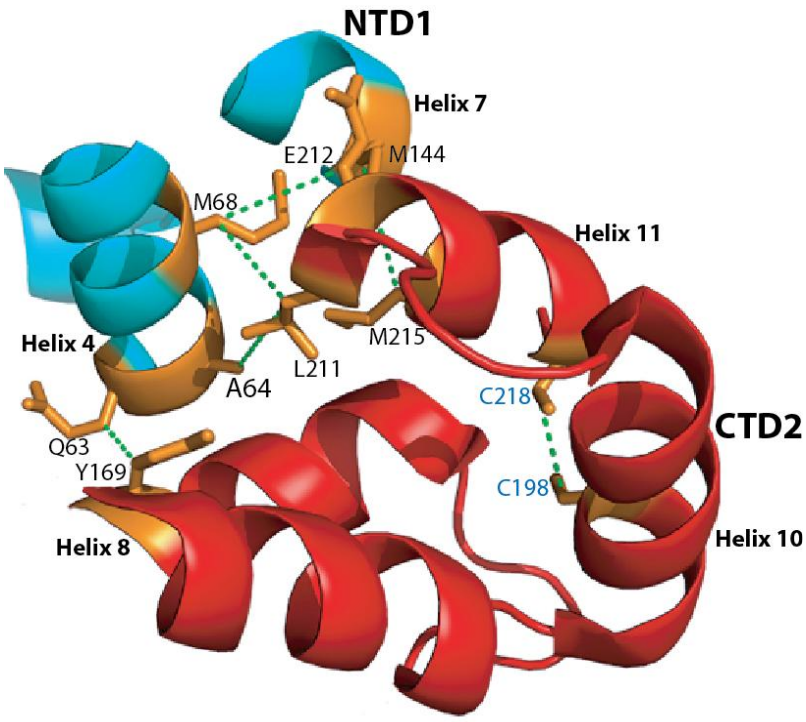

Residue (NTD1)	Residue (CTD2)	Cβ-Cβ(Å)
Q63	**Y169**	**3.6**
A64	**L211**	**7.5**
M68	**L211**	**5.2**
M68	**E212**	**5.4**
M144	**M215**	**6.5**
C198	**C218**	**4.2**

Figure 2-1: A view of the NTD-CTD interface showing an NTD (blue) from one subunit in close proximity to a CTD (red) from another subunit. The NTD helices 4 and 7 are shown in blue and the CTD helices 8 and 11 are shown in red (PDB: 3H4E). Residues mutated to cysteines for crosslinking are shown in orange and are connected by green dotted lines. The two endogenous Cys are shown for comparison. The distance, measured in angstroms, Å from a Cβ-carbon of one amino acid residue on NTD1 of one subunit to a Cβ-carbon on a second amino acid residue on CTD2 from a different subunit is shown. The Cβ-Cβ distance between endogenous cysteines is shown for comparative reasons.

Regarding the M68C/E212C mutant, analysis of virus mutants containing either individual cysteine substitution revealed that crosslinking was dependent on the presence of both substitutions (Figure 2-2C). Collectively, these data confirm that the NTD-CTD intersubunit interface is present in the hexameric unit within the capsid lattice. The formation of hexameric crosslinking within the mutant virions suggested that the NTD-CTD interface is likely to play an important role in capsid structure and function.

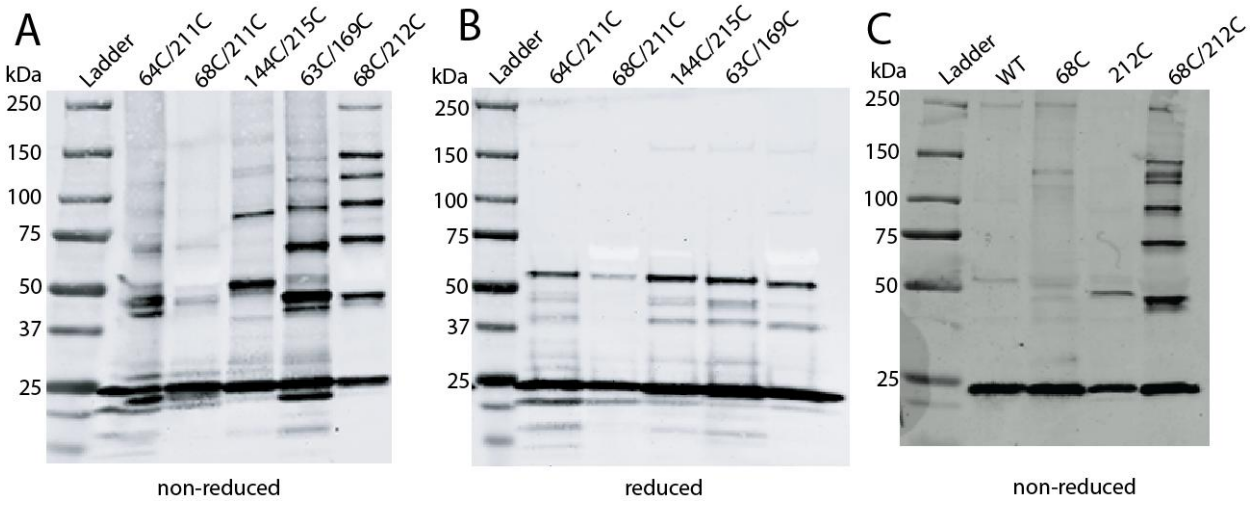

Figure 2-2: CA subunits virions with engineered cysteines at the NTD-CTD capsid interface spontaneously crosslink into hexamers in HIV-1 particles. (A, B, and C) Immunoblot analysis of viral lysate. 293T cells were transfected with mutant plasmids. The pellet was re-suspended in 1X SDS sample buffer in the absence (A) or presence (B) of β-mercaptoethanol. Samples were then separated by SDS-PAGE and analyzed by immunoblotting with CA-specific antibody. Analysis of the single mutants M68C and E212C (C), under non-reduced conditions.

NTD-CTD interface substitutions impair HIV-1 replication in T cells

To study the role of the NTD-CTD interface in HIV-1 capsid structure and function, I created a panel of HIV-1 proviruses containing single substitutions at the NTD-CTD interface. These included fourteen alanine substitutions and one aspartic acid substitution (Table 2-1). Figure 2-3A shows a view of the interface in the crystal structure, showing all residues that were mutated in this study. To characterize and evaluate the effects of the mutations on HIV-1 replication, I quantified virus accumulation in cultures of the human CEM T cell line. Cultures were inoculated with wild type and mutant viruses at low MOI, and the cultures were monitored for the accumulation of p24 or RT activity (for mutants not recognized by our ELISA primary antibody) in the culture supernatants. As expected, the wild type virus replicated efficiently in CEM cultures, peaking at day 6-9 days post-inoculation. By contrast, the Q63A, E75A and R167A mutants were markedly delayed in replication, peaking at days 18 or 15, and exhibiting peak levels lower than that of the wild type (Figure 2-3B and 2-3D). Q176A was delayed by 3 days, but reached a similar peak level as the wild type (Figure 2-3D). The Q179A mutant replicated with nearly wild-type kinetics (Figure 2-3D). However, the remaining ten mutants failed to replicate, including five NTD substitutions (H62A, A64D, M68A, E71A, K140) and five CTD mutants (R162A, V165A, D166A, E180A, M215A) (Figure 2-3C). Hence, most changes at the NTD-CTD interface resulted in severe impairments in replication in primary T cells.

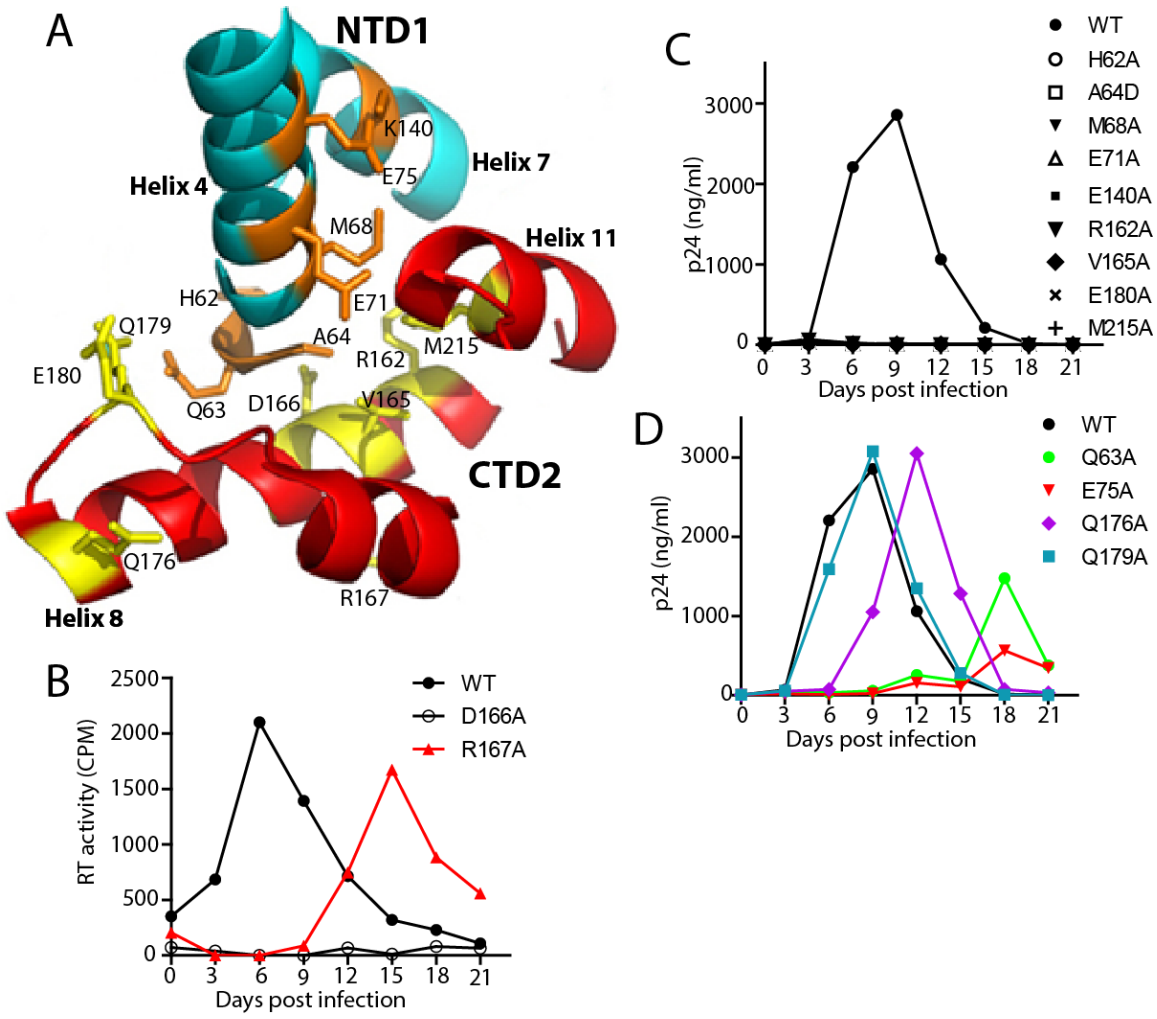

Figure 2-3: Most NTD-CTD CA interface mutants fail to replicate in CEM cells. (A) Structural view of the NTD-CTD interface showing two different subunits, NTD (blue) and CTD2 (red) and the side chains of residues targeted for mutagenesis (PDB: 3H4E). NTD side chains are shown in orange, while CTD side chains are shown in yellow. Note that NTD1 is from one subunit while CTD2 is from an adjacent subunit and the participating helices are shown. (A, B, D) CEM cells were inoculated with 5 ng of virus or a corresponding quantity based on RT units. Supernatants were sampled from the culture media after every 3 days as indicated and viral accumulation analyzed by p24 ELISA or by *in vitro* RT. The results shown are the mean of duplicate assays, (B) was independently analyzed by RT in vitro, while (C) and (D) graphs are separated for clarity.

Most changes in the NTD-CTD interface do not affect HIV-1 particle production

Substitutions in CA can inhibit particle production by perturbing lattice interfaces, altering Gag cleavage, or inhibiting protein folding or stability (Bartonova et al., 2008; Brun et al., 2008; Joshi et al., 2006; Scholz et al., 2005). To assess the effects of NTD-CTD interface substitutions on particle production, I transfected 293T cells and determined the quantity of viral proteins released into culture supernatants by RT activity assays. In most cases, particle production was similar to that of the wild type, except for H62A and K140A, which exhibited reduced particle production (Figure 2-4A), a phenotype that was not due to expression levels of Gag in the producer cells (data not shown). To determine whether Gag processing was altered by the mutations, I pelleted the viral particles and analyzed the viral proteins by SDS-PAGE and immunoblotting with a CA-specific antibody. Most of the mutants exhibited a normal banding pattern, suggesting that the observed replication defects were not caused by aberrant processing of Gag precursors. Exceptions were the H62A, K140A and M215A mutants, which exhibited additional CA-reactive bands at ≤23kD (Fig 2-4B). The precise source of these bands was not determined. Conceivably, these three mutations might have altered the tertiary and quaternary structure of the CA protein, such that sites not normally cleaved by proteases became exposed to enzyme activity resulting in non-canonical cleavage. Because proteolytic processing of Gag is initiated during HIV-1 particle assembly, the aberrant cleavage could also contribute to the impaired particle production observed for the H62A and K140A mutants (Figure 2-4A).

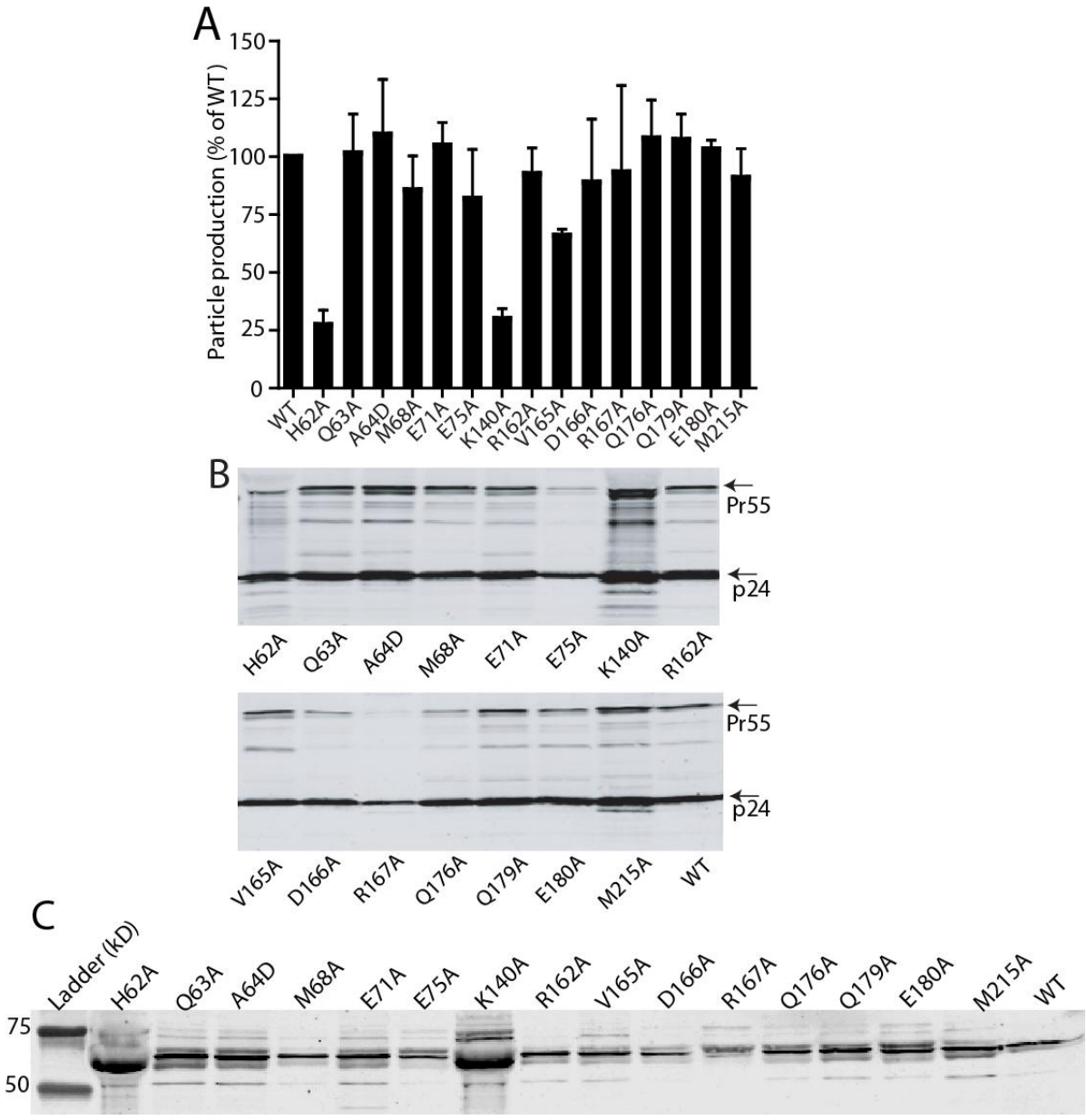

Figure 2-4: Particle production and Gag processing of HIV-1 CA NTD-CTD mutants. (A) Particle production of viral particles as measured by RT assay. (B and C) Immunoblot analysis of viral lysate. Virions were collected from transfected 293T cells, pelleted, and analyzed by SDS-PAGE and immunoblotting with a CA specific polyclonal antibody (A), or RT antibody (C).

To determine the consequences of NTD-CTD interface mutations on virus infectivity, I titrated the particles on TZM-bl indicator cells. Cells were lysed and quantified for luciferase activity, which was normalized by the input levels of RT activity in the inocula. A majority of mutants including Q63A, E71A, E75A, R167A, Q176A, E180A exhibited moderate-to-severe reductions (~10-30% of WT) in infectivity (Figure 2-5A). Infectivity was virtually abolished (<2% of WT) by the mutations H62A, A64D, M68A, K140A, V165A, D166A, M215A, while the infectivity of the Q179A mutant was similar to that of the wild type. These results suggest that the impaired replication by the mutant viruses is due to an early event in the viral life cycle, since viral production after transfection was unaffected, except for the two aforementioned mutants (H62A and K140A).

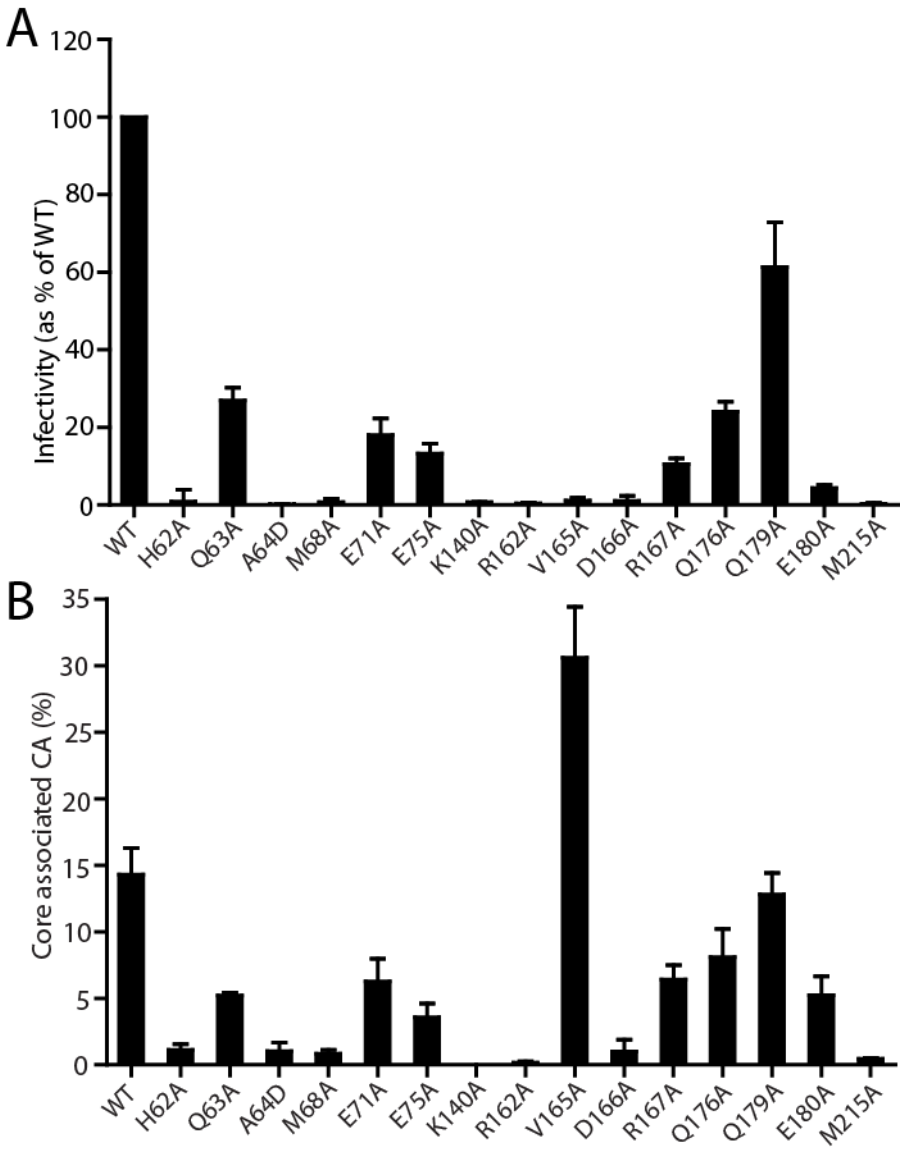

Figure 2-5: Mutations at the NTD-CTD intersubunit interface impair HIV-1 infectivity and alter capsid stability. (A) Single-cycle infectivity of the mutant virions. Virion stocks were titrated in TZM-bl reporter cells and the extent of infection was determined by quantification of luciferase reporter activity in cell lysates. Values were normalized by the corresponding values of reverse transcriptase activity in the inocula. Hence, infectivity units are RLU/RT. Results shown are the mean values of three independent experiments, where error bars represent 1 standard deviation. (B) Quantification of core-associated CA. Cores from the concentrated virions were purified, and the levels of the core-associated CA were quantified as a percentage of total virion-associated CA. The values shown are the means of three independent experiments and the error bars represent 1 standard deviation.

Point mutations at the NTD-CTD interface alter the level of CA associated with purified HIV-1 cores

The HIV-1 capsid is a metastable structure, and mutations in CA that alter the intrinsic stability of the capsid are generally deleterious to infectivity (Byeon et al., 2009; Forshey et al., 2002; Yang and Aiken, 2007). The X-ray crystal structure of the CA hexamer suggested that NTD-CTD intersubunit interactions likely contribute to capsid lattice stability (Pornillos et al., 2009). To test this hypothesis, I purified viral cores from the mutant particles and quantified the percentage of CA cosedimenting with the cores. For the wild type, a mean value of 14.3% was obtained from three independent experiments. This value is consistent with previous reports (Byeon et al., 2009; Forshey et al., 2005; Shah and Aiken, 2011a; Shi et al., 2011; Yang and Aiken, 2007; Yang et al., 2012). By contrast, a majority of the NTD-CTD interface mutants exhibited levels of core-associated CA lower than that of the wild type (Figure 2-5B). Based on these results, I have categorized the mutants as follows: hyperstable (V165A); moderately reduced stability (Q63A, E71A, E75A, R167A, Q176A, E180) and highly unstable (H62A, A64D, M68A, K140A, R162A, D166A, M215A) (Table 2-1). Importantly, the alterations in core-associated CA were correlated with the impaired infectivity for the mutant viruses (Figure 2-5A).

Cores from a subset of NTD-CTD interface mutants exhibit altered rates of uncoating in vitro

To further analyze the capsid stability of the mutants, I quantified the uncoating of cores purified from the Q63A, E71A, E75A, V165A, R167A, Q176A, Q179A, and E180A mutants. Samples of purified cores were diluted into 1X STE buffer and

incubated at 37°C for various time periods, after which the cores were pelleted and the extent of uncoating determined by quantifying the CA present in the supernatant and pellet. I observed altered rates of uncoating for a subset of the mutants. Cores from the Q63A, E75A, R167A and E180A mutants uncoated more rapidly than the wild type, while E71A, Q176A and Q179A cores uncoated with kinetics similar to the wild type (Figure 2-6D). By contrast, V165A cores uncoated more slowly than the wild type (Figure 2-6A), in concordance with the elevated level of core-associated CA exhibited by this mutant (Figure 2-5B).

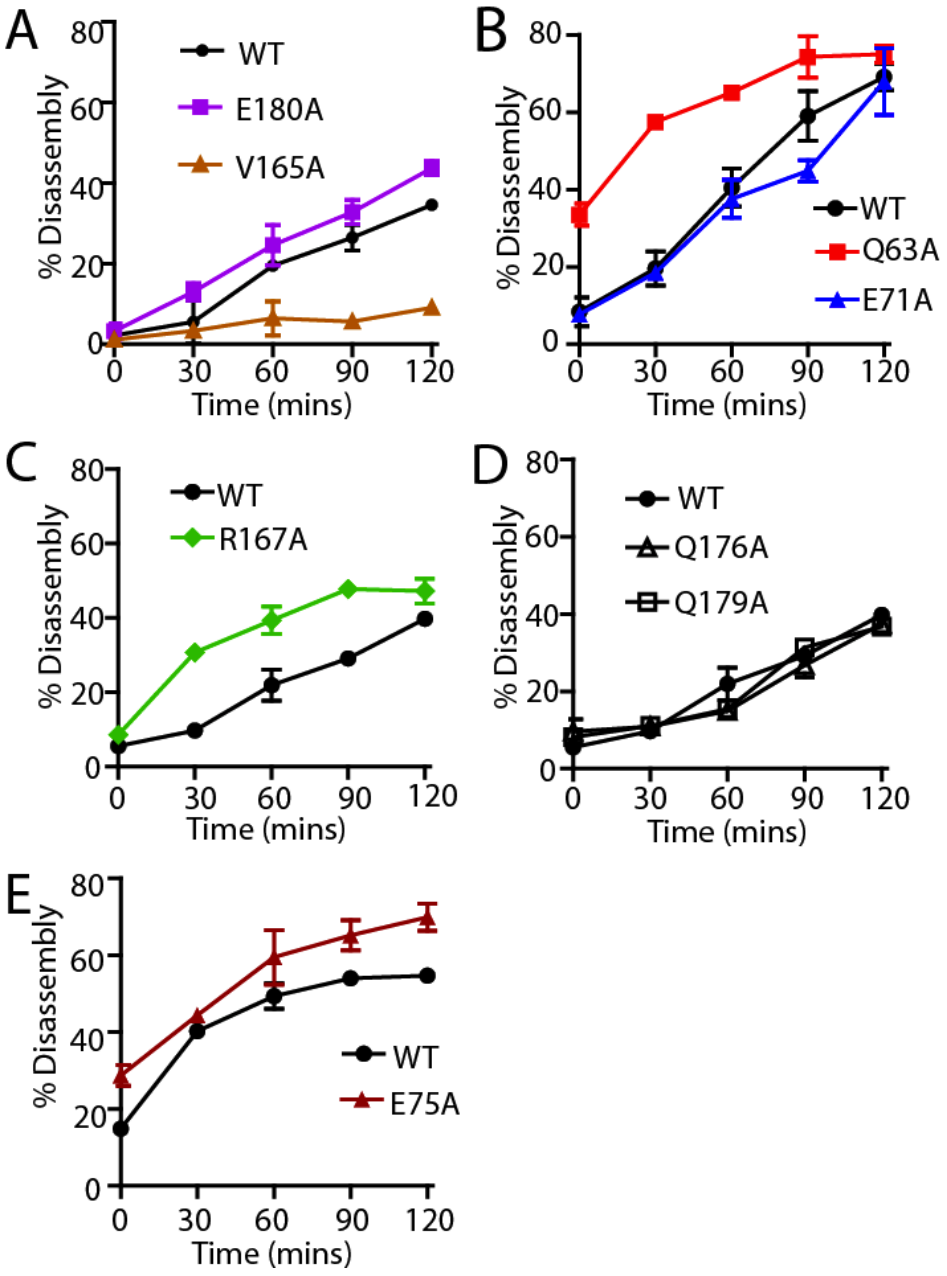

Figure 2-6: NTD-CTD CA mutant cores undergo accelerated uncoating *in vitro.* Purified HIV-1 cores were diluted in STE buffer and incubated at 37˚C for the indicated times. After pelleting the particles, the extent of uncoating was determined by quantifying CA levels in the pellets and supernatants. Shown here are the mean values of duplicate determinations with error bars representing the range of values. The results are representative of at least two independent experiments.

Based on the collective results shown in Figure 2-5B and Figure 2-6, I conclude that a majority of mutations in the NTD-CTD interface destabilize the viral capsid, while the V165A renders the capsid hyperstable (summarized in Table 2-1).

NTD-CTD interface mutants exhibiting highly unstable capsids are impaired for abrogation of restriction by TRIMCyp

TRIM5 host restriction factors inhibit retrovirus infection by inducing premature uncoating in target cells (Diaz-Griffero et al., 2007a; Diaz-Griffero et al., 2007b; Diaz-Griffero et al., 2006; Stremlau et al., 2006). Restriction by these factors is saturable and can be overcome *in trans* by virus-like particles. Our lab had shown that saturation of restriction is dependent on the stability of the HIV-1 capsid (Forshey et al., 2005; Shi and Aiken, 2006). Thus, the ability of HIV-1 particles to enhance infection of an HIV-GFP reporter virus *in trans* can be a useful probe of HIV-1 uncoating in target cells. To probe the stability of the NTD-CTD interface mutants *in vivo*, I quantified the ability of mutant virions to enhance infection by an HIV-1 reporter virus in OMK cells, which endogenously express TRIMCyp. CA mutants with moderately reduced capsid stability (Q63A, E71A, E75A, R167A, E180A, Q176A, Q179A), as well as the hyperstable mutant V165A, enhanced infection of HIV-GFP virus *in trans* (Figure 2-7A and 2-7B). By contrast, mutants with highly unstable capsids (H62A, A64D, M68A, K140A, R162A, D166A and M215A) were markedly impaired in their ability to overcome restriction by TRIMCyp (Figure 2-7C). These results suggested that the NTD-CTD mutants with unstable capsids undergo premature uncoating in target cells.

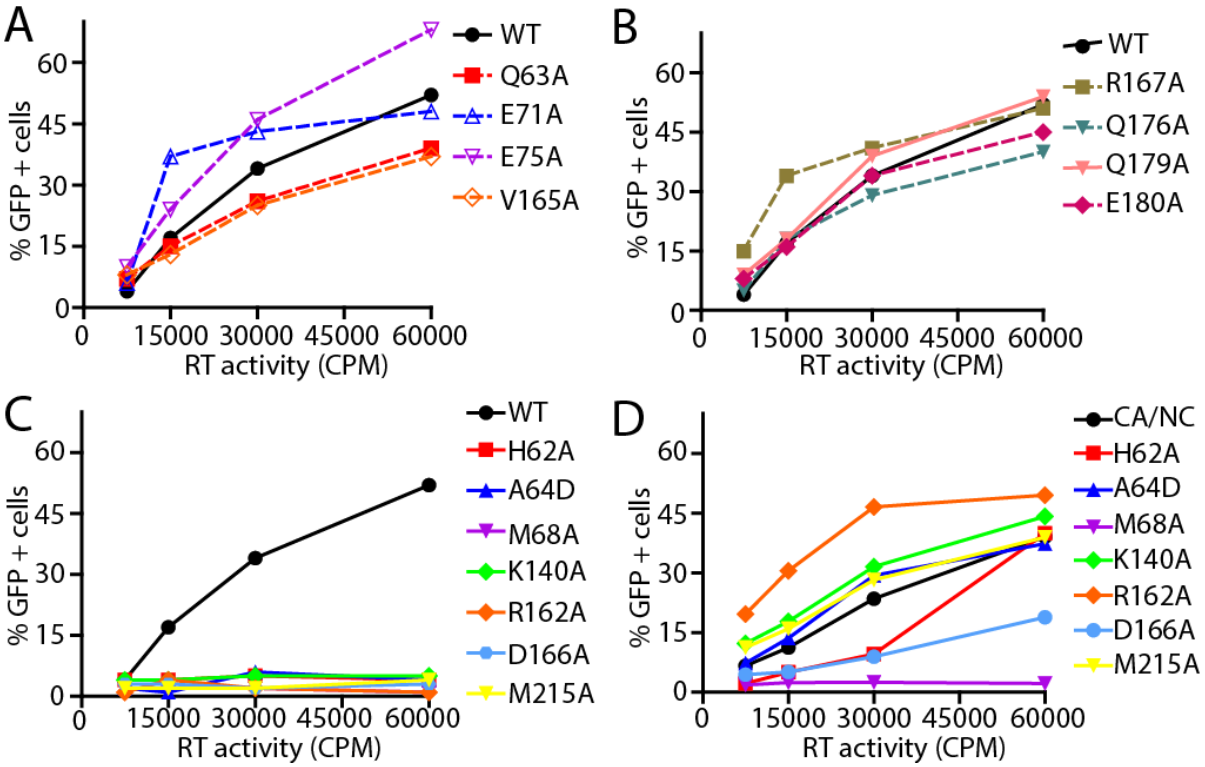

Figure 2-7: NTD-CTD CA mutants with unstable cores fail to abrogate restriction by TrimCyp. OMK cells were co-inoculated with fixed amount (5 ng) of HIV-GFP and the indicated quantities of CA mutant viruses in RT units. (A) and (B) are separated for clarity, while (C) and (D) show restrictive ability in WT background and CA/NC cleavage mutant background respectively. The results are the average of duplicate determinations and a representative of two independent experiments.

Mutations in CA can compromise the ability of the virus to engage TRIMCyp either directly by altering recognition, or indirectly by inducing premature uncoating. Our lab previously demonstrated that the addition of mutations preventing cleavage between CA and NC can rescue the ability of mutants with unstable capsids to overcome restriction, most likely by stabilizing the capsid (Forshey et al., 2005; Shi and Aiken, 2006). Although it seems unlikely that NTD-CTD interface substitutions would directly alter recognition by TRIMCyp, which binds to an exposed CA loop on the outer surface of the capsid, I nonetheless analyzed mutants containing both the NTD-CTD substitutions together with the CA-NC cleavage site mutants. In this context, all of the unstable mutants except M68A enhanced infection by HIV-1 GFP (Figure 2-7D). Thus for the majority of the unstable mutants, the failure to abrogate restriction in OMK cells can be attributed to the instability of their capsids and not to a direct effect on the CA substitutions on recognition by TRIMCyp. These data support the conclusion that NTD-CTD interface residues contribute to proper uncoating in target cells.

Mutations in the NTD-CTD interface impair HIV-1 reverse transcription in target cells

The majority of the NTD-CTD interface mutants released normal quantities of particles that were poorly infectious, indicative of an early post-entry defect. Previous studies from our laboratory and others have shown that capsid-destabilizing mutations are often associated with impairments in reverse transcription (Forshey et al., 2002; Jiang et al., 2011a; Leschonsky et al., 2007). Therefore, I employed stage-specific PCR to quantify the ability of the NTD-CTD capsid mutants to undergo reverse transcription in target cells. The mutants exhibiting altered capsid stability displayed markedly reduced

accumulation of late reverse transcripts *in vivo* (Figure 2-8). Additional experiments revealed that the mutants also produced reduced levels of early products (full-length minus strand; data not shown). My results show that the reduced infectivity of the NTD-CTD interface mutants is associated with impaired reverse transcription. Reverse transcription appeared to be correlated with capsid stability, as partially unstable CA mutants accumulated less DNA compared to WT, and no DNA products were detected for highly unstable mutants (Figure 2-8). Interestingly, the hyperstable mutant V165A was also impaired for reverse transcription in target cells.

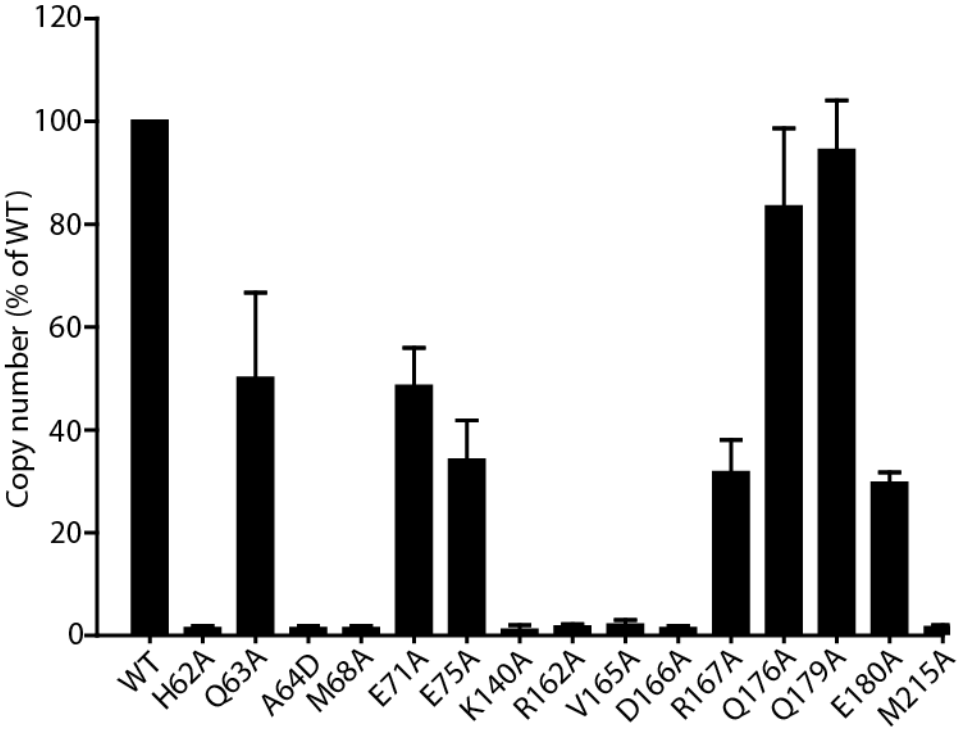

Figure 2-8: NTD-CTD CA mutants with altered capsid stability are impaired in reverse transcription in target cells. HeLa P4 cells were inoculated with equal quantities (100 ng of p24) of WT or mutant viruses. Cultures were harvested 8 hrs after infection and DNA isolated for second-strand transfer quantification by real-time PCR using the SYBR green method. Error bars represent the standard deviations from three independent experiments.

To determine whether the decrease in reverse transcription of the CA mutants in target cells is due to a decrease in virion-associated RT activity, I assayed virus stocks for exogenous RT activity and for CA antigen in parallel. The results of the two assays were concordant, indicating that the CA substitutions did not affect the levels of active RT enzyme within the particles (Figure 2-4C).

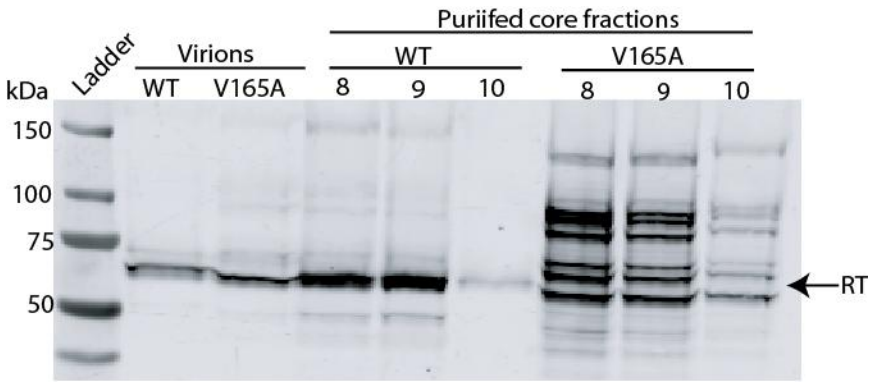

Figure 2-9. Immunoblot analysis of cores isolated from WT and V165A. Cores from the concentrated virions were purified, and fractions containing cores were biochemically analyzed by SDS-PAGE and immunoblotting using an RT specific antibody.

Ultrastructural analysis of NTD-CTD mutant virions

To examine potential effects of the NTD-CTD interface substitutions on capsid structure, we performed ultra-thin section transmission electron microscopic (TEM) analysis of WT and mutant virions produced from transfected HeLa cells. Particles associated with cells transfected with the wild type HIV-1 proviral construct exhibited various stages of morphogenesis, including budding particles and immature and mature particles, with mature particles exhibiting conical and spherical capsids near the cell surface, depending on the plane of sectioning (Figure 2-10). The conical and spherical capsids also contained an electron-dense nucleoid typical of the HIV-1 ribonucleoprotein complex.

Immature particles were apparent in both the wild type and CA mutants, but occurred at a slightly higher frequency for the mutants. Analysis of size of the particles demonstrated that most of the mutations did not alter the diameter of the particles, with three exceptions (Figure 2-11). Statistical analysis of the results indicated that E75a, K140A, and V165A each exhibited slightly elevated virion diameters compared to wild type. The E75A mutation was previously associated with altered particle size, as the double mutant E75A/E76A exhibited enlarged particles (von Schwedler et al., 2003)

With respect to capsid morphology, cones and tubes were also apparent in six of the mutants (Q63A, E75A, R162A, Q167A, Q176A, and Q179A) (Figure 2-10). However, seven of the mutants (H62A, A64D, M68A, K140A, D166A, E180A, and M215A) lacked the conical morphology of the wild type (Figure 2-10), but retained the electron core-like internal structures without clear conical capsids. V165A mutant particles appeared pleomorphic with the internal capsid exhibiting spheres and cones

varying greatly in size and shape. Overall, the effects of the mutations on capsid morphology suggest that residues at the NTD-CTD interface are important for proper capsid structure as well as stability.

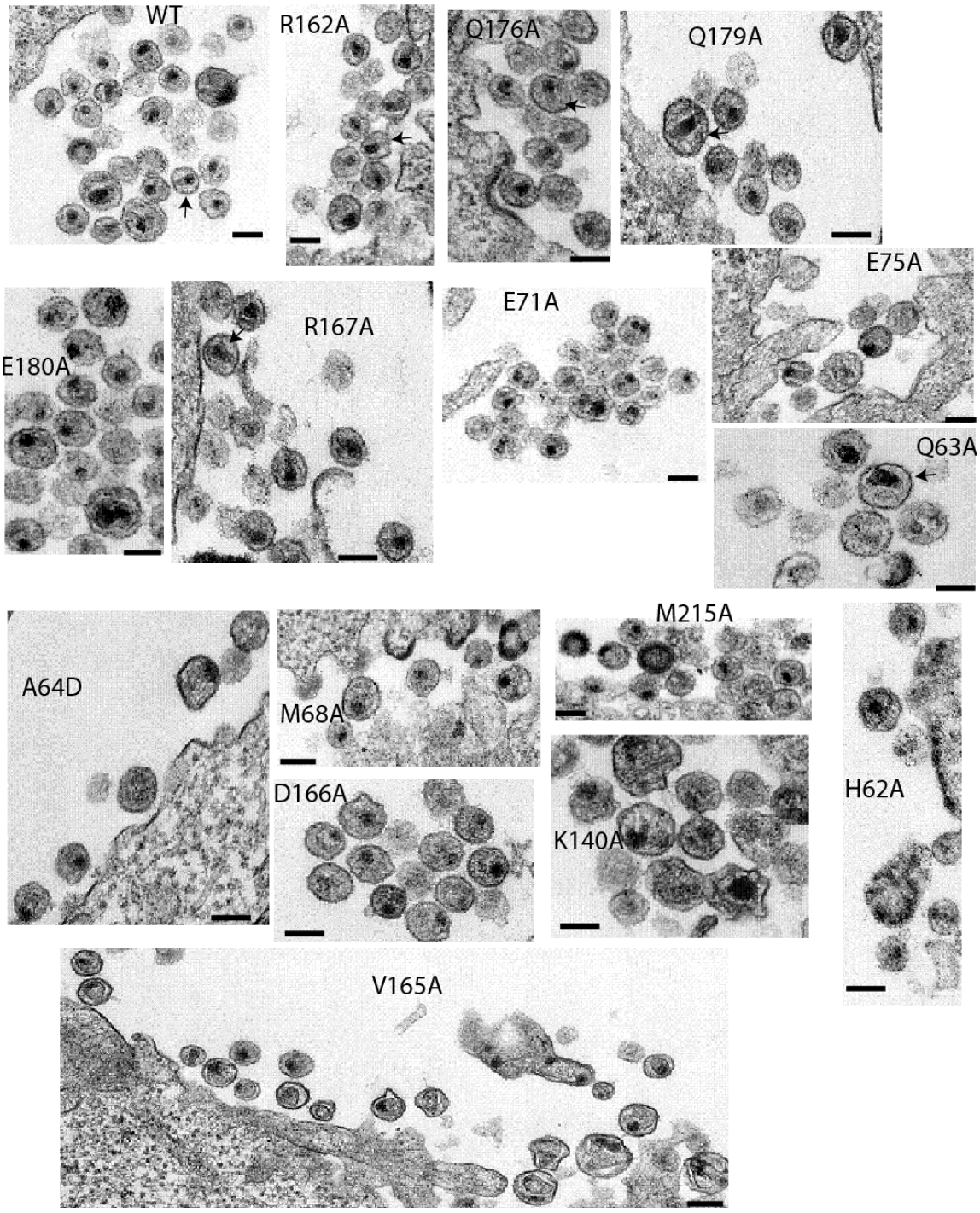

Figure 2-10. Electron microscopy of NTD-CTD interface mutants. HeLa cells were transfected with R9 plasmids containing either WT or specified mutations. 24 hr post transfection, the cells were fixed in buffer containing 2.5% glutaraldehyde. Following embedding and staining, ultrathin sections were then examined in a FEI Tecnai Spirit Twin transmission electron microscope. The scale bars are 100 nm.

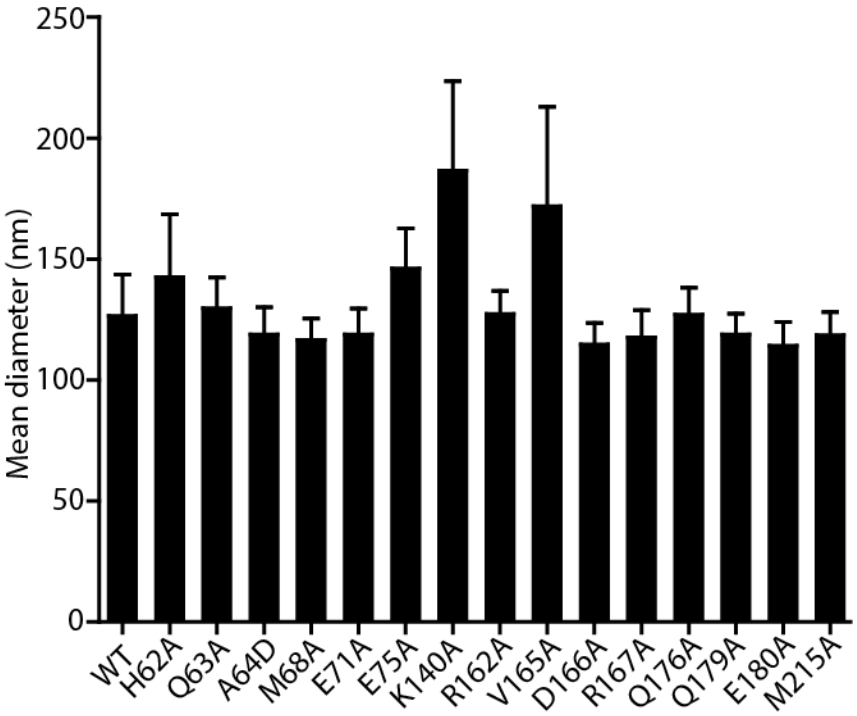

Figure 2-11. Effects of NTD-CTD interface substitutions on HIV-1 particle size. The diameter of HIV-1 particles was quantified. Shown are the mean values, with error bars represent one standard deviation.

Discussion

Our previous studies identified mutations in the NTD and CTD that are critical for HIV-1 capsid stability (Forshey and Aiken, 2003; Yang and Aiken, 2007). At the time of those studies, the positions of the mutations on the hexamer were not known, as the high-resolution structure of the hexamer had not yet been reported. Subsequent studies showed that several of the NTD substitutions that perturbed capsid stability (P38A, E45A, T54A) were located at the NTD-NTD interface (Pornillos et al., 2009), while some of the CTD substitutions (K203A, Q219A) were present at the 3-fold CTD-CTD interhexameric interface (Byeon et al., 2009). In this Chapter, I focused on the role of the NTD-CTD intersubunit interface in HIV-1 capsid structure and function.

High-resolution structural studies provided the foundation for this investigation. The CA hexamer structure suggested that the NTD-CTD interface is likely to be important for either capsid assembly or stability. Previous structural and biochemical studies of HIV-1 and other retroviral capsids demonstrated that this interface is present in the capsid lattice formed by assembly of CA in vitro (Bowzard et al., 2001; Cardone et al., 2009; Ganser-Pornillos et al., 2007; Inagaki et al., 2010; Lanman et al., 2003; Lanman et al., 2004; Lanman et al., 2002; Pornillos et al., 2009). However, the role of the NTD-CTD interface in the virion and its contribution to capsid function had not been demonstrated.

My engineered disulfide crosslinking data confirms that the NTD-CTD interface is a component of the native HIV-1 capsid lattice. Crosslinking between Cys residues at positions 68 and 212 resulted in the formation of monomer, dimer, trimer, tetramer, pentamer and hexamer bands. Lack of crosslinked CA species in the single mutants

(M68C and E212C) showed that the banding results from disulfide bonding between the engineered cysteines (Figure 2-3A). Further evidence for the NTD-CTD hexameric interface was also provided by Q63C/Y169C, A64C/L211C, M144C/M215C and M68C/L211C crosslinked mutants although with reduced efficiencies (Figure 2-3B), which did not improve upon chemical oxidation with Copper o-phenanthroline. Engineered crosslinking provides an experimental probe for the formation of an NTD-CTD interface in mutant virions. In collaboration with Dr. Peijun Zhang's group, I employed this approach to study the formation of different capsid interfaces during maturation and it may also prove useful for studying the effects of small molecules on capsid assembly and structure (Meng et al., 2012).

I also observed that amino acid substitutions at the NTD-CTD interface affect capsid assembly. Three of the mutants (A64D, M68A, and D166A) exhibited normal Gag processing, and produced particles at wild type levels. However, the virions had significant reductions in the number of conical capsids (Figure 2-9, Table 2-1). D166 is an interdomain helix-capping amino acid, whose interactions with helix 4 of an adjacent subunit provides an amino terminal capping for the NTD-CTD interaction (Pornillos et al., 2009). Other substitutions at the interface, including H62A, K140A and M215A, also perturbed capsid structure. However, these three substitutions led to altered processing of Gag, suggesting that the changes may affect capsid structure through maturation defects. A previous study of H62A had also reported that this mutant is impaired for HIV-1 capsid assembly (Noviello et al., 2011). H62 occupies the hydrophobic core of the NTD-CTD interface forming stacking interactions with F32 and Y145 (Ganser-Pornillos et al., 2007; Pornillos et al., 2009). The phenotype of the H62A mutant is also reminiscent of

the effects of CAP-1, a small molecule capsid assembly inhibitor that binds the NTD pocket and disrupts the packing of the Phe32 and Tyr145 aromatic side chains (Kelly et al., 2007; Pornillos et al., 2009). K140 and M215 lie in close proximity to the helix-capping amino acids R143 and Q219, respectively (Pornillos et al., 2009). Their proximity to helix-capping amino acids suggest that substitutions at these positions may alter contacts at the NTD-CTD interface and perturb capsid assembly. Previous work from another group had shown that the NTD-CTD interface substitutions Y169A and L211A also induced severe Gag processing defects (Bartonova et al., 2008).

A major finding from this work is that substitutions at the NTD-CTD interface alter capsid stability (Table 1). Most of the substitutions at the NTD-CTD interface produced virions with unstable capsids, all of which were poorly infectious. The mutations that destabilized the capsid *in vitro* also resulted in accelerated uncoating in target cells, as indicated by the reduced ability of the mutant particles to abrogate restriction by TRIMCyp. The in vitro disassembly data matches our in vivo abrogation of restriction assay. However, Q63A, R167A, and E180A undergo rapid uncoating in vitro, but these mutants abrogate restriction with wild type efficiency. Our understanding of abrogation is limited, however we have shown that second-site suppressor mutation to P38A, fixes the abrogation of this mutant but not its stability in vitro (Yang et al., 2012). Q179A had no apparent effect on capsid stability or viral infectivity. Structurally, Q179 is located at the end of helix 8 and is near N57, Q63 and M66. While it is not clear why the Q179A substitution had no deleterious effect, vs. the other mutations studied, the position of this side chain near the edge of the interface could be a factor.

The R162A mutant exhibited cores with conical capsids that were unstable (Figure 2-5B and Figure 2-7C). The mutant was impaired for reverse transcription in target cells (Figure 2-8) and was poorly infectious. Thus, I attribute the phenotype of this mutant to a capsid stability defect. Structurally, R162 is near the π-stack formed by Y145, H62 and F32; the R162 guanidinium group is thought to stabilize the stacking of these aromatic side chains (Pornillos et al., 2009). It is plausible that the substitution of alanine at this position changes the juxtaposition of the Y145 and F32 side chains at the NTD-CTD interface, thus altering the structure at the interface and rendering the capsid unstable.

In a previous study, I observed that a CA mutant with hyperstable capsid was functional for reverse transcription in target cells (Yang et al., 2012). Thus, I was surprised to observe that the V165A mutant, which exhibited hyperstable capsids, was impaired for reverse transcription in target cells, like the unstable mutants (Figure 2-8). Preliminary analysis of the cores purified from V165A by immunoblotting revealed that the mutant cores are enriched in unprocessed Gag and Gag-Pol (Figure 2-9). I speculate that the presence of these intermediates prevented reverse transcription by interfering with the activity of the processed RT or by perturbing capsid structure.

Virus	Mutation Location	Single-cycle infectivity (% of WT ±SD)	Replication in CEM cells[@]	% of mature cores[#]	Presence of cones/ tubes	% core-associated CA (±SD)	Disassembly in vitro	Abro-gation of restriction	Reverse transcription in cells (% of WT±SD)
WT	-	100	+++	50	+	14±2	Normal	Yes	100
H62A	Helix 4	1.0±0.3	-	10	-	1.1±0.4	ND	No	1.3±0.5
Q63A	Helix 4	27±3	+	15	+	5.2±0.2	Accelerated	Yes	50±14
A64D	Helix 4	0±0.1	-	35	-	1±0.6	ND	No	1.3±0.5
M68A	Helix 4	1.0±1	-	10	-	0.8±0.3	ND	No	1.3±0.5
E71A	Helix 4	18±4	-	20	+	6.3±2	Normal	Yes	49±6.2
E75A	Helix 4	13±3	+	20	+	3.6±1	Accelerated	Yes	34±6.2
K140A	Helix 7	1.0±0	-	20	-	0±0	ND	No	1.0±0.8
R162A	Helix 8	0±0.2	-	35	+	0.2±0.1	ND	No	1.7±0.5
V165A	Helix 8	1.0±1	-	25	a	31±4	Slowed	Yes	2.0±0.8
D166A	Helix 8	1.0±1	-	35	-	1±0.1	ND	No	1.3±0.5
R167A	Helix 8	11±2	+	35	+	6.4±1.1	Accelerated	No	32±5.2
Q176A	Helix 8	25±3	++	30	+	8.1±2	Normal	Yes	83±13
Q179A	Helix 8	62±12	+++	35	+	13±2	Normal	Yes	94±7.9
E180A	Helix 8	4±1	-	20	-	5.1±1.4	Normal	Yes	30±1.7
M215A	Helix 11	0±0.3	-	20	-	0.5±0.1	ND	No	1.5±0.5

Table 2-1: Summary of viral mutant phenotypes at the NTD-CTD interface.
[@] +++, replicates like wild type; ++, 3 days delayed; +, 15-18 days delayed; -, no replication within 30 days.
[#] mature cores exhibit an electron-dense core region, which is either bar-shaped, conical or spherical.
ND; not determined.
a; conical but aberrant cores

My results highlight the NTD-CTD intersubunit interface as a potentially attractive target for therapeutic intervention. Recently, small molecule inhibitors targeting HIV-1 CA have been identified (Blair et al., 2010; Kortagere et al., 2012; Lemke et al., 2012; Tang et al., 2003). One of these, PF-3450074 (PF74), binds to the NTD in the region of the NTD-CTD interface and destabilizes the capsid (Blair et al., 2010; Shi et al., 2011). Substitutions in the interface can lead to resistance by blocking the binding of PF74 (Shi et al., 2011), but these mutations may also result in reductions in viral fitness. Another small molecule, CAP-1, has been shown to alter subunit interactions at the NTD-CTD interface (Kelly et al., 2007; Pornillos et al., 2009; Tang et al., 2003). Our finding that many NTD-CTD interface mutants exhibit impaired replication suggests that inhibitors targeting this interface may exhibit a high barrier to emergence of resistance. Further efforts to design capsid-targeting HIV-1 inhibitors will benefit from a thorough understanding of the structure and function of the viral capsid.

CHAPTER III

GENETIC VALIDATION OF THE CRYOEM STRUCTURE OF THE HIV-1 CAPSID ASSEMBLY

Introduction

The X-ray crystal structure of HIV-1 CA hexamer has been determined from flattened sheets with the aid of stabilization and destabilization techniques of the hexamer. This provided details for intermolecular interfaces present in the capsid (Pornillos et al., 2009; Pornillos et al., 2011). While the X-ray structure is flat, the native HIV-1 capsid is curved with the architecture of a fullerene cone (Ganser et al., 1999; Li et al., 2000). This means that the X-ray crystal structure does not provide detailed atomic structural information on interhexamer interfaces. Thus, it remains unclear how the CA assembly machinery accommodates lattice curvature through intersubunit interactions at the interfaces. Byeon et al., in 2009, using cryoEM, determined a structure of the CA tube at16 Å resolution (Byeon et al., 2009). This resolution is not high enough to visualize secondary structural elements of the capsid, and so accurate and reliable atomic modeling of capsid assembly was not possible. In this present study, in collaboration with Peijun from Pittsburgh, we determined the structures of the mature HIV-1 capsid assembly at 9 Å resolution using cryoEM. My studies as described in this Chapter, employed crosslinking and single amino acid mutagenesis techniques to test the structural model of the 9 Å resolution structure of the HIV-1 CA tube from our collaborators, and validate it for HIV-1 capsid structure and stability. Our approached engineered Cys residues at the predicted interface and assessed for proximity by analyzing for disulfide linkage and

dimer formation. We also analyzed a panel of mutants at the interface for structural alterations and stability. This study provides new structural details for capsid assembly and genetic evidence of the structure determined by cryoEM. It also pinpoints the importance of the new hydrophobic interactions at the center of the three-fold interface. These residues are critically important for capsid assembly and stability, and for viral infectivity.

Results

CryoEM reconstruction of HIV-1 CA tubular assembly at 9 Å resolution

HIV-1 CA spontaneously assembles in vitro into tubes and/or cones that resemble authentic viral capsids (Li et al., 2000), from which structural investigation of CA assembly, using cryoEM, can be made. Using a novel rapid back-dilution method to instantaneously reduce salt concentrations and free protein concentration during preparation of frozen-hydrated specimens, our collaborators at the University of Pittsburgh, under the leadership of Dr. Peijun Zhang prepared cryoEM samples that diffracted to 10 Å from and the structure of the CA tubular assembly was determined at 9 Å (Figure 3-1A, B and C). Atomic modeling of the sub-nanometer resolution density map was completed using high resolution structures (3h47 of CA-NTD(Pornillos et al., 2009) and 2kod for CA-CTD(Byeon et al., 2009)) (Figure 3-1C). The linker region was built using homology modeling of applied molecular dynamics of flexible fitting (MDFF). In the cryoEM structure, the hexameric arrangement revealed similarity to the X-ray crystal structure of crosslinked hexameric CA (Figure 3-1C). However, distinct CTD dimer

conformations were present in the assembled helical tubes with varying dimerization helix 9 crossing angles ranging from 71 degrees to 95 degrees (Figure 3-1E), confirming an earlier suggestion that the CTD interface is plastic (Byeon et al., 2012). The angular variability at the CTD led us to posit that curvature in the capsid assembly is provided by CTD orientations and intrinsic flexibility, but with fixed principal hydrophobic contacts at W184 and M185. Mutating any of these residues leads to impairment in particle assembly (Gamble et al., 1997). From the cryoEM structure, new and important structural details at the three-fold trimer interface were revealed. The trimer interface revealed a highly conserved patch of hydrophobic residues with A204 and I201 at the center of the hydrophobic core, flanked by L205 all situated on one face of Helix 10 (Figure 3-2). The entire hydrophobic core is itself surrounded by a belt of polar K203 and E213 residues of opposite charges that frame the hydrophobic core (Figure 3-2). The alanine mutants of K203 and E213 were previously shown to be critically important for HIV-1 capsid stability and infectivity; mutations K203A destabilized and E213A stabilized the capsid lattice (Byeon et al., 2009; Forshey et al., 2002).

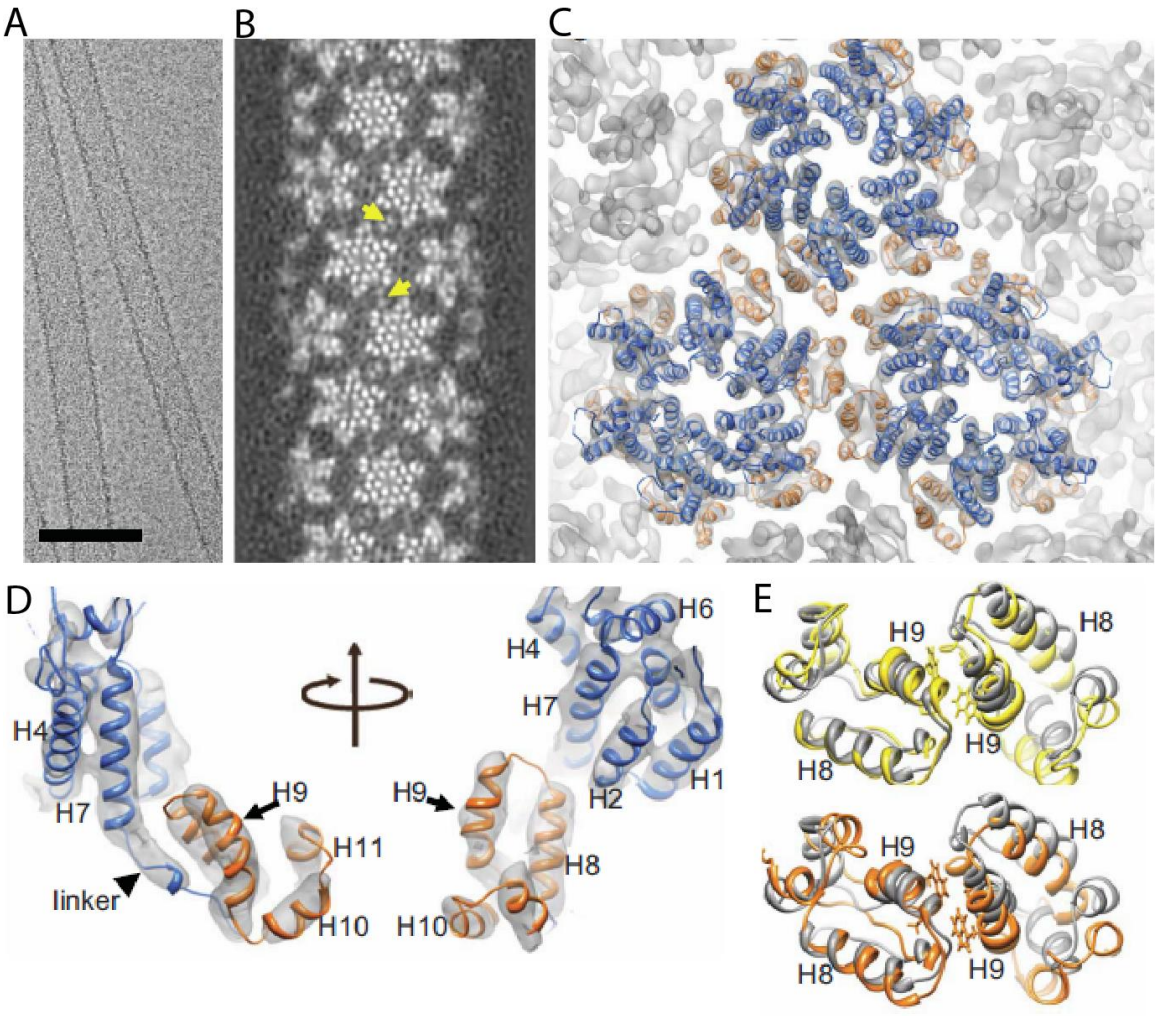

Figure 3-1. CryoEM reconstruction of a HIV-1 CA tubular assembly at 9 Å resolution and Molecular Dynamics Flexible Fitting (MDFF). (A) CryoEM image of recombinant A92E CA tubular assembly. (B) Electron density map of the A92E CA tube with (-12, 11) helical symmetry. Pairs of helices H9, located between adjacent hexamers, are indicated by yellow arrows. (C) All-atom MDFF model of HIV-1 capsid assembly, superimposed with the electron density map contoured at 4.0σ. Three CA hexamers are shown with NTDs and CTDs colored in blue and orange, respectively. (D) Superposition of the density map and the MDFF model of a CA molecule viewed from two different angles. Individual α-helices are labeled. Arrows point to the kinked helix H9 and the arrowhead points to the linker and the 310 helix. (E) Two CTD dimer structures along -1 (orange) and 11 (yellow) helical directions, superimposed with the NMR solution dimer structure (gray, 2kod). Two hydrophobic residues at the interface, W184 and M185, are shown in ball and stick representation. Figure provided by Dr. Peijun Zhang and used with permission.

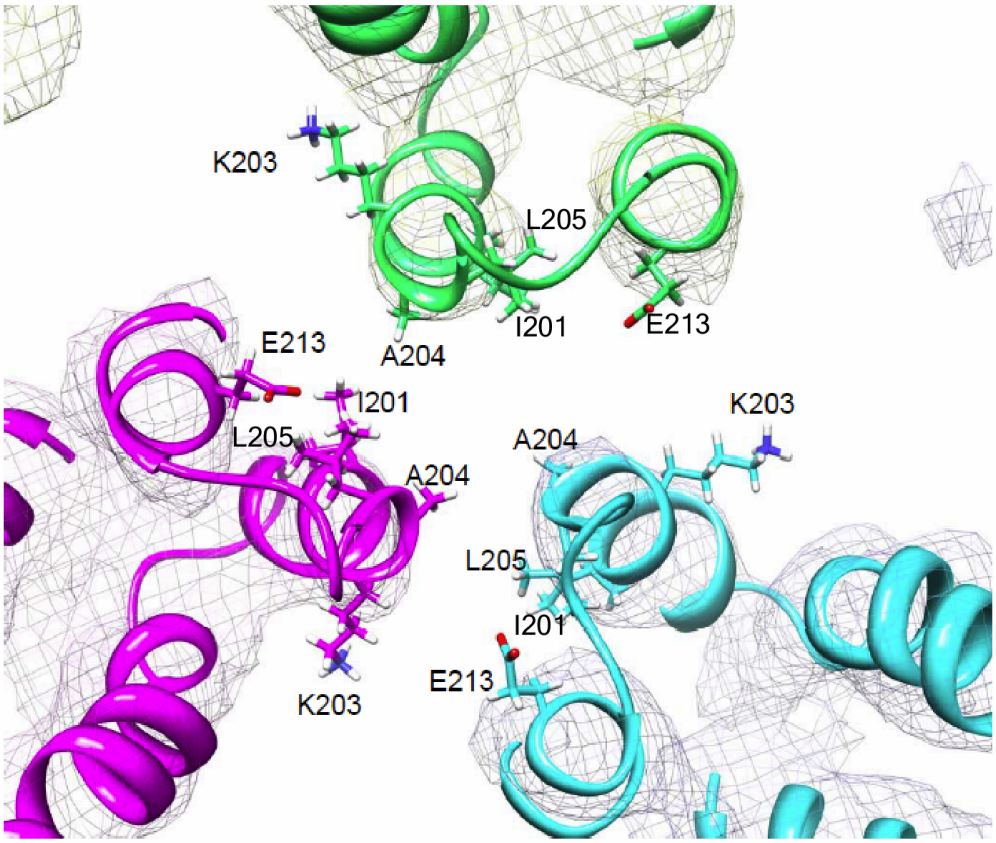

Figure 3-2: Detailed view of the hydrophobic trimer interface. Purple, blue and green ribbons are superimposed on the density map (gray mesh) and represent helix 10 from individual hexamers interacting at the trimer interface. Side chains of residues are shown in stick representation.

A204C forms a crosslinked dimer in mature HIV-1 virions

To validate the cryoEM model, we asked whether specific amino acid substitutions in key regions, would affect HIV-1 capsid structure and function. Based on the structure, we predicted that introduction of a Cys at position 204 would result in spontaneous disulfide bond formation in mature HIV-1 particles. This prediction was based on the backbone distance of A204 (5.3 Å) at the center of the hydrophobic core. The A204C spontaneously formed a dimer band in mature HIV-1 virions (Figure 3-3A). Upon treatment with reducing agent, the dimer band formed by A204C was converted into the monomeric form (Figure 3-3B), demonstrating that the dimer species were stabilized by disulfide bond interactions. However, introduction of A204C into a maturation-defective Gag in which the cleavage sites between CA-SP1-NC were mutated the dimer was absent, suggesting that the hydrophobic CTD trimer interface is specific to the mature capsid. This result agrees well with our maturation studies, which indicated that the trimer interface is fully formed only after complete cleavage of CA-SP1 (Meng et al., 2012) and discussed in Chapter IV of this dissertation. In addition, A204C CA protein exhibited higher assembly efficiency compared to wild type greater than 90%, verses 10-15% of wild type (Figure 3-3C). Moreover, the A204C CA protein assembled into short tubes and closed cones, similar to authentic lentiviral cores (Figure 3-4A) verses the long tubes formed by wild type CA protein. Sections of transfected HeLa cells revealed that A204C produced conical capsids when examined by transmission electron microscopy (Figure 3-4B). These observations suggest that there is pentamer incorporation in A204C assemblies, suggestive of a role for HIV-1 capsid assembly. Collectively, these data

validate conclusions from the 9 Å cryoEM structural model of the HIV-1 capsid that the A204 residue is at the center of the hydrophobic interface.

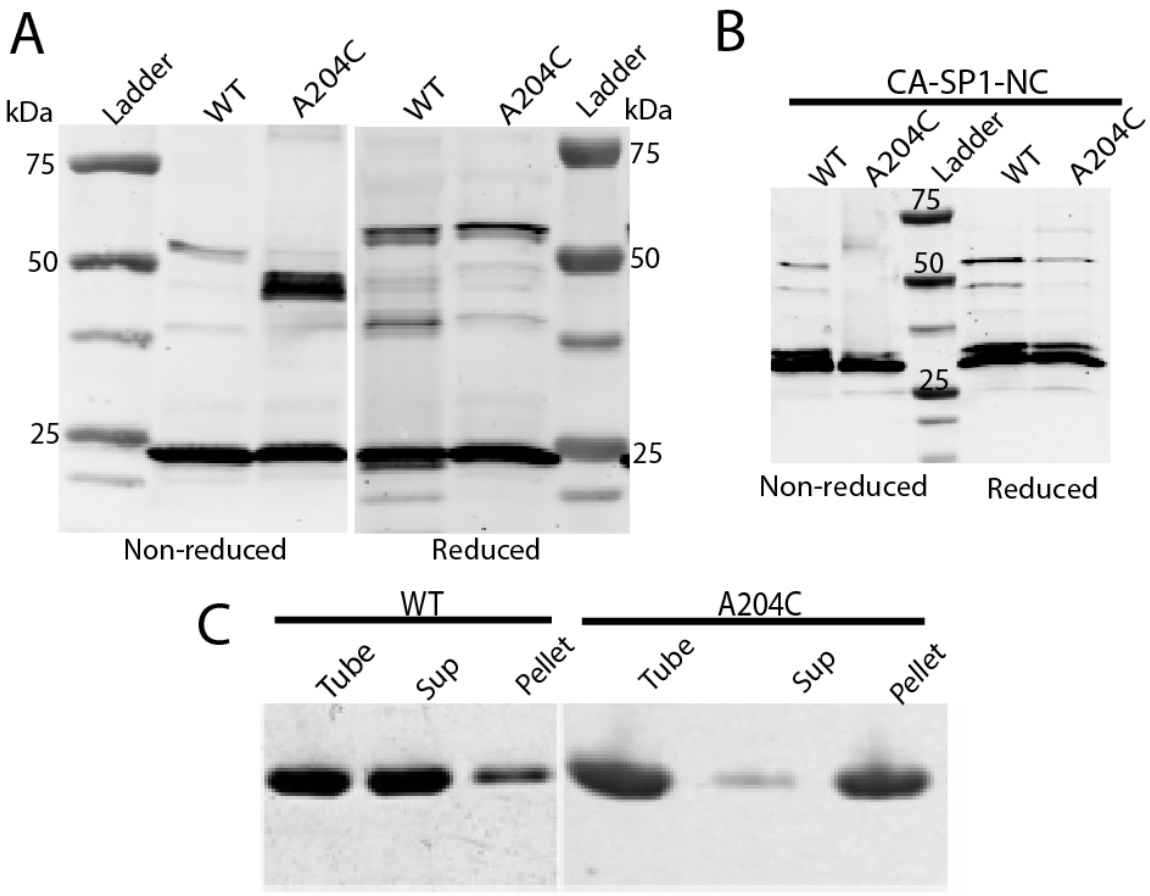

Figure 3-3: Mutational validation of the hydrophobic trimer interface. (A and B) Spontaneous disulfide crosslinking of A204C mature and maturation-defective (CA-SP1-NC) virions. Wild type virions and mutant particles carrying A204C mutation substitution were pelleted and analyzed by non-reducing and reducing 4-20% polyacrylamide gradient gels and subsequently by western blotting with specific anti-CA rabbit polyclonal antibody. (C) Assembly of wild type and A204C proteins in vitro, stained with Coomassie blue.

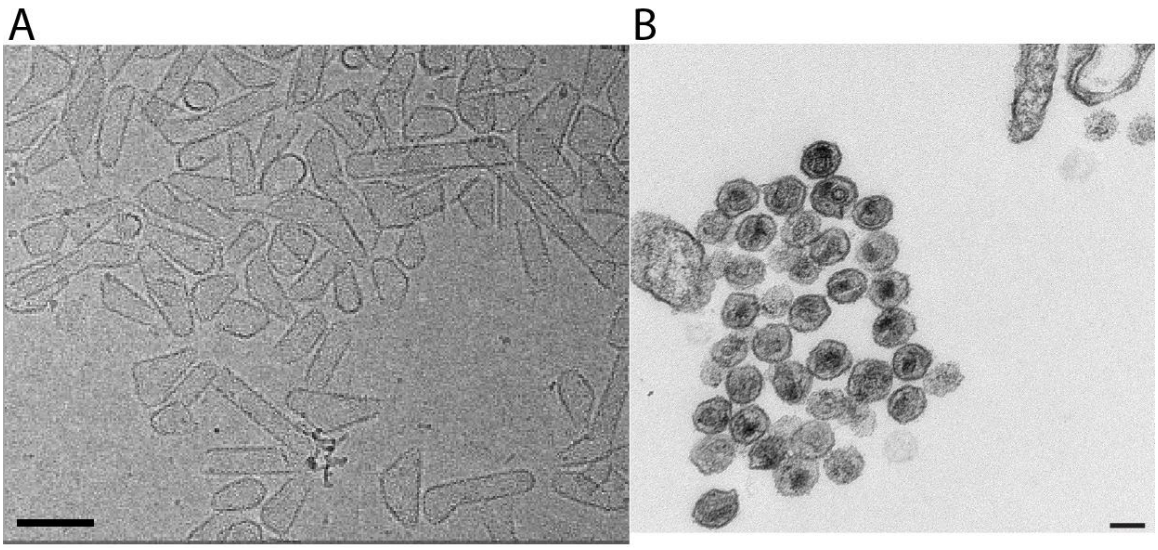

Figure 3-4: Cone formation of A204C in vitro and in virus particles. (A) Negative stain EM micrographs analysis of in vitro assembly of purified recombinant A204C CA protein. (B) Electron micrographs of fixed, pelleted, and thin-sectioned virus particles. A204C virions exhibit cone-shaped cores. Scale bars represent 100 nm. Peijun provided panel A.

Mutations altering hydrophobic residues at the trimer interface result in severe impairments in infectivity

Substitutions in CA can inhibit particle production by perturbing lattice interface interactions, altering Gag cleavage, or inhibiting protein folding or stability (Bartonova et al., 2008). To assess the effects of hydrophobic residues substitutions on HIV-1 particle production, I transfected 293T cells and determined the quantity of viral proteins and the activity of RT released into culture supernatants. In most cases, particle production was similar to that of the wild, except for L205D and I201D (Figure 3-5A), which exhibited reduced particle production. To determine whether Gag processing was altered by the mutations, pelleted and normalized viral particles were analyzed for viral protein by SDS-PAGE and immunoblotted with a CA-specific antibody. Most mutants exhibited a normal banding pattern similar to wild type, but for L205K, L205V and L205A (Figure 3-5B) that exhibited a band < 25 kDa. The protein identity was not determined and could be as result of altered cleavage of Gag. The results suggest that no major alterations occur as a result of the engineered mutations.

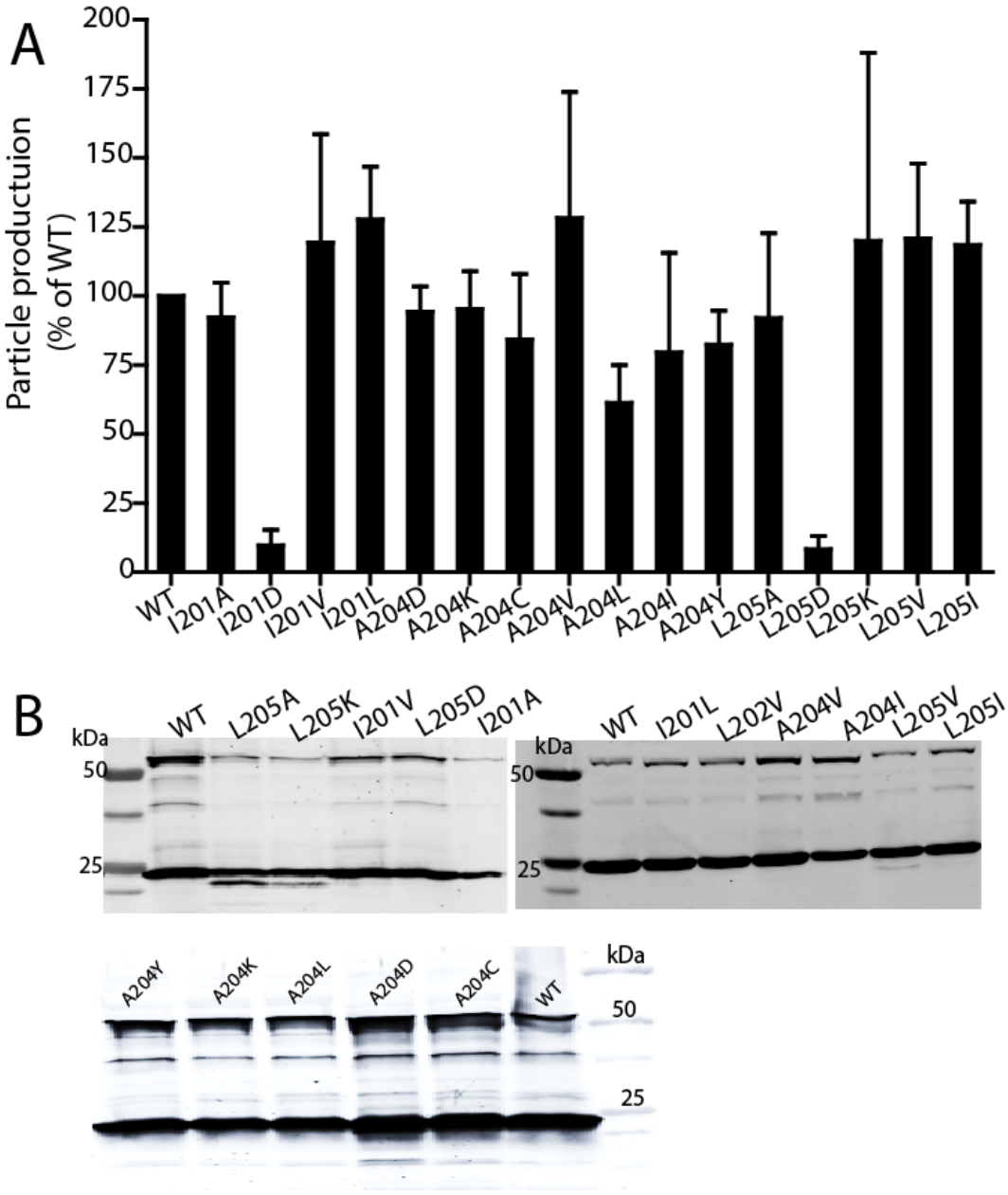

Figure 3-5. Production of viral particles and processing of Gag. (A) Particle production was measured by RT activity and values represent % of WT from three independent experiments, hence error bars represent one SD. (B) Immunoblot analysis of viral lysate. Virions were collected from transfected 293T cells, pelleted, and analyzed by SDS-PAGE and immunoblotting with a CA specific polyclonal antibody.

To determine the consequences of these hydrophobic residues mutations on virus infectivity, we titrated polar charged mutant particles on TZM-bl indicator cells. The cells were lysed and quantified for luciferase activity, which was normalized by the input levels of RT activity in the inocula. Mutant virions with polar residues substituted for hydrophobic residues exhibited essentially no infectivity (I201D, A204D, A204K, L205D), but for A205K, which exhibited, reduced infectivity compared to wild type. Hydrophobic replacements at the CTD-CTD trimer interface largely retained infectivity (I201V/L, A204V/L, L205V/I). However, the degree of infectivity retained by A204 mutants, L205A and I201A suggested that the size and nature of the charge are critically important at the CTD-CTD hydrophobic trimer core (Figure 3-6A). The results with charge residues suggest that the impaired infection of the mutant viruses is due to a defect in an early stage in the viral life cycle, since viral production after transfection was unaffected, except for the two aforementioned mutants (I201D and L205D).

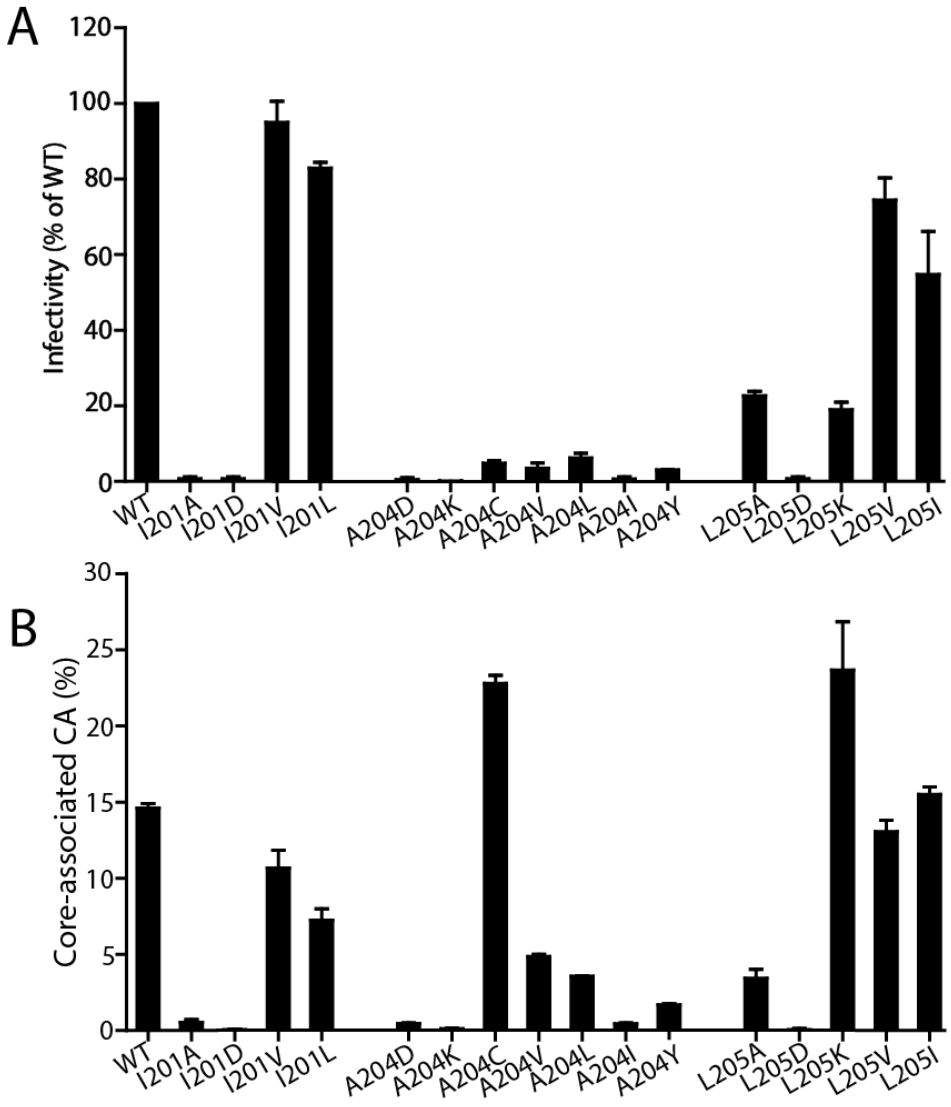

Figure 3-6: Single-cycle infectivity and core-associated CA of mutant virions at the hydrophobic core of the trimer interface**.** (A) Virion stocks were titrated in TZM-bl reporter cells and the extent of infection was determined by quantification of luciferase reporter activity in cell lysates. Values were normalized by the corresponding values of reverse transcriptase activity in the inocula. Hence, infectivity units are RLU/RT. Results shown are the mean values of three independent experiments, where error bars represent 1 standard deviation. (B) Purified HIV-1 cores were diluted in STE buffer and incubated at 37˚C for the indicated times. After pelleting the particles, the extent of uncoating was determined by quantifying CA levels in the pellets and supernatants. Shown here are the mean values of duplicate determinations with error bars representing the range of values. The results are representative of at least two independent. The values shown are the means of three independent experiments and the error bars represent 1 standard deviation.

Point mutations of the hydrophobic residues at the trimer interface alter the level of CA associated with purified HIV-1 cores

The cryoEM structure of the CA hexamer suggested that hydrophobic residues at the trimer intersubunit interactions likely contribute to capsid lattice stability. To test this hypothesis, I purified viral cores from the mutant particles and quantified the percentage of CA co-sedimenting with the cores. The majority of the mutants exhibited reduced levels of core-associated CA than the wild type, except for I201V/L and L205V/I, which was similar to wild type. There was a slight reduction in the core-associated CA of A204V. Core-associated CA levels for A204C and L205K were higher than that of the wild type (Figure 3-6B). Based on these results, we categorized the mutants as follows: wild type stability (I201V/L, L205V/I), hyperstable (A204C and L205K), moderately reduced stability (A204I/V/L/Y, L205A), and highly unstable (A204D/K, I201A/D, L205D). These alterations in core-associated CA were correlated with the impaired infectivity for the mutant viruses (Figure 3-6B). We conclude that the hydrophobic interactions at the CTD trimer interface are critical for formation and stability of the viral capsid.

Cores from a subset of hydrophobic mutants exhibit altered rates of uncoating in vitro

To further investigate the effects of the interface mutations on capsid stability I quantified the uncoating of cores purified from the A204C, I201V, L205A, and L205K mutants in vitro. We observed altered rates of uncoating for a subset of the

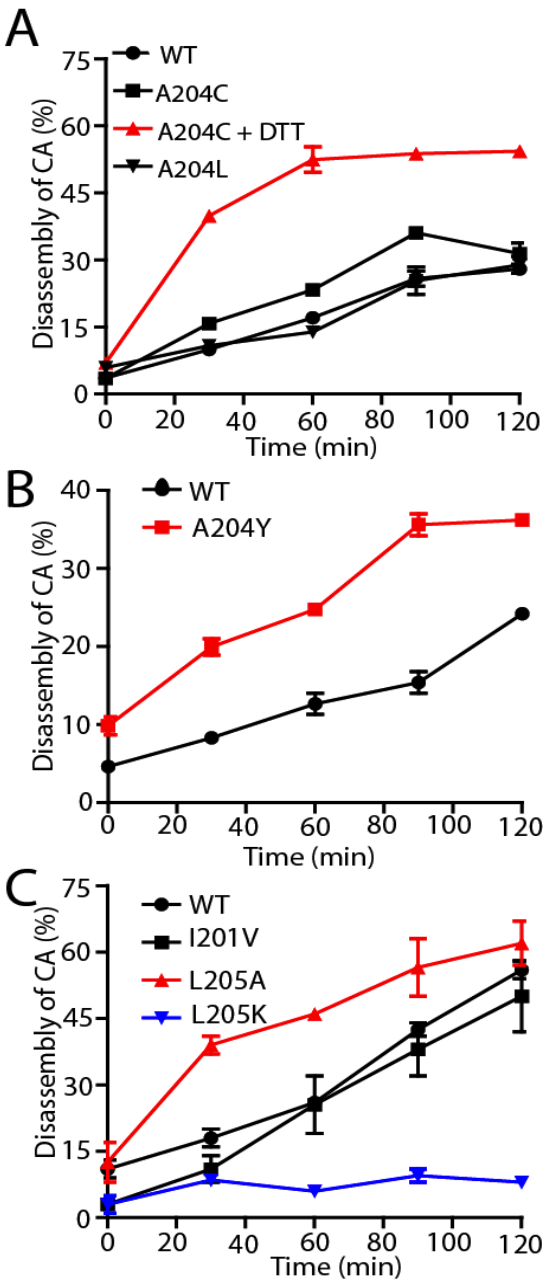

Figure 3-7: HIV-1 cores containing trimer interface substitutions exhibit altered uncoating kinetics in vitro. Purified HIV-1 cores were diluted in STE buffer and incubated at 37˚C for the indicated times. After pelleting the particles, the extent of uncoating was determined by quantifying CA levels in the pellets and supernatants. Shown here are the mean values of duplicate determinations with error bars representing the range of values. The results are representative of at least two independent experiments.

mutants. Cores from the A204Y and L205A mutants uncoated more rapidly than the wild type, while A204L and I201V uncoated with kinetics similar to the wild type (Figure 3-7B and C). In contrast, L205K cores uncoated more slowly than the wild type (Figure 3-7C), in concordance with the elevated level of core-associated CA exhibited by this mutant (Figure 3-6B). When the uncoating of A204C was performed in the presence of DTT, a reducing agent, A204C rapidly disassembled but the wild type was relatively unaffected (Figure 3-7A). These results suggest that these residues are important for the proper stabilization of the capsid.

Hydrophobic core mutants at the CTD-CTD trimer interface are impaired in reverse transcription in target cells

I employed stage-specific PCR to quantify the ability of CTD-CTD interface hydrophobic CA mutants to undergo reverse transcription in target cells. My results agree well with predictions from infectivity data and showed reduced late reverse transcription products in target cells (Figure 3-8). Reverse transcription appeared to be correlated with the degree of capsid stability, as partially unstable CA mutants accumulated reduced HIV-1 DNA relative to wild type, and no DNA products were detected for highly unstable mutants. As control, EFV treated samples did not accumulate late reverse transcripts controlling for background levels. I therefore conclude that mutations at the CTD-CTD trimer interface are impaired in infectivity due to an inability to efficiently undergo reverse transcription in target cells.

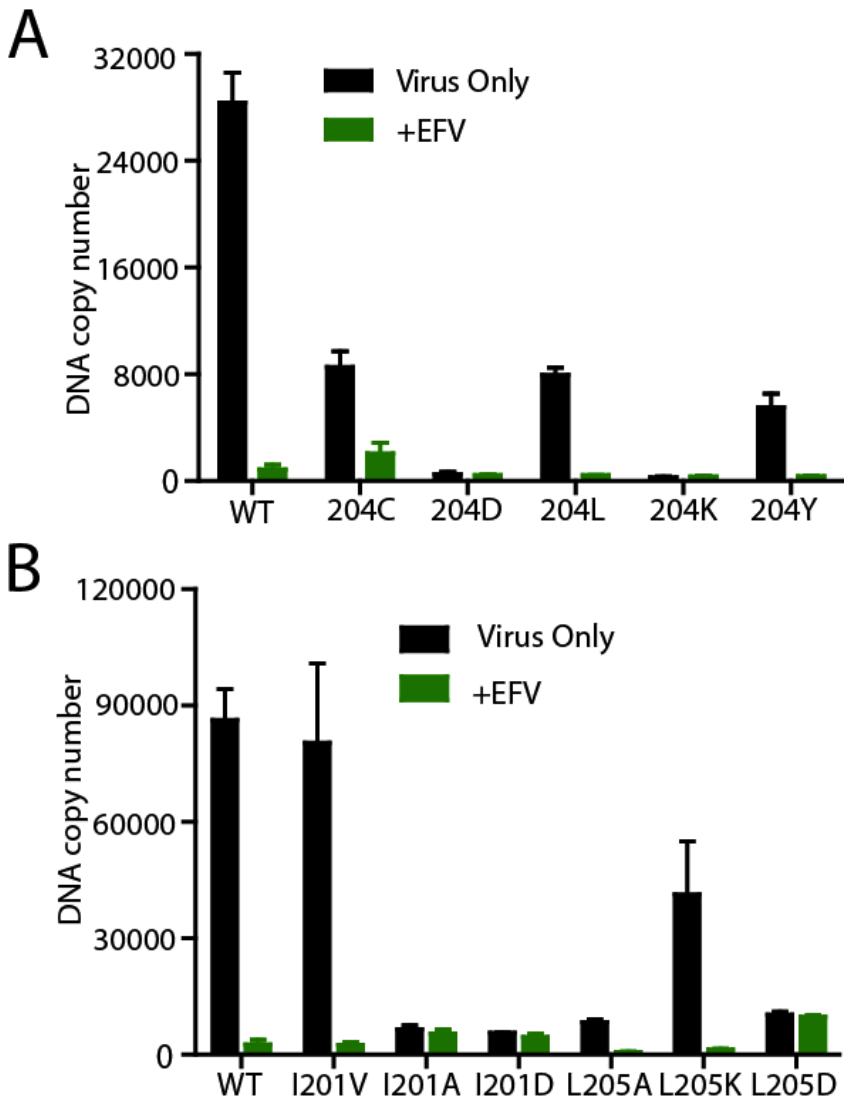

Figure 3-8: Hydrophobic core CA mutants with altered capsid stability are impaired in reverse transcription in target cells. HeLa P4 cells were inoculated with equal quantities (100 ng of p24) of WT or mutant viruses in the absence or presence of EFV. Cultures were harvested 8 hr after infection and DNA isolated for second-strand transfer quantification by real-time PCR using the SYBR green method. A and B were done at different times and presented separately for clarity. Error bars represent the standard deviations from triplicate infections.

Discussion

Previous studies of the structure of the tubular HIV-1 capsid assembly observed strong density at the trimer interface at 16 Å resolution. Mutational analysis of charge residues at this interface, E213 and K203, revealed that this interface is important for capsid stability (Byeon et al., 2009; Forshey et al., 2002). In the present study, our collaborators determined the structure of capsid at 9 Å resolution. This new high-resolution structure revealed a patch of hydrophobic residues in the center of the three-helix bundle at A204, I201, and L205 that were not revealed in the previous studies. I performed a functional analysis of these residues and the results revealed important new information about these hydrophobic residues and about the importance of the trimer interface in HIV-1 capsid function.

Analysis of A204C revealed that this mutation confers hyperstability to the capsid and causes a tenfold reduction in infectivity. Electron microscopic analysis of virions revealed that the mutant makes conical capsids. Assembly of the recombinant protein in vitro revealed that A204C CA protein assembled with greater efficiency than wild type protein. What was most interesting though was the fact that A204C assembled predominantly into cones as opposed to the long elongated tubes of wild type. This means that the mutation renders efficient incorporation of pentamer. This phenotype was also observed with A204L (data not shown). Previously it was noted that electrostatic alterations at the six-fold axis (NTD-NTD), specifically R18A, L, or V mutations shift the assembly to the formation of pentamers (Yeager, 2011). It should also be noted that assembly of N21C/A22C leads to the accumulation of pentamer band when assembly is analyzed by non-reducing SDS-PAGE and the accumulation of rounded spheres that

matches an icosahedron of 20 hexamers and 12 pentamers (Pornillos et al., 2010). The question that arises is how do independent alterations at both domains lead to incorporation of the pentamers in the assembled protein? These integrated observations lead us to suggest that electrostatic destabilization at the NTD-NTD interfaces is counterbalanced by the stabilizing hydrophobic interaction at the three-fold axis leading to the incorporation of pentamers. Therefore, independent enhancement of interactions at the trimer interface would result in incorporation of pentamers as in A204C and A204L assemblies. This observation in conjunction with the fact that trimer contacts are absent in the planar 2D crystal of the CA assembly (Ganser-Pornillos et al., 2007) suggest that the trimer interface is essential for curvature of the capsid. The fact that A204 mutants are impaired for infectivity with hydrophobic substitutions may be related to the structure of the hydrophobic core, where substitution of bulkier hydrophobic residues may lead to overcrowding and make the capsid unstable. More so, the phenotype with A204C/L in vitro assembly suggest there is a change in the intrinsic assembly program that shifts the balance from predominantly tubes (seen in wild type) to cones seen in these two mutants. The formation of cones in high frequency by these mutants is interesting because the wild type rarely forms cones when assembled in vitro. The wild type virus normally forms cones during maturation.

The different phenotypes of the mutations at the hydrophobic interface suggest that charge is extremely important at this interface; whereas in most cases the electrostatic charges were deleterious, hydrophobic substitutions could be tolerated to some extent. A previous study showed that the double mutant I201A/L202A is severely impaired in infectivity; however, I201V, a revertant to I201A, replicated with wild type

efficiency (Joshi et al., 2006). Our results here for I201V and I201L are in accord with this observation and highlight the importance of size and hydrophobicity of residues at the trimer interface. Interestingly, I201V confers resistance to PF-46396 and Beviramat (Li et al., 2003; Zhou et al., 2004).

Residue L205, which is slightly peripheral to I201 and A204, was particularly intriguing. L205D mutant was severely impaired in infectivity, while the infectivity of L205A and L205K were reduced but not completely abolished. In vitro, the L205A capsid was very unstable while L205K was hyperstable. No cores were isolated from L205D (very unstable), while cores isolated from L205V and L205I were similar to wild type in core-associated CA. This leads us to suggest that replacement of L with A, another hydrophobic residue, partially maintains the hydrophobicity of this interface, but the amount of hydrophobicity is likely insufficient for optimal stability. However, changing L to K may produce a new set of interactions where lysine may attract a neighboring negative charge such as E213, leading to stabilization of the interface. On the other hand, L205D results in repulsive forces that destabilize the capsid. Previous studies had shown that E213A/Q are both hyperstable, raising possible scenarios on the role of charge at E213. One possibility is that charge neutralization around this locus makes the capsid hyperstable.

CHAPTER IV

PROTEASE CLEAVAGE LEADS TO THE FORMATION OFA MATURE TRIMER INTERFACE IN THE HIV-1 CAPSID

Introduction

The Gag polyprotein represents the major viral structural element that is cleaved during maturation by protease into MA, CA, NC, P6, and the two spacer proteins SP1 and SP2. Cleavage results in conformational changes that convert a spherical core of an immature, non-infectious viral particle into a conical core of a mature, infectious viral particle. The core of the mature virus is surrounded by the capsid, which is made up of a lattice of CA hexamers and pentamers. Recent structural studies of in vitro assembled CA revealed that the lattice is held together by several intermolecular intersubunit interactions that include an NTD-NTD, CTD-CTD dimer, NTD-CTD, and CTD-CTD trimer interfaces in mature HIV-1 capsid (Byeon et al., 2009; Pornillos et al., 2009). While the structure of the mature viral particle is moderately well understood, the structural rearrangements that accompany the morphogenesis of the immature particle to a mature particle remain unknown. Hence, the presence of these intersubunit interactions in immature viral particles and the mechanism of maturation are not known. It is therefore not known if the capsid interfaces present in mature HIV-1 virions are similar to those present in immature virions or in maturation intermediates.

Several maturation models have been proposed. Based on structural studies conducted by Briggs et al. (Briggs et al., 2006), it was proposed that CA monomers or hexamers reassemble de novo after proteolysis of Gag. In this case, it is assumed that the

intersubunit interfaces present in immature lattice are different from those present in the mature HIV-1 capsid lattice. It has also been proposed that contacts in immature capsid lattice are very similar to contacts in the mature capsid. This is based on the theory that a major conformational switch occurs during maturation that converts an immature lattice into a mature lattice (Ivanov et al., 2007; von Schwedler et al., 1998). This Chapter describes work that I performed in collaboration with Dr. Peijun Zhang's group from the University of Pittsburgh. The group under the auspices of Peijun Zhang determined the cryoEM structure of tubular assemblies of HIV-1 CA-SP1-NC protein and compared it with the cryoEM structure of CA, while I focused on testing the structural model in virus particles. Our results support a maturation model in which there is a remodeling of the capsid interfaces rather than complete disassembly and reassembly of the lattice. Specifically, using cryoEM and crosslinking in assembled protein and in HIV-1 virions, our data show that proteolytic cleavage during maturation leads to the reorganization of the polypeptide, resulting in the formation of the CTD-CTD trimer interface. Our analysis also includes in vitro studies and studies in mutant HIV-1 particles containing CA-SP1, a relevant biological intermediate in the process of maturation.

Approach

CA-SP1-NC protein was assembled in the presence of nucleic acid resulting in the formation of CA-SP1-NC tubes and CA tubes. The best density maps from CA-SP1-NC tubes and CA tubes were used for structural analysis. High resolution structures of the NTD and CTD of CA proteins were used to dock into the density maps

generated from these tubes using a correlation-based automated rigid-body fitting method (Byeon et al., 2009). Our collaborators in Pittsburgh (Drs Zhang, Meng, Xhou) performed the structural studies. The structural model predicted intersubunit contacts at some interfaces and not others. I used engineered Cys-Cys disulfide crosslinking in assembled protein of CA, CA-SP1, and CA-SP1-NC to probe for the presence of contacts predicted by the structural model. The assembled proteins were analyzed by SDS-PAGE and western blot. In vitro studies were verified using the same Cys substitutions in mature HIV-1 particles containing mutations resulting in the accumulation of oligomers formed by engineered disulfide interactions in CA-SP1-NC and CA-SP1 backgrounds and the degree and number of oligomers formed were analyzed.

Results

Determination of the pseudo-atomic structure of CA-SP1-NC

The tubes generated from CA-SP1-NC and CA assemblies exhibited striking differences. Notably, the CA-SP1-NC tubes exhibited a double layer density with inner and outer diameters of 270±8Å and 468±10Å respectively, while the tubes from assembled CA only contained a single layer density (Figure 4-1). A detailed comparison of the density maps of CA-SP1-NC and CA is shown in Figure 4-1D-I. The Zhang lab used high-resolution structures of CA-NTD and CA-CTD domains to separately dock into the CA-SP1-NC density maps using a correlation-based automated rigid-body fitting method (Byeon et al., 2009). Shown in Figure 4-2A is a view of the tube surfaces

obtained after docking high resolution structures of individual NTD and CTD domains to generate pseudo-atomic structures of CA and CA-SP1-NC. The pseudo-atomic structure of CA in this study was similar to previous structure (Byeon et al., 2009). For clarity the pseudo-atomic structure of CA reported in a previous study is shown in Figure 4-2. (Byeon et al., 2009). The structure of CA-SP1-NC revealed the presence of some previously characterized capsid interfaces: a CTD-CTD dimer, an NTD-NTD and an NTD-CTD (Byeon et al., 2009; Pornillos et al., 2009) that were also present in the mature CA density map (Figure 4-2A and B). Our results showed that interactions between neighboring CA-SP1-NC hexamers are mediated primarily by the CTD-CTD dimers, similar to mature CA and that hexamer formation is mediated by the NTD-NTD interactions (Figure 4-2A and B). However, the CTD-CTD trimer interface that is present in the mature CA was absent from the CA-SP1-NC map (Figure 4-2A and 4-2B). Superposition of the CA monomer with CA-SP1-NC protein revealed that the NTDs of both structures aligned well, except for the CTD that did not (Figure 4-2C). Specifically, the CTD of CA-SP1-NC was rotated 34 degrees relative to the NTD, suggesting that this could be the reason why the CTD-CTD trimer interface was not apparent in the structure.

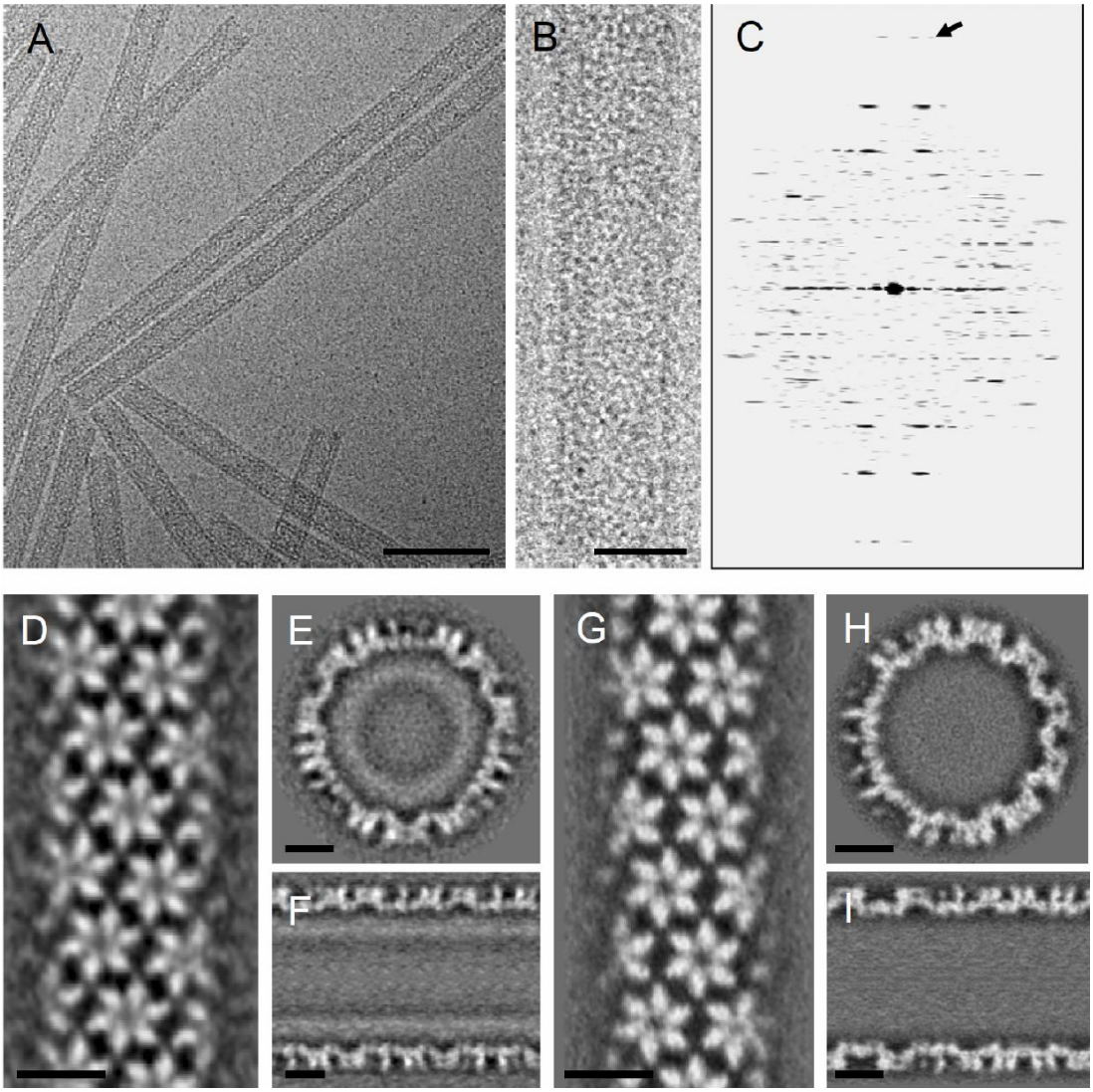

Figure 4-1: CryoEM and image reconstruction of HIV-1 CA CA-SP1-NC and CA tubular assemblies. (A-B) CryoEM micrographs of recombinant HIV CA-SP1-NC assembled into tubes. (C) The computed Fourier transformation of the tube shown in B. The arrow points to the layerline at 23 Å resolution. (D-F) Final density map of CA-SP1-NC tubes helical family, displayed as three orthogonal slices: parallel to the tube axis and close to the surface (D), perpendicular to the tube axis (E), and parallel to the and through the tube axis (F). (G-I) The final density map of CA tubes helical family displayed as in (D-F). Scale bars represent 100 nm in (A), 25 nm in (B) and 10 nm in (D-H).

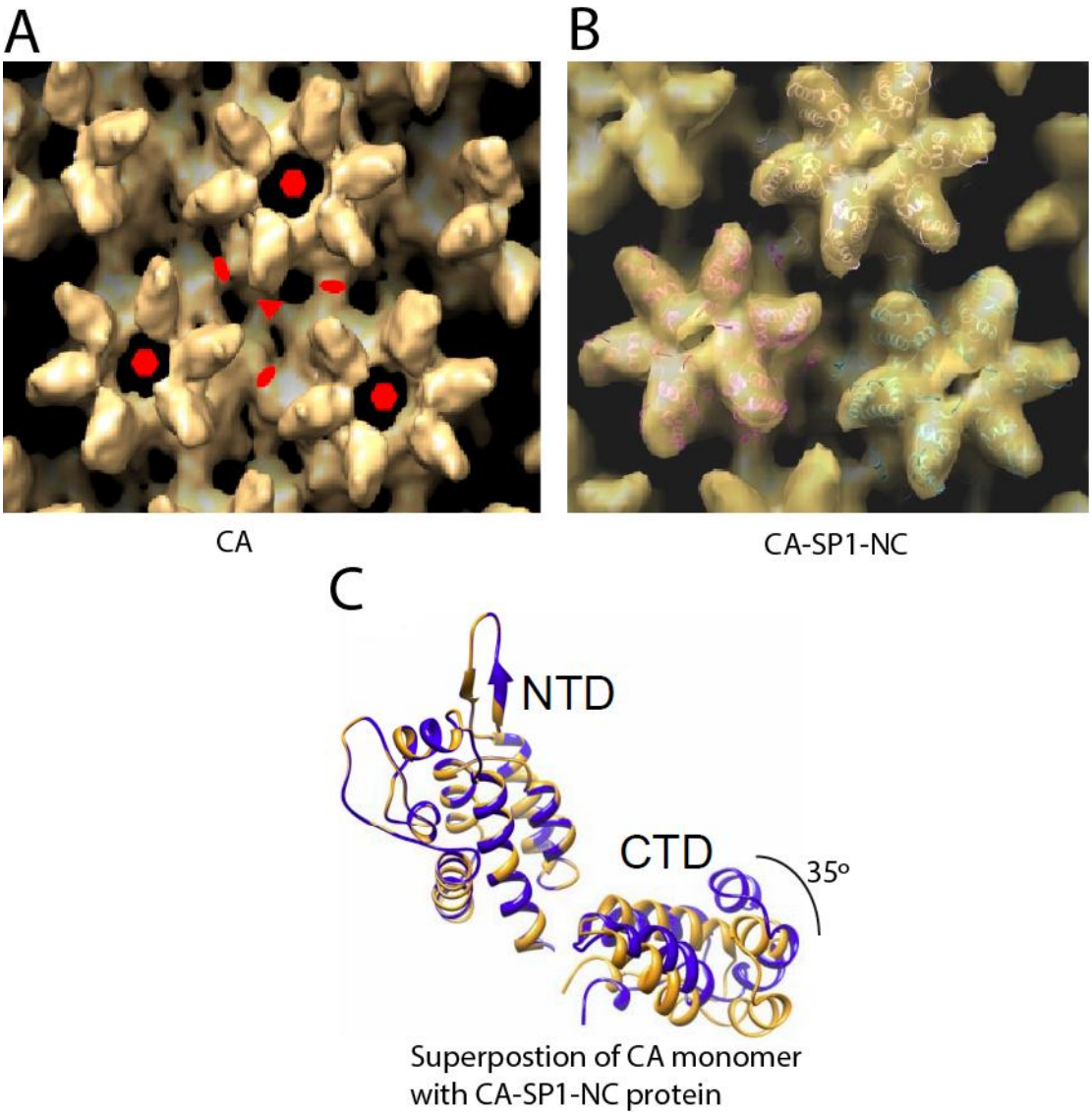

Figure 4-2: Molecular docking of the CA-SP1-NC density map. (A) Density map of CA (image obtained from Byeon 2009) showing NTD-NTD, CTD-CTD dimer and CTD-CTD trimer densities. (B) Docking of the CA-NTD (PDB 3h47) and CA-CTD (PDB 2kod) domain models, independently, into the CA region (gold) of the density map showing a view onto the tube surface with a conspicuously absent density at the trimer interface when compared with (A). (C) Superposition of the CA monomer model from the assembled CA structure (gold) and that from the assembled CA-SP1-NC structure (blue).

Structural reorganization in the HIV-1 capsid assembly upon proteolytic cleavage

Our pseudo-atomic structural model of the CA-SP1-NC structure in comparison with that of CA revealed structural differences between the two assemblies. As mentioned earlier, the major structural difference was observed at the CTD, where the CTD was rotated 34 degrees relative to the NTD through a flexible hinge in CA-SP1-NC. To test whether the structural deviation affects intersubunit interface formation during assembly, we performed a detailed comparative analysis of the intermolecular NTD-NTD and the CTD-CTD trimer interfaces. Previous work had shown that the presence of these interfaces in mature HIV-1 particles can be studied by testing the proximity of pairs of residues on the lattice surface by engineered disulfide crosslinking (Byeon et al., 2009; Falke and Koshland, 1987; Pornillos et al., 2009; Pornillos et al., 2011). These included P17/T19 or A14/E45, and P207/T216, for the NTD-NTD and CTD-CTD trimer interfaces, respectively. The results in Table 4-1 show the average distance of Cα-Cα of the pairs used for comparison in CA and CA-SP1-NC structures. The NTD-NTD interface that forms hexamer interactions in assembled CA was retained in CA-SP1-NC assembly and displayed comparatively similar Cα-Cα distances when P17/T19 intersubunit pairs were compared (Table 4-1). This pair is located in the center of the 18-helix barrel and close to its surface, with an average distance difference of ~1.7 Å, suggesting that the contacts are likely maintained in both the CA-SP1-NC and CA structures. By contrast, the A14/E45 pair that is halfway into the hexameric barrel exhibited an average deviation of 3.9 Å, but with variability among pairs in the CA-SP1-NC structure.

	Intrahexamer		Intrahexamer		Interhexamer trimer	
Cα- Cα Distance(Å)	**CA 14/45**	**CA-SP1-NC 14/45**	**CA 17/19**	**CA-SP1-NC 17/19**	**CA 207/216**	**CA-SP1-NC 207/216**
1-2	8.0	10.2	5.0	5.6	9.6	20.1
2-3	8.1	9.8	5.4	6.6	8.1	18.6
3-4	7.9	12.1	6.5	7.5	10.6	19.9
4-5	8.5	12.7	6.9	8.6		
5-6	8.0	13.8	6.6	9.2		
6-1	8.3	13.3	7.2	10.3		
Average	8.1	12.0	6.3	8.0	9.6	19.6

Table 4-1: Cα-Cα distance (Å) of selected pairs at the intersubunit interfaces, where 14/45 and 17/19 represent the NTD-NTD interface and 207/216 represent the CTD-CTD trimer interface. The Cα-Cα distance is between adjacent CA molecules.

Four of the six pairs displayed an average Cα-Cα distance of ~13.0 Å, while the remaining two pairs were shown to be closer to each other at about 10 Å apart. This distance variation was absent for the assembled CA structure that maintained an average constant Cα-Cα distance of 8.1±0.2 Å. However, the major difference in the CA-SP1-NC assembly, when compared to CA assembly, occurred at the CTD-CTD trimer intermolecular interface. Using the P207/T216 pair as a gauge for CTD-CTD trimer interactions with a Cα-Cα distance of 9 Å in CA structure, the average Cα-Cα distance was measured at 20 Å in CA-SP1-NC, suggesting that the major structural change that occurs during cleavage and maturation is at the formation of the trimer interface. This result agrees well with the absence of density at this interface in CA-SP1-NC tubes. Overall, the comparison of the intersubunit interfaces in the CA and CA-SP1-NC tubes indicates that the trimer interface is altered or absent in CA-SP1-NC.

Probing structural alterations during HIV-1 maturation: analysis of intermolecular contacts formed during assembly by chemical crosslinking

Using the above residues as probes for the different capsid interfaces, I analyzed the cryoEM structural model for the presence of capsid interfaces from which we could infer intermolecular contacts. Using the contacts described above, we engineered Cys mutants at these residues: P17C/T19C and A14C/E45C for NTD-NTD crosslinking, and P207C/T216C for CTD-CTD trimer interface crosslinking. The crosslinking was assayed by SDS-PAGE analysis of spontaneous disulfide bind formation of the mutants. Crosslinking of P17C/T19C in assembled CA and CA-SP1-NC agreed well with structural predictions and displayed a similar ladder of oligomers (Figure 4-3A). The results suggested that the contacts at the NTD-NTD interface are unperturbed during

cleavage of Gag. Assembled A14C/E45C protein was much less efficient at crosslinking in CA-SP1-NC, forming predominantly a dimer band as opposed to efficient hexamer formation in assembled CA (Figure 4-3B). This result was consistent with the cryoEM structural model that showed only two residues in close proximity (Figure 4-3B), and the differences, if any, were subtle. However, when we compared crosslinking of P207C/T216C in assembled CA and in assembled CA-SP1-NC, there was a profound difference in crosslinking patterns between the two assemblies (Figure 4-3C). Specifically, there was no accumulation of a trimer band in CA-SP1-NC, while the trimer band accumulated well in CA assemblies. This was consistent with the altered arrangement at the trimer interface as predicted from the cryoEM structure (Figure 4-3C).

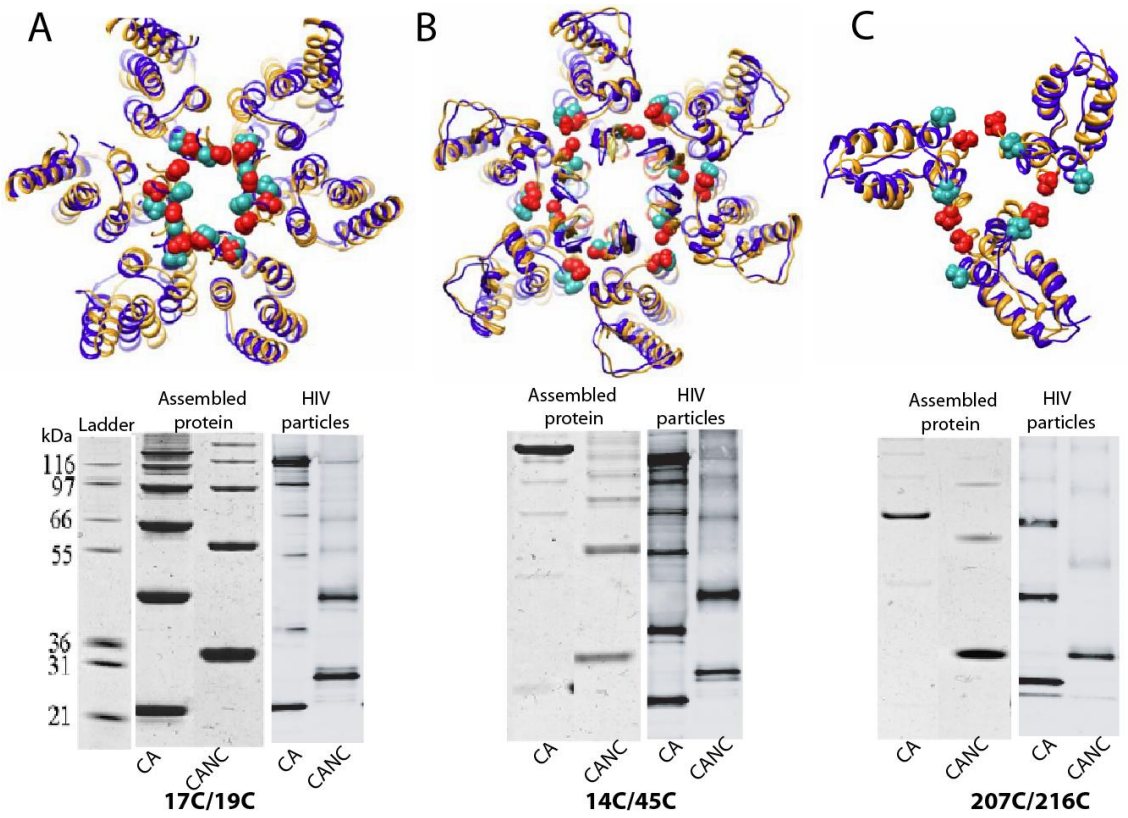

Figure 4-3: Comparison of the intermolecular interfaces and chemical crosslinking patterns between CA and CA-SP1-NC structures. (A–C, top panel) Superposition of the CA-NTD models at the NTD interfaces (A&B) and CA-CTD models at the trimer interface (C), with assembled CA structure (gold) and that from the assembled CA-SP1-NC structure (blue). Space-filling representation highlights the specific residue pairs: 17/19 in (A), 14/45 in (B) and 207/216 in (C), with red corresponding to those from CA and cyan to those from CA-SP1-NC. (A-C, bottom panel) Non-reducing SDS-PAGE analysis of in vitro disulfide crosslinked assembled CA and CA-SP-NC assemblies stained with Coomassie blue and non-reducing SDS-PAGE analysis of crosslinking of HIV-1 particles and cleavage-defective HIV-1 CA-SP-NC particles. Proteins were detected by immunoblotting with a CA-specific antibody.

To test our in vitro studies with HIV-1 particles, I engineered corresponding double Cys mutations at the NTD and CTD domains of CA in HIV-1 clones, and tested their ability to crosslink in CA and CA-SP1-NC particles. The CA-SP1-NC contains mutations that block cleavage between CA-SP1 and SP1-NC but contains active protease that cleaves processing sites in Gag(Wiegers et al., 1998). Mutant particles obtained from the supernatant of transfected 293T cells were assessed for spontaneous crosslinking by non-reducing SDS-PAGE and immunoblotting. My results with P17C/T19C CA-SP1-NC particles were surprisingly different from what was predicted by cryoEM structure and crosslinking in vitro with 17C/19C CA-SP1-NC. P17C/T19C in CA-SP1-NC formed only a dimer with very faint higher molecular weight bands (Fig 4-3A bottom-right panel). The results of A14C/E45C crosslinking pattern were similar to in vitro observations as it readily crosslinked into a dimer in CA-SP1-NC virions and into a hexamer in A14C/E45C CA virions (Figure 4-3B). P207C/T216C HIV-1 particles in the CA-SP-NC background did not form a trimer band as expected (Figure 4-3C bottom-right panel). Altogether, our results in vitro and in virions substantially agree with the structural model, leading us to conclude that it is the CTD-CTD trimer interface that is distinctly different in CA verses CA-SP1-NC assemblies.

Structural reorganizations in HIV-1 capsid assembly upon proteolytic cleavage

Our results with CA-SP1-NC particles suggested that cleavage by protease may result in proper orientation of the CTD terminal domain of CA and in turn form the trimer interface. To further analyze the effects of cleavage on tube structure, we performed CA-SP1-NC protease digestion of preassembled tubes and unassembled CA-SP1-NC protein

in vitro in order to mimic the process of maturation, and determined the effects on interface formation by analyzing disulfide crosslinking. In the absence of assembly, cleavage of CA-SP1-NC occurred primarily at the CA-SP1 site, yielding CA and SP1-NC as by-products (Figure 4-4A). However, a distinct cleavage pattern was observed when CA-SP1-NC assemblies were tested. When preassembled, the efficiency of cleavage at the CA-SP1 junction was reduced, likely as a result of cleavage site occlusion from the less flexible SP1 region in the assembled lattice. However, cleavage between SP1 and NC was enhanced, liberating CA-SP1 and NC as the major products, similar to initial cleavage of Gag during virion maturation (Figure 4-4A).

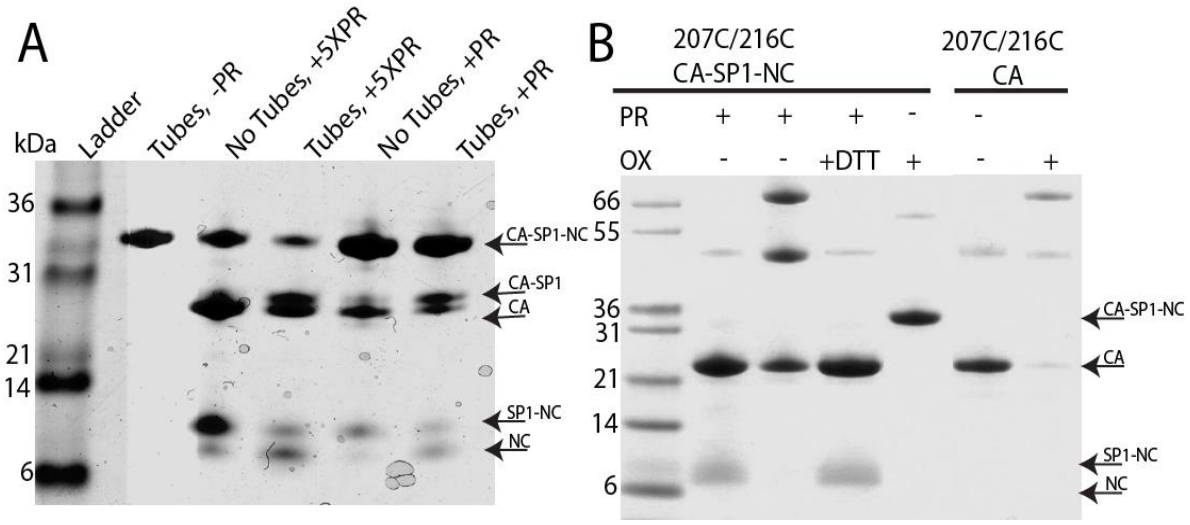

Figure 4-4: Protease cleavage of CA-SP1-NC assemblies. (A) SDS-PAGE analysis of HIV-1 protease (PR)-treated, unassembled soluble CA-SP1-NC (No tubes), and CA-SP1-NC tubular assemblies (Tubes), visualized by Coomassie Blue staining. The cleavage products, CA-SP1, CA, SP1-NC, and NC are labeled. Samples treated with 5 times more protease were marked as x5. (B) Non-reducing SDS-PAGE analysis of crosslinked, protease-treated CA-SP1-NC 207C/216C assembly.

We then asked whether the CTD would re-orient properly and form the mature trimer interface once cleavage of CA-SP1-NC tubes was complete. As predicted, the protease cleaved assembled 207C/216C protein in the CA-SP1-NC background formed crosslinks of dimers and trimers that were very similar to those formed in the 207C/216C CA assembly (Figure 4-4B). This supports the hypothesis that optimal trimer contacts are formed upon complete cleavage of SP1 from CA.

During peer review of this work, it was suggested that the CA-SP1-NC is not a good model for the assembly intermediate, since it is itself not a biological intermediate during the process of maturation. Taking this into consideration, I sought to validate my studies with CA-SP1 virus particle. To evaluate spontaneous disulfide crosslinking of the NTD-NTD pairs in CA-SP1 virus particles, I used the same interacting pairs as employed in the studies of recombinant CA and CA-SP1-NC assemblies. Analysis by non-reducing SDS-PAGE and immunoblotting with CA specific antibody showed that there was no difference between the efficiency of crosslinking of P17C/T19C or A14C/E45C particles in CA-SP1 as compared to CA (Figure 4-5A). Also, the NTD-CTD interface was fully formed in CA-SP1, with no difference when compared to NTD-CTD in CA particles (Figure 4-5B). By contrast, there was a reduction in trimer formation in P207C/T216C CA-SP1 verses CA. Specifically, trimer band formation in CA-SP1-NC was much less efficient than in CA. I also observed that there was a small percentage of higher order oligomers in CA-SP1-NC compared to CA. Our results with cryoEM structural model, validated by crosslinking, suggested that the trimer interface in HIV-1 capsid is fully formed only after full cleavage of Gag, further suggesting that the CA-SP1 particles

exhibit an immature CA-CTD trimer interface similar to CA-SP1-NC, but with NTD-NTD and NTD-CTD interfaces that are similar to those in mature capsid.

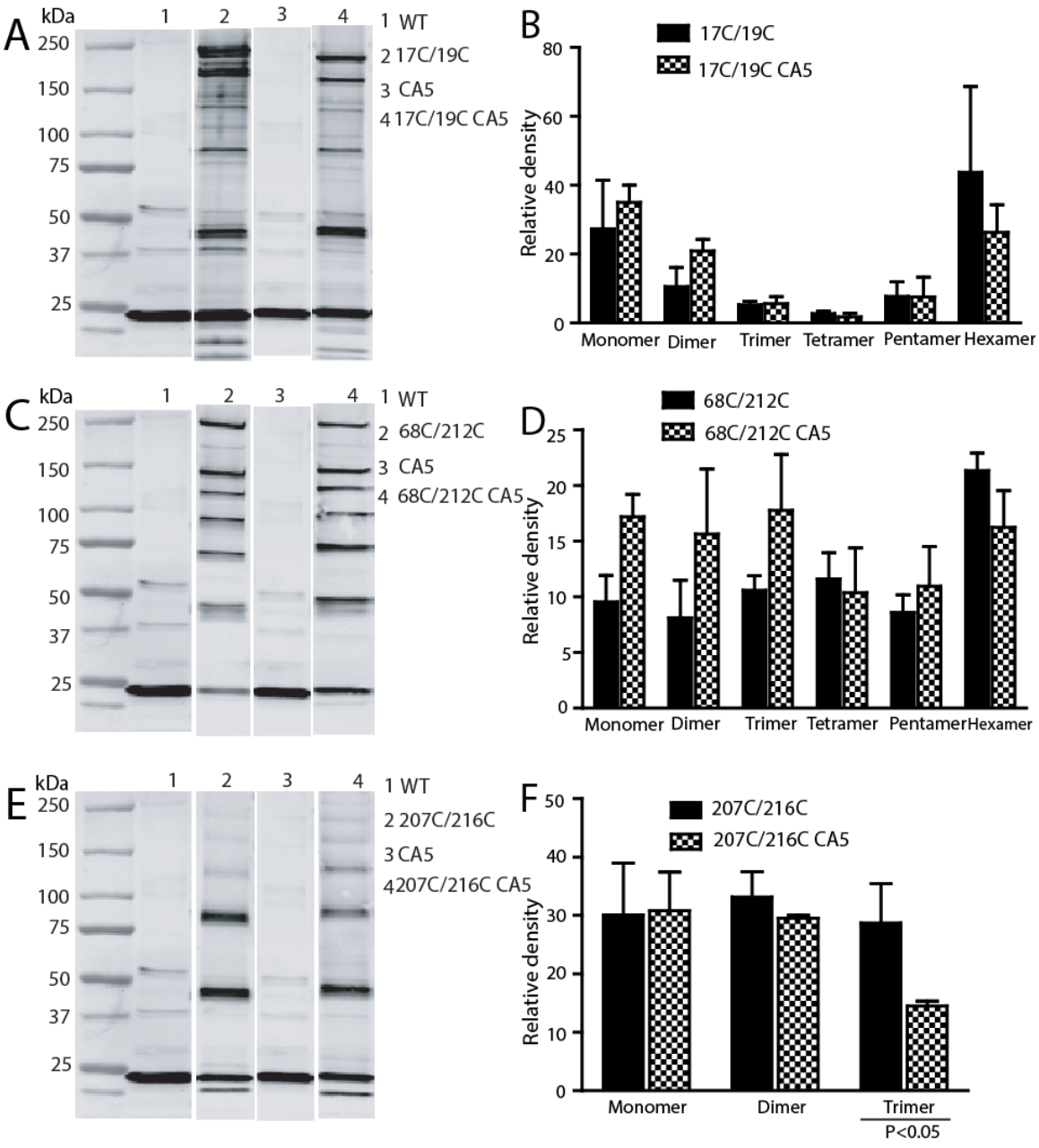

Figure 4-5: Chemical crosslinking analysis of the HIV-1 maturation intermediate CA5 particles that retain CA-SP1 linkage. (A, C, and E) Non-reducing SDS-PAGE analysis of crosslinking in mature wild type and CA-SP1 cleavage-defective (CA5) particles. Proteins were detected by immunoblotting with a CA-specific antibody. (B, D, and F) Quantification of oligomer forms of CA in wild type and CA5 of 17C/19C (B), 68C/212C (D) and 207C/216C (F) crosslinked particles as determined from 3 independent experiments. Note that (A, C and E) are representative experiments. Error bars represent SD of quantified bands from three independent experiments.

Discussion

In this study, my collaborators and I used structural and biochemical approaches on assembled proteins, and crosslinking analyses of HIV-1 particles, to study the mechanism of interface formation in capsid maturation. Our structural data showed that in CA-SP1-NC, the CTD of CA is rotated 34 degrees relative to the NTD through a flexible hinge suggesting that the hinge plays a critical role in conformational changes upon protease cleavage. Previously, this linker hinge region has been attributed to controlling the multiple conformations that are required for proper capsid assembly (Cardone et al., 2009; Du et al., 2011). A recent mutational analysis of the hinge region suggested that the linker NTD-CTD sequence is critical for proper assembly of the capsid (Jiang et al., 2011a). Our results underscore the importance of the hinge region in mature capsid formation, and they show that flexibility allows rotation to position the CTD of CA to make optimal contacts for trimer interface formation.

We were surprised to observe that P17C/T19C did not form higher-ordered oligomers in HIV-1 particles containing mutations that block cleavage between CA-SP1-NC. This cannot be readily explained given that this pair appeared to be in close proximity to interact. However, given that these pairs are inferred from structural models, they may not be the most optimal pairs with which to study the NTD-NTD interface, or the structural model may not be accurate. The latter seems less likely, since most of the predictions were verified by the crosslinking in virus particles. In addition, crosslinking may also depend on the geometry of the lattice.

Based on our findings, we propose a model for the mechanism of HIV-1 capsid maturation with regard to the C terminus of CA. Our model suggests that in immature

assemblies, initially only the SP1-NC cleavage site is readily accessible to the viral protease. Cleavage between SP1 and NC releases NC and the viral RNA making the CA-SP1 cleavage site available. The protease then cleaves at CA-SP1, releasing CA. The sequential cleavage that results in the release of NC-RNA and SP1 not only destabilizes the immature lattice, but also allows the CTD of CA to reorient itself relative to the NTD forming the mature contacts that are required for efficient formation of the CTD-CTD trimer interface.

Gag cleavage by protease occurs in the order SP1-NC>MA-CA≥SP2-p6>NC-SP2>CA-SP1 (Pettit et al., 1998; Wiegers et al., 1998), and CA-SP1-NC does not accumulate during HIV-1 maturation. This could mean that CA-SP1-NC is not a relevant structural intermediate with which to study maturation, given that NC is released before MA. However, we think that CA-SP1-NC is a relevant model for the assembly intermediate. Our reasoning is based on the fact that cleavage of MA, as reported by high-resolution structures, does not appear to affect the CA-CTD structure, but rather results in the formation of a beta-hairpin at the N-terminus of the CA-NTD (Kelly et al., 2006; Tang et al., 2002). Cleavage of MA-CA is important in the formation of the beta-hairpin (Cortines et al., 2011; Tang et al., 2002; von Schwedler et al., 1998; Wildova et al., 2008), but the role of the beta-hairpin in mature HIV-1 capsid formation is not well understood. Our studies support prior knowledge that the NTD of CA-SP1-NC may fold in a manner similar to mature conformations. However, the orientation of CA-CTD is strikingly different in CA from that of CA-SP1-NC, with the CA-CTD conformations in CA-SP1-NC at its immature-like state. This is exemplified by lack of CTD trimer interface density at this locus and validated by in vitro and in vivo disulfide crosslinking

experiments of the 207C/216C. Our results with HIV-1 particles in the CA-SP1 background further demonstrate that the release of SP1 is critical for the formation of the trimer interface, corroborating that the CA-SP1-NC exhibit an immature trimer interface similar to CA-SP1. This result further validates the CA-SP1-NC as a structural model for viral maturation.

Results from our studies suggest that the release of SP1 is critical for the formation of a mature trimer interface in HIV-1 capsid. The trimer interface may therefore control mature capsid structure. Viral mutants with substitutions in the CA protein that prevent cleavage between CA and SP1 contain unstable, incompletely formed spherical capsids (Wiegers et al., 1998). Previous studies identified mutations in the CTD-CTD trimer interface including Q219A, K203A, E213A, and E213Q, which alter the intrinsic stability of the viral capsid and impair infectivity without altering the structure of the capsid (Byeon et al., 2009; Forshey et al., 2002). This suggests that the trimer interface is important for both capsid structure and stability. CA-SP1 cleavage is also a target of the small molecule inhibitor Bevirimat that binds and inhibits HIV-1 maturation by blocking cleavage of this site (Blair et al., 2009; Li et al., 2003; Zhou et al., 2004). Since Bevirimat is purported to stabilize an immature lattice, it can be inferred that cleavage of SP1 results in the conversion of an intermediary immature capsid into a mature capsid (Keller et al., 2011), which is consistent with a Gag mutant that is defective in CA-SP1 cleavage. Another inhibitor has also been found to bind and act in a manner similar to Bevirimat, but comes from a different class of compounds (Blair et al., 2009). It would be ideal to make HIV-1 particles in the presence of Bevirimat and analyze the formation of capsid interfaces. The results from such experiments can further

inform of the effects of Bevirimat in interface formation. Since Bevirimat prevents cleavage between CA-SP1, I predict that the effects of Bevirimat will be similar to those of CA-SP1. In summary, structural insights into the formation of the mature CA-CTD trimer interface upon cleavage of Gag represent a significant advance in our understanding of HIV-1 maturation. These experimental findings about the trimer interface are of great interest as they answer some of the basic questions about maturation and may also be important for developing new HIV-1 maturation inhibitors.

CHAPTER V

SUMMARY AND FUTURE DIRECTIONS

Uncoating is still a poorly understood step in the HIV-1 life cycle. The characterization of viral determinants of uncoating is crucial for advancement in HIV-1 basic biology and drug development to target HIV/AIDS. My results, as discussed in Chapters II and III of this dissertation, have shown that intersubunit interfaces (NTD-CTD and CTD-CTD trimer interfaces) are critically important for assembly and stability of the HIV-1 capsid. These genetic studies were based on the X-ray structural model of the capsid for NTD-CTD (Pornillos et al., 2009), and on a cryoEM model of the capsid generated at 9 Å by Dr. Peijun Zhang and her group at the University of Pittsburgh School of Medicine. These structures enabled the mutational analysis of CA positions to: (1) validate the structural models by engineered disulfide crosslinking, and (2) determine the functional role of the intersubunit interfaces. The ability to relate structure to function, as described in Chapters II and III, provides valuable fundamental knowledge about capsid stability and assembly and the role of specific residues located at the interfaces. Based on these data and work from previous studies, capsid stability appears to be coordinated between intersubunit interfaces: the NTD-CTD and CTD-CTD trimer interfaces analyzed here, and residues that were later identified to contribute to the NTD-NTD interactions reported in previous studies (Pornillos et al., 2009). The results from Chapter III also provide new and important information about the hydrophobic core of the trimer interface.

Our present understanding of the interfaces in the HIV-1 capsid comes mainly from structural studies using recombinant proteins and from crosslinking analysis, and these techniques have limitations. A functional approach to establish the presence of an interface would be complementary. The prevalence of charged residues at some of the interfaces (NTD-NTD and NTD-CTD in particular) suggests that major interactions are electrostatic. Studies in Chapter II of my dissertation show that altering the charges at the interface by alanine mutations results in dramatic impairment of viral infectivity and alter capsid stability. One way to functionally confirm the role of charge-charge interactions at interfaces in the mature HIV-1 capsid would be to perform structure-guided charge reversal of amino acids suspected for possible interaction. Mutant viruses with these substitutions would be studied for infectivity and characterized with other biochemical assays. For example, K140 lies in close proximity to E212, and a mutant K140E/E212K could be made and analyzed as proposed, while the single mutants could be used as controls. If charge interactions are important, it would be noted that charge reversal will maintain wild type activity of infectivity and stability. This would mean that the residues are in contact and interact in the virus. However, these charges could also organize water molecules that can mediate intersubunit interactions. Altogether, these results could link the structure of the capsid interfaces and the functional role of residues at those interfaces.

The presence of the capsid interfaces could also be functionally demonstrated through the generation of pseudo-revertants of HIV-1 mutants. Although reversion is stochastic, mutations on one arm of the interface could be corrected by alterations in the other interacting surface. The critical side chain amino acid mutants that show poor infectivity due to changes in the stability of the capsid could be adapted for growth by serial passaging in

CEM cells and analyzing the RT activity every two days. Wherever there is growth, DNA will be isolated and sequence for possible reversion. Historically, second-site compensatory changes have provided valuable information on the relationship between protein structure and function and have defined potential intermolecular and intramolecular interactions in HIV-1 and other retroviruses (Bowzard et al., 2001; Cimarelli et al., 2000; Freed and Martin, 1996; Ono et al., 1997). P38A is a poorly infectious virus that contains unstable capsids. When P38A was selected for second-site reversions, T216I was identified as a second-site suppressor (Yang et al., 2012). This result suggested that the CTD-CTD trimer interface can offset deleterious defects induced at the NTD-NTD interface. Therefore, all interfaces are involved in balancing the stability of the capsid.

The structural mechanism of disassembly of the capsid is also very important, since disassembly should not happen too soon (unstable CA mutants, action of small molecule compounds such as PF74, activity of host factors such as TRIM5α), or too late (hyperstable CA mutants and action of small molecule compound BI-1) (Blair et al., 2010; Byeon et al., 2009; Forshey et al., 2002; Stremlau et al., 2004; Yang and Aiken, 2007; Yang et al., 2012). The disassembly of the capsid may happen as a response to cues such as reverse transcription and or binding to host factors (Hulme et al., 2011; Yang et al., 2012). However, we do not know whether uncoating occurs by the systematic release of monomeric CA, single hexameric CA or by the release of strands of CA hexamers. This may depend on which of the capsid interfaces fall apart during the process of uncoating. Since intersubunit interfaces hold the capsid units together, it is conceivable to ask the essential question about disassembly: which of the interfaces comes apart first, or where on the capsid surface is the process of uncoating initiated? Based on my data,

obtained by analysis of capsid mutants at the NTD-CTD and CTD-CTD interfaces using biochemical approaches (in vitro uncoating, core-associated CA, abrogation of restriction) and similar analysis of the NTD-NTD and some at the CTD-CTD interface from published observations, intersubunit interfaces do not show dominance of any interface in controlling capsid stability. These results suggest that all capsid interfaces are critically important in stabilizing the capsid. However, looking at the architecture of the capsid intrahexameric interactions are formed by two large interfaces, NTD-CTD, and NTD-NTD interactions. I speculate that the sum total of the energy generated by these intrahexameric interactions may make it difficult to break intrahexameric bonds, making interhexameric contacts with only one interface, the CTD-CTD interface, the more liable interface to initiate disassembly. This conceptual model is indirectly supported by studies with TRIM5α disassembly of tubes assembled in vitro. Binding of TRIM5α to assembled tubes released discrete linear fragments. The release of these fragments was reduced when the CTD-CTD trimer interface was stabilized using engineered Cys disulfide crosslinking, which was not the case when the NTD-NTD interface was stabilized by engineered Cys disulfide crosslinking (Zhao et al., 2011). This result suggests that one way to break the capsid is to strip the hexamers apart at the CTD-CTD trimer interface leaving a string of hexamers held by NTD-NTD and NTD-CTD bonds. Future studies can focus on the structural aspects to understand how the capsid is disassembled; i.e. which capsid interface is critical for uncoating or which of the capsid interfaces fall apart to initiate uncoating. Applying the techniques of crosslinking and factors that affect capsid stability can do this. Briefly, this would require HIV-1 mutant cores (stabilized by disulfide linkages at different interfaces) and recombinant proteins (with similar

mutations). Previous work from our laboratory showed that capsid stability is affected by small molecule compounds, cellular factors, temperatures, and pH (Blair et al., 2010; Forshey et al., 2002). To study how the capsid falls apart, HIV-1 cores will be isolated from mutant viruses stabilized by engineered Cys disulfide crosslinking and allowed to undergo uncoating at different time points and using the various parameters. Pelleted samples would then be analyzed by non-reducing SDS-PAGE /immunobloting and by negative stain and observed by transmission electron microcopy. An analysis of the kinetics of uncoating and the dissociated fragments or oligomers formed from partially or fully disassembled disulfide-stabilized CA can provide knowledge about the disassembly of the HIV-1 capsid. Alternatively, or in addition to the above, assembled protein with these crosslinks would be analyzed in a similar way as purified cores. Several outcomes are possible, but the most desirable outcome is that which shows rapid disassembly of one interface in the presence of uncoating promoting conditions but not in its absence. This, if present for only one interface would mean this probably is the interface that initiates uncoating. This should be supported by analysis by negative stain of partially uncoated CA.

Much is known about the structure of the mature HIV-1 capsid and the various interfaces present. This structure shows that the mature capsid is composed of four intersubunit interfaces that help form the mature capsid: NTD-NTD and NTD-CTD intrahexameric interfaces and a CTD-CTD dimer and CTD-CTD trimer interhexameric interfaces, and that the conical shape of the mature core results from the uneven distribution of pentamers in its hexameric lattice. We also know that the immature HIV-1 Gag lattice is hexameric, but no evidence for pentamer inclusions exists. Moreover, there

is no detailed understanding of the immature lattice, and it remains unknown what happens during maturation with respect to interface formation: whether the hexameric lattice in the immature completely disassembles and reassemble de novo during maturation or whether the subunits in the hexameric assembly rearrange to form the mature HIV-1 capsid. This has given rise to two maturation models.

1. Disassembly and reassembly model of maturation.

This model postulates that the hexameric Gag lattice completely disassembles during maturation and reassembles upon the completion of Gag processing. According to the model, cleavage of Gag results in complete disruption of the hexameric lattice to CA dimers. Assumptions for this model comes from structural studies conducted recently where it was proposed that CA monomers or dimers or hexamers reassemble de novo after proteolysis of Gag (Briggs et al., 2006). This proposal was based on the observation that there is an inherent relationship between the cap diameter at the wide end of the core and the virion size, which was not the case with the cap diameter at the narrow end. This observation led them to assume that the immature capsid has to disassemble and reassemble de novo with the cone growing from the narrow end of the capsid. Recent structural studies of the Mason Pfizer monkey virus suggested that the NTD-CTD interface that is structurally and functionally present in mature retrovirus capsid is absent in assemblies of uncleaved Gag, and argued that intrahexameric interactions in immature retrovirus capsids were formed by CTD-CTD interactions (Bharat et al., 2012). A similar inference about the NTD-CTD interface was suggested following experiments using hydrogen-deuterium exchange (Lanman et al., 2004; Monroe et al., 2010). H/D exchange mass spectrometry deals with the exchange of amide protons that are unprotected, with

those in solution (deuterium). Protons that are protected by participating in subunit interactions are not be available for amide exchange. Monroe et al., (2010) showed with immature virus-like particles rapid exchange of deuterium occurred in the peptide residues that participate in an NTD-CTD interface mature viral-like particles, indicating that the NTD-CTD interactions are not yet formed in the immature virus. Furthermore, a recent study suggested that the position of the NTD of CA in immature HIV-1 virus is quite different from its position in the mature virus, arguing that the interactions that exist in the immature must therefore be different from those in mature virus (Briggs et al., 2009). The implication that arises from this model is that contacts that are present in the immature capsid must be different from those in the mature capsid, but may also argue that large conformational changes happen during maturation. All together, this suggests that the immature capsid may disassemble and then reassemble de novo to form the mature capsid, and that he capsid interfaces in immature maybe different from those in the mature capsid.

2. Subunit rearrangement model of maturation.

This model proposes that complete disassembly of subunits is not required for maturation and formation of mature capsid interfaces. In this model, the mature capsid is formed through the slight alterations in intersubunit contacts during Gag cleavage, specifically upon the release of SP1, without lattice disassembly. In this case, intersubunit contacts in the immature capsid are very similar to those in mature viruses. The model is based on the theory that a major conformational switch occurs during maturation that converts an immature lattice into a mature lattice (Ivanov et al., 2007; von Schwedler et al., 1998). Evidence for this model comes from studies using hydrogen-deuterium

exchange experiments, and electron cryotomography (Monroe et al., 2010; Wright et al., 2007), where both suggest the presence of an NTD-NTD interface making similar contacts as those seen in the mature HIV-1 capsid, but different lattice spacing in mature and immature. Hence, this model implies that contacts present in the immature are largely present in the mature capsid. However, having similar contacts does not exclude disassembly as a mechanism for maturation, but it appears unlikely that an immature virus would disassemble completely just to reassemble with the same contacts.

A powerful technique that I developed to probe the presence of capsid interface formed in mature virus particles (NTD-CTD in Chapter II, CTD-CTD trimer interface in Chapter III) has many applications, one of which can be applied in the study of maturation and interface formation. This technique, as described in Materials and Methods, utilizes engineered disulfide crosslinking at predicted residues based on structural proximity of ~5 Å and geometric accommodation. Viral particles made with Cys mutations at these positions are then analyzed by non-reducing SDS-PAGE and immunobloting with anti-CA antibody. I have shown in Chapter IV of my dissertation (Figure 4-5) that engineered disulfide crosslinking of the NTD-NTD and NTD-CTD interfaces in CA-SP1 background show the accumulation of higher-order oligomers similar in pattern and efficiency to those obtained from engineered Cys in wild type. However, the efficiency of crosslinking at the trimer interface of CA-SP1 appeared to less efficient compared to that in CA. Using CA-SP1-NC as a model for immature HIV-1, I also showed that cleavage of the CA-SP1 transforms an immature virus into a mature virus with the formation of a mature trimer interface, but did not have an effect on the formation of the NTD-NTD and NTD-CTD interfaces. These results support that subunit

rearrangement model of maturation and suggest that cleavage of CA-SP1 rearranges the lattice leading to the formation of a mature trimer interface.

The determination of the cryoEM structure of CA-SP1-NC and the mutational analysis studies revealed changes that occur during maturation of the capsid. These studies concentrated on assembled CA-SP1-NC and CA-SP1. However, CA-SP1 is produced during the later steps in the maturation process, and CA-SP1-NC is not a true maturation intermediate. Early and "true" processing intermediates have not been assessed for interface formation while the formation of capsid interfaces in fully assembled, unprocessed Gag has not been studied. As part of the future studies it is important to know the nature of interactions in the Gag lattice and subsequent intermediates. Specifically, I propose to analyze the capsid interfaces in the mature virions, compared to the immature or these maturation intermediates. This can be done using the engineered disulfide crosslinking.

The novel application of crosslinking can be applied to unprocessed Gag, MA-CA-SP1, and mutant viruses containing engineered cysteines. Specifically, 207C/216C, 14C/45C, 17C/19C, 68C/212C, 204C mutations will be made in MA-CA, PR-, MA-CA-SP1. These are cleavage defective HIV-1 mutants that contain substitutions in the cleavage sites and prevent protease from cleavage at those sites. An analysis of the banding pattern obtained from non-reducing SDS-PAGE would provide insight into which of the two maturation models is likely. If, for example, a hexameric ladder is obtained from crosslinking of the A14C/E45C in the MA-CA-SP1 background, it would indicate that this interface is present in this intermediate structure and supports the subunit rearrangement model of maturation. Alternatively, the absence of crosslinking

would mean that this interface is not present in the MA-CA-SP1 intermediate. It is important to note that crosslinking analysis of these intermediates alone cannot satisfactorily answer these questions and so a complete answer would have to include high-resolution structures of these intermediates.

Another maturation step that may be linked with interface formation and critical for maturation is the formation of the β-hairpin. Cleavage at the MA-CA site is important and results in the formation of a β-hairpin structure, which is anchored by a salt bridge formed between Asp51 and Pro1. It has also been suggested that if the β-hairpin is not formed, the NTD-NTD interface may not be formed (Gross et al., 1998; Kelly et al., 2006; Pornillos et al., 2010; von Schwedler et al., 1998). Formation of the β-hairpin may occur in order to facilitate proper positioning of both CTD and NTD domains for eventual formation of mature capsid interfaces. However, the high resolution structure of the CA hexamer did not show evidence for any involvement of the β-hairpin in intersubunit interactions, yet the formation of this structure is vital for mature capsid formation, essential in the assembly of the capsid, but itself is not sufficient to make a mature capsid. (Mortuza et al., 2004; Pornillos et al., 2009; von Schwedler et al., 1998). This means that the consequence of β-hairpin formation on capsid interfaces is not known. Mutations in CA that prevent cleavage between MA and CA has transdominant infectivity impairments (Lee et al., 2009). This could be as a result of preventing proper juxtaposition of CA elements used in the formation of an essential interface during maturation.

It has long been assumed that cleavage at the MA-CA junction leads to formation of the β-hairpin. However, recent studies suggest that cleavage of the MA-CA does not

immediately result in the folding of the β-hairpin, but that folding and formation of the β-hairpin occurs following cleavage at CA-SP1 (Monroe et al., 2010). This data raises questions about the timing of the β-hairpin formation and its role in capsid interface formation. The effects of structural alterations at the N-terminal domain of CA in interface formation are not known. If the β-hairpin is formed only after cleavage of CA-SP1 as suggested by recent studies, then my crosslinking results suggest that β-hairpin formation is not required for NTD-NTD and NTD-CTD interface formation. As discussed in Chapter IV (Figure 4-5), crosslinking of 17C/19C, and 68C/212C (NTD-NTD and NTD-CTD interfaces respectively) in the CA-SP1 background show that these mutants efficiently form disulfide bonds that oligomerize to form hexamers. I have made similar observations with 14C/45C (data not shown). However, formation of the CTD-CTD trimer interface was less efficient and thus is dependent upon cleavage of SP1 from CA. This result shows that formation of the β-hairpin is not required for interface formation.

Analysis of the MA-CA intermediate for interface formation is paramount to understanding the consequence of β-hairpin for interface formation (if any), and when folding of the β-hairpin actually occurs. In a paper published in 2010, Prevelige's group observed, by hydrogen/deuterium exchange, that the NTD-NTD interface in particles containing uncleaved MA-CA is protected from H/D exchange in a manner similar to mature virus (Monroe et al., 2010). This suggests that similar CA-CA interactions are present in both MA-CA and mature virions. Analysis of the oligomeric states of CA proteins released from the disulfide stabilized cores in the MA-CA background by non-reducing SDS-PAGE and the extent of crosslinking may be helpful. Additionally, a

systematic mutational analysis of the β-hairpin to test for mutations that affect interface formation would be important. It has been shown that the D51A substitution in CA disrupts β-hairpin formation (Abdurahman et al., 2007). Additionally, one could graft the β-hairpin of a related virus (MLV) onto the HIV-1 CA protein sequence. Engineering these mutations in the viruses containing engineered disulfide crosslinks can be used to analyze if formation of any of the interfaces is perturbed. This would answer whether formation of the β-hairpin is important for interface formation. I, in collaboration with Dr. Peijun Zhang's group, have begun to undertake this work to specifically understand the transition from the immature Gag lattice to the mature capsid lattice, and the conformational changes that take place during maturation, using both biochemical assays and high-resolution structures of the immature Gag lattice and its maturation intermediates.

In summary, my research has shown that the NTD-CTD interface and the CTD-CTD trimeric interface are critically important for HIV-1 capsid assembly and stability. I have also shown that the CTD-CTD trimer interface is formed only after cleavage of CA-SP1. A detailed understanding of how the capsid is assembled or stabilized, and how it uncoats, represents an important advance for HIV-1 capsid biology and highlights the viral capsid as an attractive target for anti-HIV therapy.

CHAPTER VI

MATERIALS AND METHODS

Cells

The 293T, HeLa-P4, HeLa, TZM-bl, OMK cells used in these studies were cultured in Dulbecco's modification of Eagle's medium (DMEM; Cellgro) supplemented with 10% fetal bovine serum (FBS), penicillin (50 IU/ml), and streptomycin (50 µg/ml). All cells were cultured in a humidified 37˚C incubator containing 5% CO_2. CEM cells were cultured in RPMI 1640 medium supplemented with 10% FBS, penicillin (50 IU/ml), streptomycin (50 µg/ml) and in a humidified 37˚C incubator containing 5% CO_2.

Viruses

R9 is a wild type HIV-1 proviral DNA construct that has complete open reading frames for all HIV-1 structural and accessory genes. Point mutations in the CA region of proviral HIV-1 R9 plasmid (H62A, Q63A, A64D, M68A, E71A, E75A, K140A, R162A, V165A, D166A, R167A, Q176A, Q179A, E180A and M215A or A204C, A204D, A204K, A204L, A204Y, I201A, I201D, I201V, L205A, L205D, L205K) and the double cysteine mutants (M68C/E212C, Q63C/Y169C, M68C/E211C, A64C/E211C, M144C/M215C) were introduced by PCR mutagenesis. The mutant viral fragments were reintroduced into R9 with the unique restriction site pairs BssHII-ApaI, Spe1-ApaI, and BssHII-Spe1, depending on the location of the residue on the CA region. Viruses used for the abrogation-of-restriction assay were Env-deficient R9 mutants pseudotyped by the

vesicular stomatitis virus glycoprotein (VSV-G) (Forshey et al., 2005) and were generated by transferring the BssHII-Apa1 fragments from the CA mutants of R9 to R9ΔE. CA-SP1-NC and CA-SP1 cleavage mutants were generated as described (Wiegers et al., 1998). CA-SP1-NC amino-terminal mutants (H62A, A64D, M68A, K140A) were generated by transferring the BssHII-SpeI fragment of their R9 CA mutant viruses into CA-SP1-NC ΔE (Wyma et al., 2004). CA-SP1-NC carboxyl-terminal mutants (R162A, V165A, D166A, M215A, A204D, A204K, and A205D) and the double cysteine cleavage mutants were created by segment overlap PCR copying of their R9 CA mutants and the cleavage sites of CA-SP1-NC. The regions of the mutants insert on the viral plasmid corresponding to the PCR-generated fragment were sequenced to confirm the presence of these mutations and absence of extraneous mutations.

Virus stocks were produced by calcium phosphate transient transfection (Chen and Okayama, 1987) of 293T cells in which 20 μg of plasmid DNA was used per 2.0 x 10^6 cells in 10 cm dishes as previously described (Chen and Okayama, 1987). Pseudotyped particles were produced by cotransfection 15 μg of Env-defective proviral constructs with 5 μg of plasmid pHCMV-G (Yee et al., 1994). 12-16 hours after transfection, the supernatant was removed from the plate and the cells were washed with sterile PBS before adding fresh media. The culture supernatants were harvested 48 hr after transfection and filtered through a 0.45 μm-pore-size filters. Viral aliquots were frozen at -80°C and virus production quantified by p24 ELISA as previously described (Wehrly and Chesebro, 1997) or by RT activity (Aiken, 1997). For experiments involving qPCR detection of HIV-1 cDNA, particles were produced using the TransIT®-293 Transfection Reagent according to the manufacturer's protocol (Mirus).

Single-cycle assay of HIV-1 infectivity

Viral infectivity was assessed by titration on TZM-bl cells (Wei et al., 2002). The TZM-bl cell line is a HeLa cell clone engineered to express CD4+, CXCR-4 and CCR5. These cells contain Tat-responsive luciferase and LacZ reporters. HIV-1 viral stocks were serially diluted in culture medium containing polybrene or DEAE-dextran (8 μg/ml or 20 μg/ml, respectively), and samples (100 μl total volume) were used to inoculate TZM-bl target cells seeded the day before (15,000 cells per well in 96-well plates). The cultures were maintained for an additional 48 hr prior to lysis and detection with a luciferase substrate, (Steady-Glo, Promega). To determine the extent of infection, the luminescence reading in relative light units (RLU) was measured in a Topcount instrument (Perkin Elmer). The corrected RLU values were normalized by RT or p24 to calculate the specific infectivity of the viruses in RLU/RT or RLU/p24.

Viral replication assay

Viral stocks were inoculated on CEM (40,000 cells/well in 96-well plate) cells at low MOI. Samples of culture supernatants were withdrawn every 3 days and an equal volume of fresh media added to the wells. Culture supernatants were quantified by p24 ELISA or by RT activity as previously described (Wehrly and Chesebro, 1997) or by RT activity (Aiken, 1997).

Crosslinking assay

Viruses were produced by transfection of the mutant plasmids and pelleted by ultracentrifugation (100,000 x*g*, 30 min) through a 20% sucrose cushion. The pellet was

dissolved in SDS sample buffer in the presence or absence of reducing agent, β-mercaptoethanol. Samples were heated at 95˚C for 5 min and then analyzed by SDS-PAGE. CA was detected by immunoblotting using a rabbit polyclonal specific CA antibody. The secondary antibody, anti-rabbit antibody, was conjugated to Alexa Fluor 680 for Odyssey analysis.

Transmission electron microscopy

Cultured HeLa cells were transfected with 2.5 μg of viral DNA plasmids using the TransIT-HeLaMonster transfection kit (Mirus) according to the manufacturer's protocol. 24 hr after transfection, cells were washed with phosphate buffered saline (PBS) and fixed with 2.5% glutaraldehyde. The fixed cells were detached from the plates by gentle scraping, pelleted by centrifugation at 4˚C and the pellet incubated for 3 hr in an ice-water bath. Following incubation, the cells were washed several times with PBS and the cell pellet was shipped to Electron Microscopy BioServices (Gaithersburg, MD) for embedding, sectioning, and microscopic examination. Pellets were post-fixed in 1% osmium tetroxide and washed in ultra pure water. The samples were then bloc-stained with 2% uranyl acetate and dehydrated in ethanol. Ultra-thin sections were cut and mounted onto 200 mesh copper grids and post-stained with uranyl acetate and Reynolds's Lead Citrate; and examined in a FEI Tecnai Spirit Twin Transmission Electron Microscope at 80kV at a minimum magnification of 30,000X. In some cases, samples were fixed differently. Samples were fixed on a 35 mm dish for about two hours and the cells were never scraped from the plate surface. After fixing the cells the fixative was

removed and the plate, washed twice with sterile 1X PBS before filling the plate with sterile 1X PBS, sealed and sent off for analysis.

Isolation of HIV-1 cores

HIV-1 cores were isolated and characterized as previously described (Shah and Aiken, 2011a). Supernatants from transfected 293T cells were filtered through a 0.45 µm-pore filter to remove cellular debris before ultracentrifugation (120,000 x*g* for 3 hr at 4˚C using Beckman rotor SW-32Ti) through a cushion of 20% sucrose in PBS buffer to concentrate the virions before core isolation. The viral pellet was re-suspended in 250 µL 1X STE buffer (10 mM Tris-HCl, 100 mM NaCl, 1 mM EDTA, pH 7.4) and incubated on ice for 2 hr prior to ultracentrifugation (120,000 x g) over a 10 ml linear sucrose gradient (70% to 30% in STE buffer) overlaid with 15% sucrose solution containing 1% Triton X-100 and 7.5% sucrose barrier cushion on top. An overnight (16 hr to 18 hr) ultracentrifugation using the Beckman SW-32Ti rotor at 4˚C, partitioned the CA assoluble CA (primarily on the top of the gradient) and core-associated CA (found mostly in the bottom fractions of the gradient). For each virus, the level of core-associated CA was determined as a percentage of the total CA in the gradient (based on ELISA). I used a commercial ELISA (SAIC, Frederick) to analyze the D166A and R167A mutants, which were not detected by the standard ELISA.

In vitro uncoating assay

The assay was carried out as previously reported (Shah and Aiken, 2011a), with the following modifications. Frozen aliquots of purified HIV-1 cores (300 µl) were

thawed and diluted in 300 µl of cold STE buffer. 100 µl of the diluted cores were mixed with 150 µl of 1X STE buffer and incubated at 37˚C in a final concentration of 10 µg/ml of BSA. Immediately following incubation, the reaction was stopped by placing the tube in an ice-water bath for 10 min, and then tubes were centrifuged at 100,000 x*g* (Beckman TLA-55 rotor at 45,000 rpm) for 20 min at 4˚C to pellet the remaining cores. The supernatant was removed, while the pellet was dissolved in 250 µl of p24 ELISA sample diluent (10% calf serum and 0.5% Triton X-100 in phosphate-buffered saline). The CA content in both fractions (pellet and supernatant) was quantified by p24 ELISA, and the extent of uncoating was determined as the ratio of CA in the supernatant to the total CA quantity in the reaction.

Abrogation-of-restriction assay

The reporter virus, HIV-1-GFP pseudotyped with VSV-G, was used to infect OMK (owl monkey kidney) cells, as previously described (Forshey et al., 2005). 20,000 OMK cells per well in 12-well plate were seeded 24 hr before infection. To identify the appropriate dose of the reporter virus to use, it was first titrated on OMK cells to determined the dose of GFP reporter virus required to achieve an infection level of ~0.5% just before the inflection point in the infection curve. With a fixed concentration of reporter virus, and increasing concentrations of test viruses, the mixture in a 600 µl final volume of media containing 8 µg/ml polybrene, was used to infect OMK cells, adding fresh media after 24 hr. After 48 hr, cells were dissociated with trypsin and fixed by the addition of an equal volume of PBS containing 4% paraformaldehyde. GFP expression

was quantified by flow cytometry using an Accuri C6 flow cytometer. The percentage of GFP-expressing cells was determined from a minimum of 10,000 cells analyzed.

Assay of reverse transcription in target cells

For analysis of viral DNA synthesis by qPCR, virus were produced by transfecting 293T cells using the 293T transfection reagent (Mirus), according to the manufacturer's protocol, with a few modifications. We found this transfection procedure to be effective at for minimizing levels of carryover plasmid DNA, thereby providing acceptable backgrounds in the PCR-based assay of reverse transcription. Briefly, 8 hr post transfection the media was removed and the cells washed with PBS before replenishing media. Viruses were harvested 36-48 hr later. Virus stocks were pretreated with 20 μg of DNase 1, 10 μM $MgCl_2$, and 1 μM of $CaCl_2$ at 37˚C for 1 hr to remove contaminating plasmid from transfection and 100 ng of p24 was used to infect 100,000 HeLa P4 cells per well in a 12-well plate. For control, parallel infections were performed in the presence of 1 μM Efavirenz, a reverse transcription inhibitor. After 8 hr of infection cells were harvested by detaching with trypsin and DNA isolated. To harvest the cells, the supernatant was removed and the cells were washed once with 1 ml of PBS before trypsinization. Cells were pelleted and washed again with 0.5 ml of PBS and the pellet resuspended in 100 μl PCR lysis buffer (10 mM Tris-HCl, 1 mM EDTA, 0.2 mM $CaCl_2$, 0.001% Triton X-100, 0.001% SDS, 1 mg/ml proteinase K) and incubated at 58˚C for 1 hr, followed by heat inactivation at 95˚C for 15 minutes. Viral DNA was quantified by real-time PCR using a Stratagene MX-3000p instrument with SYBR Green detection. The reaction mixture contained 5 μl of infected lysate, 12.5 μl of 2X SYBR Green PCR

Master Mix (Roche), and 500 nM of each primer. Second strand reverse transcription products were amplified using 5-AGCAGCTGCTTTTTGCCTGTACT-3 as the sense primer and 5-CCTGCGTCGAGAGAGCTCCTCTGG-3′, as the reverse primer. The thermal cycling conditions were set at 50°C for 2 min and 95°C for 10 min, followed by 40 cycles of 95°C for 15 secs and 65°C for 45 secs. I tested how much DNA was loaded to qPCR reactions by measuring the absorbance at A260 in each lysate, and the quantities of DNA analyzed were within 5% of one another.

Protein expression and purification

Plasmids for the expression of full-length HIV-1 CA proteins were obtained as described in virus constructs. An NdeI/XhoI fragment was amplified from WT and mutant plasmids 5' GGAATCCCATATGCCTATAGTGCAGAACCTCCAGGGG as sense primer and 5' CCCCTCGAGTCACAAAACTCTTGCTTTATGGCCGGG as anti-sense primer. This PCR amplified fragment was cloned into the NdeI/XhoI region of the pET21a and the regions of the mutations corresponding to the PCR-generated fragment were sequenced to confirm the presence of these mutations and absence of extraneous mutations. The CA proteins were expressed in *E*. coli BL21-DE3 and purified as previously described (Ganser et al., 1999) and eluted using a UnosphereQ column (Bio-Rad) with increasing concentrations of NaCl, ranging from 0.6 M to 1 M. The protein was then dialyzed into 50 mM Na_2PO_4 buffer, pH 8 before concentration using a Centriprep centrifugal filter (Millipore). Concentrated protein solution was quantified and stored in aliquots frozen at -80˚C until needed.

In vitro capsid assembly and analysis

80 µl of the purified crosslinked mutant CA proteins were assembled in vitro by rapid dilution into buffer containing 2 M NaCl for 1 hr at room temperature. The final concentration of the protein was 40 µM; and 1 mM for NaCl. The assembled protein was centrifuged and the pellet resuspended in minimal volume of assembly buffer. Samples were stained with 1% uranyl acetate for electron microscopic analysis.

REFERENCES

Abdurahman, S., Youssefi, M., Hoglund, S., and Vahlne, A. (2007). Characterization of the invariable residue 51 mutations of human immunodeficiency virus type 1 capsid protein on in vitro CA assembly and infectivity. Retrovirology *4*, 69.

Aiken, C. (1997). Pseudotyping human immunodeficiency virus type 1 (HIV-1) by the glycoprotein of vesicular stomatitis virus targets HIV-1 entry to an endocytic pathway and suppresses both the requirement for Nef and the sensitivity to cyclosporin A. Journal of virology *71*, 5871-5877.

Aiken, C. (2006). Viral and cellular factors that regulate HIV-1 uncoating. Curr Opin HIV AIDS *1*, 194-199.

Aiken, C. (2009). Cell-free assays for HIV-1 uncoating. Methods Mol Biol *485*, 41-53.

Ako-Adjei, D., Johnson, M.C., and Vogt, V.M. (2005). The retroviral capsid domain dictates virion size, morphology, and coassembly of gag into virus-like particles. Journal of virology *79*, 13463-13472.

Arhel, N.J., Souquere-Besse, S., Munier, S., Souque, P., Guadagnini, S., Rutherford, S., Prevost, M.C., Allen, T.D., and Charneau, P. (2007). HIV-1 DNA Flap formation promotes uncoating of the pre-integration complex at the nuclear pore. The EMBO journal *26*, 3025-3037.

Bartonova, V., Igonet, S., Sticht, J., Glass, B., Habermann, A., Vaney, M.C., Sehr, P., Lewis, J., Rey, F.A., and Krausslich, H.G. (2008). Residues in the HIV-1 capsid assembly inhibitor binding site are essential for maintaining the assembly-competent quaternary structure of the capsid protein. The Journal of biological chemistry *283*, 32024-32033.

Berthet-Colominas, C., Monaco, S., Novelli, A., Sibai, G., Mallet, F., and Cusack, S. (1999). Head-to-tail dimers and interdomain flexibility revealed by the crystal structure of HIV-1 capsid protein (p24) complexed with a monoclonal antibody Fab. The EMBO journal *18*, 1124-1136.

Bharat, T.A., Davey, N.E., Ulbrich, P., Riches, J.D., de Marco, A., Rumlova, M., Sachse, C., Ruml, T., and Briggs, J.A. (2012). Structure of the immature retroviral capsid at 8 A resolution by cryo-electron microscopy. Nature *487*, 385-389.

Blair, W.S., Cao, J., Fok-Seang, J., Griffin, P., Isaacson, J., Jackson, R.L., Murray, E., Patick, A.K., Peng, Q., Perros, M.*, et al.* (2009). New small-molecule inhibitor class targeting human immunodeficiency virus type 1 virion maturation. Antimicrobial agents and chemotherapy *53*, 5080-5087.

Blair, W.S., Pickford, C., Irving, S.L., Brown, D.G., Anderson, M., Bazin, R., Cao, J., Ciaramella, G., Isaacson, J., Jackson, L.*, et al.* (2010). HIV capsid is a tractable target for small molecule therapeutic intervention. PLoS pathogens *6*, e1001220.

Bowzard, J.B., Wills, J.W., and Craven, R.C. (2001). Second-site suppressors of Rous sarcoma virus Ca mutations: evidence for interdomain interactions. Journal of virology *75*, 6850-6856.

Briggs, J.A., Grunewald, K., Glass, B., Forster, F., Krausslich, H.G., and Fuller, S.D. (2006). The mechanism of HIV-1 core assembly: insights from three-dimensional reconstructions of authentic virions. In Structure, pp. 15-20.

Briggs, J.A., Riches, J.D., Glass, B., Bartonova, V., Zanetti, G., and Krausslich, H.G. (2009). Structure and assembly of immature HIV. Proceedings of the National Academy of Sciences of the United States of America *106*, 11090-11095.

Briggs, J.A., Simon, M.N., Gross, I., Krausslich, H.G., Fuller, S.D., Vogt, V.M., and Johnson, M.C. (2004). The stoichiometry of Gag protein in HIV-1. Nature structural & molecular biology *11*, 672-675.

Briggs, J.A., Wilk, T., Welker, R., Krausslich, H.G., and Fuller, S.D. (2003). Structural organization of authentic, mature HIV-1 virions and cores. The EMBO journal *22*, 1707-1715.

Brun, S., Solignat, M., Gay, B., Bernard, E., Chaloin, L., Fenard, D., Devaux, C., Chazal, N., and Briant, L. (2008). VSV-G pseudotyping rescues HIV-1 CA mutations that impair core assembly or stability. Retrovirology *5*, 57.

Byeon, I.J., Hou, G., Han, Y., Suiter, C.L., Ahn, J., Jung, J., Byeon, C.H., Gronenborn, A.M., and Polenova, T. (2012). Motions on the millisecond time scale and multiple conformations of HIV-1 capsid protein: implications for structural polymorphism of CA assemblies. Journal of the American Chemical Society *134*, 6455-6466.

Byeon, I.J., Meng, X., Jung, J., Zhao, G., Yang, R., Ahn, J., Shi, J., Concel, J., Aiken, C., Zhang, P.*, et al.* (2009). Structural convergence between Cryo-EM and NMR reveals intersubunit interactions critical for HIV-1 capsid function. Cell *139*, 780-790.

Cardone, G., Purdy, J.G., Cheng, N., Craven, R.C., and Steven, A.C. (2009). Visualization of a missing link in retrovirus capsid assembly. Nature *457*, 694-698.

Chen, C., and Okayama, H. (1987). High-efficiency transformation of mammalian cells by plasmid DNA. Molecular and cellular biology *7*, 2745-2752.

Cimarelli, A., Sandin, S., Hoglund, S., and Luban, J. (2000). Basic residues in human immunodeficiency virus type 1 nucleocapsid promote virion assembly via interaction with RNA. J Virol *74*, 3046-3057.

Cortines, J.R., Monroe, E.B., Kang, S., and Prevelige, P.E., Jr. (2011). A retroviral chimeric capsid protein reveals the role of the N-terminal beta-hairpin in mature core assembly. Journal of molecular biology *410*, 641-652.

Datta, S.A., Temeselew, L.G., Crist, R.M., Soheilian, F., Kamata, A., Mirro, J., Harvin, D., Nagashima, K., Cachau, R.E., and Rein, A. (2011). On the role of the SP1 domain in HIV-1 particle assembly: a molecular switch? Journal of virology *85*, 4111-4121.

Diaz-Griffero, F., Kar, A., Lee, M., Stremlau, M., Poeschla, E., and Sodroski, J. (2007a). Comparative requirements for the restriction of retrovirus infection by TRIM5alpha and TRIMCyp. Virology *369*, 400-410.

Diaz-Griffero, F., Kar, A., Perron, M., Xiang, S.H., Javanbakht, H., Li, X., and Sodroski, J. (2007b). Modulation of retroviral restriction and proteasome inhibitor-resistant turnover by changes in the TRIM5alpha B-box 2 domain. Journal of virology *81*, 10362-10378.

Diaz-Griffero, F., Vandegraaff, N., Li, Y., McGee-Estrada, K., Stremlau, M., Welikala, S., Si, Z., Engelman, A., and Sodroski, J. (2006). Requirements for capsid-binding and an effector function in TRIMCyp-mediated restriction of HIV-1. Virology *351*, 404-419.

Dismuke, D.J., and Aiken, C. (2006). Evidence for a functional link between uncoating of the human immunodeficiency virus type 1 core and nuclear import of the viral preintegration complex. Journal of virology *80*, 3712-3720.

Dorfman, T., Bukovsky, A., Ohagen, A., Hoglund, S., and Gottlinger, H.G. (1994). Functional domains of the capsid protein of human immunodeficiency virus type 1. Journal of virology *68*, 8180-8187.

Du, S., Betts, L., Yang, R., Shi, H., Concel, J., Ahn, J., Aiken, C., Zhang, P., and Yeh, J.I. (2011). Structure of the HIV-1 full-length capsid protein in a conformationally trapped unassembled state induced by small-molecule binding. Journal of molecular biology *406*, 371-386.

Falke, J.J., and Koshland, D.E., Jr. (1987). Global flexibility in a sensory receptor: a site-directed cross-linking approach. Science *237*, 1596-1600.

Forshey, B.M., and Aiken, C. (2003). Disassembly of human immunodeficiency virus type 1 cores in vitro reveals association of Nef with the subviral ribonucleoprotein complex. Journal of virology *77*, 4409-4414.

Forshey, B.M., Shi, J., and Aiken, C. (2005). Structural requirements for recognition of the human immunodeficiency virus type 1 core during host restriction in owl monkey cells. Journal of virology *79*, 869-875.

Forshey, B.M., von Schwedler, U., Sundquist, W.I., and Aiken, C. (2002). Formation of a human immunodeficiency virus type 1 core of optimal stability is crucial for viral replication. Journal of virology *76*, 5667-5677.

Franke, E.K., Yuan, H.E., and Luban, J. (1994). Specific incorporation of cyclophilin A into HIV-1 virions. Nature *372*, 359-362.

Freed, E.O. (2001). HIV-1 replication. Somatic cell and molecular genetics *26*, 13-33.

Freed, E.O., and Martin, M.A. (1996). Domains of the human immunodeficiency virus type 1 matrix and gp41 cytoplasmic tail required for envelope incorporation into virions. J Virol *70*, 341-351.

Fuller, S.D., Wilk, T., Gowen, B.E., Krausslich, H.G., and Vogt, V.M. (1997). Cryo-electron microscopy reveals ordered domains in the immature HIV-1 particle. Current biology : CB *7*, 729-738.

Gallo, S.A., Puri, A., and Blumenthal, R. (2001). HIV-1 gp41 six-helix bundle formation occurs rapidly after the engagement of gp120 by CXCR4 in the HIV-1 Env-mediated fusion process. Biochemistry *40*, 12231-12236.

Gamble, T.R., Vajdos, F.F., Yoo, S., Worthylake, D.K., Houseweart, M., Sundquist, W.I., and Hill, C.P. (1996). Crystal structure of human cyclophilin A bound to the amino-terminal domain of HIV-1 capsid. Cell *87*, 1285-1294.

Gamble, T.R., Yoo, S., Vajdos, F.F., von Schwedler, U.K., Worthylake, D.K., Wang, H., McCutcheon, J.P., Sundquist, W.I., and Hill, C.P. (1997). Structure of the carboxyl-terminal dimerization domain of the HIV-1 capsid protein. Science *278*, 849-853.

Ganser, B.K., Li, S., Klishko, V.Y., Finch, J.T., and Sundquist, W.I. (1999). Assembly and analysis of conical models for the HIV-1 core. Science *283*, 80-83.

Ganser-Pornillos, B.K., Cheng, A., and Yeager, M. (2007). Structure of full-length HIV-1 CA: a model for the mature capsid lattice. Cell *131*, 70-79.

Ganser-Pornillos, B.K., Yeager, M., and Sundquist, W.I. (2008). The structural biology of HIV assembly. Current opinion in structural biology *18*, 203-217.

Gitti, R.K., Lee, B.M., Walker, J., Summers, M.F., Yoo, S., and Sundquist, W.I. (1996). Structure of the amino-terminal core domain of the HIV-1 capsid protein. Science *273*, 231-235.

Gross, I., Hohenberg, H., Huckhagel, C., and Krausslich, H.G. (1998). N-Terminal extension of human immunodeficiency virus capsid protein converts the in vitro assembly phenotype from tubular to spherical particles. Journal of virology *72*, 4798-4810.

Hatziioannou, T., Perez-Caballero, D., Yang, A., Cowan, S., and Bieniasz, P.D. (2004). Retrovirus resistance factors Ref1 and Lv1 are species-specific variants of TRIM5alpha. Proceedings of the National Academy of Sciences of the United States of America *101*, 10774-10779.

Hulme, A.E., Perez, O., and Hope, T.J. (2011). Complementary assays reveal a relationship between HIV-1 uncoating and reverse transcription. Proceedings of the National Academy of Sciences of the United States of America *108*, 9975-9980.

Inagaki, N., Takeuchi, H., Yokoyama, M., Sato, H., Ryo, A., Yamamoto, H., Kawada, M., and Matano, T. (2010). A structural constraint for functional interaction between N-terminal and C-terminal domains in simian immunodeficiency virus capsid proteins. Retrovirology *7*, 90.

Ivanov, D., Tsodikov, O.V., Kasanov, J., Ellenberger, T., Wagner, G., and Collins, T. (2007). Domain-swapped dimerization of the HIV-1 capsid C-terminal domain. Proceedings of the National Academy of Sciences of the United States of America *104*, 4353-4358.

Jiang, J., Ablan, S.D., Derebail, S., Hercik, K., Soheilian, F., Thomas, J.A., Tang, S., Hewlett, I., Nagashima, K., Gorelick, R.J.*, et al.* (2011a). The interdomain linker region of HIV-1 capsid protein is a critical determinant of proper core assembly and stability. Virology *421*, 253-265.

Jiang, J.Y., Ablan, S.D., Derebail, S., Hercik, K., Soheilian, F., Thomas, J.A., Tang, S.X., Hewlett, I., Nagashima, K., Gorelick, R.J.*, et al.* (2011b). The interdomain linker region of HIV-1 capsid protein is a critical determinant of proper core assembly and stability. Virology *421*, 253-265.

Joshi, A., Nagashima, K., and Freed, E.O. (2006). Mutation of dileucine-like motifs in the human immunodeficiency virus type 1 capsid disrupts virus assembly, gag-gag interactions, gag-membrane binding, and virion maturation. Journal of virology *80*, 7939-7951.

Keller, P.W., Adamson, C.S., Heymann, J.B., Freed, E.O., and Steven, A.C. (2011). HIV-1 maturation inhibitor bevirimat stabilizes the immature Gag lattice. Journal of virology *85*, 1420-1428.

Kelly, B.N., Howard, B.R., Wang, H., Robinson, H., Sundquist, W.I., and Hill, C.P. (2006). Implications for viral capsid assembly from crystal structures of HIV-1 Gag(1-278) and CA(N)(133-278). Biochemistry *45*, 11257-11266.

Kelly, B.N., Kyere, S., Kinde, I., Tang, C., Howard, B.R., Robinson, H., Sundquist, W.I., Summers, M.F., and Hill, C.P. (2007). Structure of the antiviral assembly inhibitor CAP-1 complex with the HIV-1 CA protein. Journal of molecular biology *373*, 355-366.

Khorasanizadeh, S., Campos-Olivas, R., and Summers, M.F. (1999). Solution structure of the capsid protein from the human T-cell leukemia virus type-I. Journal of molecular biology *291*, 491-505.

Kingston, R.L., Fitzon-Ostendorp, T., Eisenmesser, E.Z., Schatz, G.W., Vogt, V.M., Post, C.B., and Rossmann, M.G. (2000). Structure and self-association of the Rous sarcoma virus capsid protein. Structure *8*, 617-628.

Kortagere, S., Madani, N., Mankowski, M.K., Schon, A., Zentner, I., Swaminathan, G., Princiotto, A., Anthony, K., Oza, A., Sierra, L.J., *et al.* (2012). Inhibiting Early-Stage Events in HIV-1 Replication by Small-Molecule Targeting of the HIV-1 Capsid. Journal of virology *86*, 8472-8481.

Kotov, A., Zhou, J., Flicker, P., and Aiken, C. (1999). Association of Nef with the human immunodeficiency virus type 1 core. Journal of virology *73*, 8824-8830.

Lanman, J., Lam, T.T., Barnes, S., Sakalian, M., Emmett, M.R., Marshall, A.G., and Prevelige, P.E., Jr. (2003). Identification of novel interactions in HIV-1 capsid protein assembly by high-resolution mass spectrometry. Journal of molecular biology *325*, 759-772.

Lanman, J., Lam, T.T., Emmett, M.R., Marshall, A.G., Sakalian, M., and Prevelige, P.E., Jr. (2004). Key interactions in HIV-1 maturation identified by hydrogen-deuterium exchange. Nature structural & molecular biology *11*, 676-677.

Lanman, J., Sexton, J., Sakalian, M., and Prevelige, P.E., Jr. (2002). Kinetic analysis of the role of intersubunit interactions in human immunodeficiency virus type 1 capsid protein assembly in vitro. Journal of virology *76*, 6900-6908.

Lee, S.K., Harris, J., and Swanstrom, R. (2009). A strongly transdominant mutation in the human immunodeficiency virus type 1 gag gene defines an Achilles heel in the virus life cycle. Journal of virology *83*, 8536-8543.

Lemke, C.T., Titolo, S., von Schwedler, U., Goudreau, N., Mercier, J.F., Wardrop, E., Faucher, A.M., Coulombe, R., Banik, S.S., Fader, L., *et al.* (2012). Distinct effects of two HIV-1 capsid assembly inhibitor families that bind the same site within the N-terminal domain of the viral CA protein. Journal of virology *86*, 6643-6655.

Leschonsky, B., Ludwig, C., Bieler, K., and Wagner, R. (2007). Capsid stability and replication of human immunodeficiency virus type 1 are influenced critically by charge and size of Gag residue 183. The Journal of general virology *88*, 207-216.

Li, F., Goila-Gaur, R., Salzwedel, K., Kilgore, N.R., Reddick, M., Matallana, C., Castillo, A., Zoumplis, D., Martin, D.E., Orenstein, J.M., *et al.* (2003). PA-457: a potent HIV inhibitor that disrupts core condensation by targeting a late step in Gag processing. Proceedings of the National Academy of Sciences of the United States of America *100*, 13555-13560.

Li, S., Hill, C.P., Sundquist, W.I., and Finch, J.T. (2000). Image reconstructions of helical assemblies of the HIV-1 CA protein. Nature *407*, 409-413.

Li, Y., Kar, A.K., and Sodroski, J. (2009). Target cell type-dependent modulation of human immunodeficiency virus type 1 capsid disassembly by cyclophilin A. Journal of virology *83*, 10951-10962.

Luban, J. (1996). Absconding with the chaperone: essential cyclophilin-Gag interaction in HIV-1 virions. Cell *87*, 1157-1159.

Luban, J., Bossolt, K.L., Franke, E.K., Kalpana, G.V., and Goff, S.P. (1993). Human immunodeficiency virus type 1 Gag protein binds to cyclophilins A and B. Cell *73*, 1067-1078.

Mateu, M.G. (2002). Conformational stability of dimeric and monomeric forms of the C-terminal domain of human immunodeficiency virus-1 capsid protein. Journal of molecular biology *318*, 519-531.

Meng, X., Zhao, G., Yufenyuy, E., Ke, D., Ning, J., Delucia, M., Ahn, J., Gronenborn, A.M., Aiken, C., and Zhang, P. (2012). Protease Cleavage Leads to Formation of Mature Trimer Interface in HIV-1 Capsid. PLoS pathogens *8*, e1002886.

Miller, M.D., Farnet, C.M., and Bushman, F.D. (1997). Human immunodeficiency virus type 1 preintegration complexes: studies of organization and composition. Journal of virology *71*, 5382-5390.

Momany, C., Kovari, L.C., Prongay, A.J., Keller, W., Gitti, R.K., Lee, B.M., Gorbalenya, A.E., Tong, L., McClure, J., Ehrlich, L.S.*, et al.* (1996). Crystal structure of dimeric HIV-1 capsid protein. Nature structural biology *3*, 763-770.

Monroe, E.B., Kang, S., Kyere, S.K., Li, R., and Prevelige, P.E., Jr. (2010). Hydrogen/deuterium exchange analysis of HIV-1 capsid assembly and maturation. Structure *18*, 1483-1491.

Mortuza, G.B., Haire, L.F., Stevens, A., Smerdon, S.J., Stoye, J.P., and Taylor, I.A. (2004). High-resolution structure of a retroviral capsid hexameric amino-terminal domain. Nature *431*, 481-485.

Neira, J.L. (2009). The capsid protein of human immunodeficiency virus: designing inhibitors of capsid assembly. FEBS J *276*, 6110-6117.

Nisole, S., Lynch, C., Stoye, J.P., and Yap, M.W. (2004). A Trim5-cyclophilin A fusion protein found in owl monkey kidney cells can restrict HIV-1. Proceedings of the National Academy of Sciences of the United States of America *101*, 13324-13328.

Noviello, C.M., Lopez, C.S., Kukull, B., McNett, H., Still, A., Eccles, J., Sloan, R., and Barklis, E. (2011). Second-site compensatory mutations of HIV-1 capsid mutations. Journal of virology *85*, 4730-4738.

Ono, A., Huang, M., and Freed, E.O. (1997). Characterization of human immunodeficiency virus type 1 matrix revertants: effects on virus assembly, Gag processing, and Env incorporation into virions. J Virol *71*, 4409-4418.

Owens, C.M., Song, B., Perron, M.J., Yang, P.C., Stremlau, M., and Sodroski, J. (2004). Binding and susceptibility to postentry restriction factors in monkey cells are specified by

distinct regions of the human immunodeficiency virus type 1 capsid. Journal of virology *78*, 5423-5437.

Owens, C.M., Yang, P.C., Gottlinger, H., and Sodroski, J. (2003). Human and simian immunodeficiency virus capsid proteins are major viral determinants of early, postentry replication blocks in simian cells. Journal of virology *77*, 726-731.

Pettit, S.C., Sheng, N., Tritch, R., Erickson-Viitanen, S., and Swanstrom, R. (1998). The regulation of sequential processing of HIV-1 Gag by the viral protease. Advances in experimental medicine and biology *436*, 15-25.

Phillips, J.M., Murray, P.S., Murray, D., and Vogt, V.M. (2008). A molecular switch required for retrovirus assembly participates in the hexagonal immature lattice. The EMBO journal *27*, 1411-1420.

Pornillos, O., Ganser-Pornillos, B.K., Banumathi, S., Hua, Y., and Yeager, M. (2010). Disulfide bond stabilization of the hexameric capsomer of human immunodeficiency virus. Journal of molecular biology *401*, 985-995.

Pornillos, O., Ganser-Pornillos, B.K., Kelly, B.N., Hua, Y., Whitby, F.G., Stout, C.D., Sundquist, W.I., Hill, C.P., and Yeager, M. (2009). X-ray structures of the hexameric building block of the HIV capsid. Cell *137*, 1282-1292.

Pornillos, O., Ganser-Pornillos, B.K., and Yeager, M. (2011). Atomic-level modelling of the HIV capsid. Nature *469*, 424-427.

Sayah, D.M., Sokolskaja, E., Berthoux, L., and Luban, J. (2004). Cyclophilin A retrotransposition into TRIM5 explains owl monkey resistance to HIV-1. Nature *430*, 569-573.

Scholz, I., Arvidson, B., Huseby, D., and Barklis, E. (2005). Virus particle core defects caused by mutations in the human immunodeficiency virus capsid N-terminal domain. Journal of virology *79*, 1470-1479.

Shah, V.B., and Aiken, C. (2011a). In vitro uncoating of HIV-1 cores. Journal of visualized experiments : (57), e3384, DOI: 103791/3384.

Shah, V.B., and Aiken, C. (2011b). In vitro uncoating of HIV-1 cores. Journal of Visulized Experiments: (57), e3384, DOI: 103791/3384, (57), e3384, DOI: 3310.3791/3384.

Shah, V.B., Shi, J., Hout, D.R., Oztop, I., Krishnan, L., Ahn, J., Shotwell, M.S., Engelman, A., and Aiken, C. (2013). The host proteins transportin SR2/TNPO3 and cyclophilin A exert opposing effects on HIV-1 uncoating. Journal of virology *87*, 422-432.

Shi, J., and Aiken, C. (2006). Saturation of TRIM5 alpha-mediated restriction of HIV-1 infection depends on the stability of the incoming viral capsid. Virology *350*, 493-500.

Shi, J., Zhou, J., Shah, V.B., Aiken, C., and Whitby, K. (2011). Small-molecule inhibition of human immunodeficiency virus type 1 infection by virus capsid destabilization. Journal of virology *85*, 542-549.

Stremlau, M., Owens, C.M., Perron, M.J., Kiessling, M., Autissier, P., and Sodroski, J. (2004). The cytoplasmic body component TRIM5alpha restricts HIV-1 infection in Old World monkeys. Nature *427*, 848-853.

Stremlau, M., Perron, M., Lee, M., Li, Y., Song, B., Javanbakht, H., Diaz-Griffero, F., Anderson, D.J., Sundquist, W.I., and Sodroski, J. (2006). Specific recognition and accelerated uncoating of retroviral capsids by the TRIM5alpha restriction factor. Proceedings of the National Academy of Sciences of the United States of America *103*, 5514-5519.

Tang, C., Loeliger, E., Kinde, I., Kyere, S., Mayo, K., Barklis, E., Sun, Y., Huang, M., and Summers, M.F. (2003). Antiviral inhibition of the HIV-1 capsid protein. Journal of molecular biology *327*, 1013-1020.

Tang, C., Ndassa, Y., and Summers, M.F. (2002). Structure of the N-terminal 283-residue fragment of the immature HIV-1 Gag polyprotein. Nature structural biology *9*, 537-543.

Ternois, F., Sticht, J., Duquerroy, S., Krausslich, H.G., and Rey, F.A. (2005). The HIV-1 capsid protein C-terminal domain in complex with a virus assembly inhibitor. Nature structural & molecular biology *12*, 678-682.

Towers, G.J., Hatziioannou, T., Cowan, S., Goff, S.P., Luban, J., and Bieniasz, P.D. (2003). Cyclophilin A modulates the sensitivity of HIV-1 to host restriction factors. Nature medicine *9*, 1138-1143.

von Schwedler, U.K., Stemmler, T.L., Klishko, V.Y., Li, S., Albertine, K.H., Davis, D.R., and Sundquist, W.I. (1998). Proteolytic refolding of the HIV-1 capsid protein amino-terminus facilitates viral core assembly. The EMBO journal *17*, 1555-1568.

von Schwedler, U.K., Stray, K.M., Garrus, J.E., and Sundquist, W.I. (2003). Functional surfaces of the human immunodeficiency virus type 1 capsid protein. Journal of virology *77*, 5439-5450.

Wacharapornin, P., Lauhakirti, D., and Auewarakul, P. (2007). The effect of capsid mutations on HIV-1 uncoating. Virology *358*, 48-54.

Wehrly, K., and Chesebro, B. (1997). p24 antigen capture assay for quantification of human immunodeficiency virus using readily available inexpensive reagents. Methods *12*, 288-293.

Wei, P., Garber, M.E., Fang, S.M., Fischer, W.H., and Jones, K.A. (1998). A novel CDK9-associated C-type cyclin interacts directly with HIV-1 Tat and mediates its high-affinity, loop-specific binding to TAR RNA. Cell *92*, 451-462.

Wei, X., Decker, J.M., Liu, H., Zhang, Z., Arani, R.B., Kilby, J.M., Saag, M.S., Wu, X., Shaw, G.M., and Kappes, J.C. (2002). Emergence of resistant human immunodeficiency virus type 1 in patients receiving fusion inhibitor (T-20) monotherapy. Antimicrobial agents and chemotherapy *46*, 1896-1905.

Wiegers, K., Rutter, G., Kottler, H., Tessmer, U., Hohenberg, H., and Krausslich, H.G. (1998). Sequential steps in human immunodeficiency virus particle maturation revealed by alterations of individual Gag polyprotein cleavage sites. Journal of virology *72*, 2846-2854.

Wildova, M., Hadravova, R., Stokrova, J., Krizova, I., Ruml, T., Hunter, E., Pichova, I., and Rumlova, M. (2008). The effect of point mutations within the N-terminal domain of Mason-Pfizer monkey virus capsid protein on virus core assembly and infectivity. Virology *380*, 157-163.

Wilk, T., Gross, I., Gowen, B.E., Rutten, T., de Haas, F., Welker, R., Krausslich, H.G., Boulanger, P., and Fuller, S.D. (2001). Organization of immature human immunodeficiency virus type 1. Journal of virology *75*, 759-771.

Worthylake, D.K., Wang, H., Yoo, S., Sundquist, W.I., and Hill, C.P. (1999). Structures of the HIV-1 capsid protein dimerization domain at 2.6 A resolution. Acta crystallographica Section D, Biological crystallography *55*, 85-92.

Wright, E.R., Schooler, J.B., Ding, H.J., Kieffer, C., Fillmore, C., Sundquist, W.I., and Jensen, G.J. (2007). Electron cryotomography of immature HIV-1 virions reveals the structure of the CA and SP1 Gag shells. The EMBO journal *26*, 2218-2226.

Wyma, D.J., Jiang, J., Shi, J., Zhou, J., Lineberger, J.E., Miller, M.D., and Aiken, C. (2004). Coupling of human immunodeficiency virus type 1 fusion to virion maturation: a novel role of the gp41 cytoplasmic tail. Journal of virology *78*, 3429-3435.

Yang, R., and Aiken, C. (2007). A mutation in alpha helix 3 of CA renders human immunodeficiency virus type 1 cyclosporin A resistant and dependent: rescue by a second-site substitution in a distal region of CA. Journal of virology *81*, 3749-3756.

Yang, R., Shi, J., Byeon, I.J., Ahn, J., Sheehan, J.H., Meiler, J., Gronenborn, A.M., and Aiken, C. (2012). Second-site suppressors of HIV-1 capsid mutations: restoration of intracellular activities without correction of intrinsic capsid stability defects. Retrovirology *9*, 30.

Yeager, M. (2011). Design of in vitro symmetric complexes and analysis by hybrid methods reveal mechanisms of HIV capsid assembly. Journal of molecular biology *410*, 534-552.

Yee, J.K., Friedmann, T., and Burns, J.C. (1994). Generation of high-titer pseudotyped retroviral vectors with very broad host range. Methods in cell biology *43 Pt A*, 99-112.

Zhao, G., Ke, D., Vu, T., Ahn, J., Shah, V.B., Yang, R., Aiken, C., Charlton, L.M., Gronenborn, A.M., and Zhang, P. (2011). Rhesus TRIM5alpha disrupts the HIV-1 capsid at the inter-hexamer interfaces. PLoS pathogens *7*, e1002009.

Zhou, J., Yuan, X., Dismuke, D., Forshey, B.M., Lundquist, C., Lee, K.H., Aiken, C., and Chen, C.H. (2004). Small-molecule inhibition of human immunodeficiency virus type 1 replication by specific targeting of the final step of virion maturation. Journal of virology *78*, 922-929.